



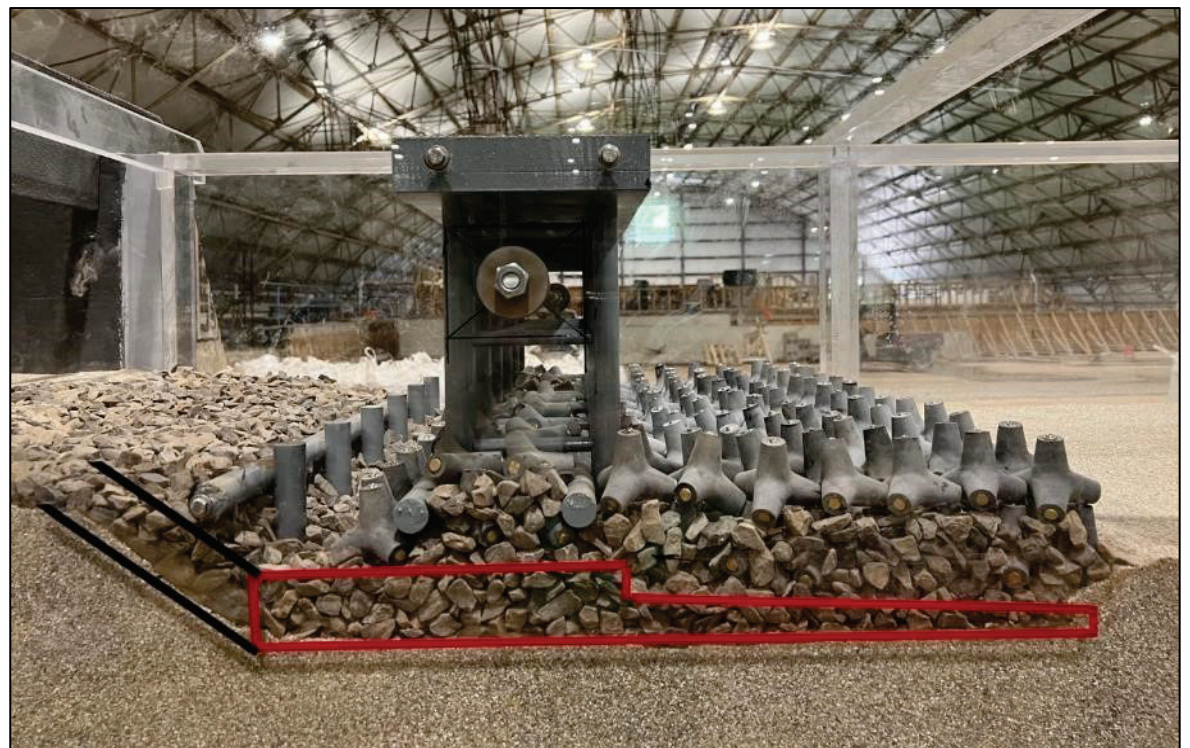
US Army Corps
of Engineers®
Engineer Research and
Development Center



Evaluation of a Permeable Dam as an Erosion Control Structure on Coca River, Ecuador

Efraín Ramos-Santiago, Yamiretsy Pagán-Albelo, Jeremy A. Sharp,
Curtis L. Blades, and Kevin L. Pigg

June 2023



The US Army Engineer Research and Development Center (ERDC) solves the nation's toughest engineering and environmental challenges. ERDC develops innovative solutions in civil and military engineering, geospatial sciences, water resources, and environmental sciences for the Army, the Department of Defense, civilian agencies, and our nation's public good. Find out more at www.erdclibrary.on.worldcat.org/discovery.

To search for other technical reports published by ERDC, visit the ERDC online library at <http://www.erdclibrary.on.worldcat.org/discovery>.

Evaluation of a Permeable Dam as an Erosion Control Structure on the Coca River, Ecuador

Efraín Ramos-Santiago, Yamiretsy Pagán-Albelo, Jeremy A. Sharp,
Curtis L. Blades, and Kevin L. Pigg

*US Army Engineer Research and Development Center
Coastal and Hydraulics Laboratory
3909 Halls Ferry Road
Vicksburg, MS 39180-6199*

Final Report

DISTRIBUTION STATEMENT A. Approved for public release; distribution unlimited.

Prepared for Mobile District, US Army Corps of Engineers
PO Box 2288
Mobile, AL 36628-0001

Under Funding via Labor Charge Code

Abstract

The effort performed here describes the process to evaluate the scour-protection performance of the proposed permeable dam. The US Engineer Research and Development Center, Coastal and Hydraulics Laboratory, built a 1:50 Froude scaled movable bed section model of the permeable dam structure and tested in a specialized flume that simulates regressive erosion propagation. Profiles were collected at various times to track the progression of the scour. Tests evaluated variations of the proposed structure, which included tetrapods, riprap, bridge piers, and longitudinal piles. For the various proposed alternatives, a total of six tests were conducted. The collected profiles show the ability or inability of each alternative and its associated performance. From this analysis, untethered tetrapods could not effectively arrest the local scour around the structure. However, large rock along with invert control stopped the regressive erosion and held the upstream grade.

DISCLAIMER: The contents of this report are not to be used for advertising, publication, or promotional purposes. Citation of trade names does not constitute an official endorsement or approval of the use of such commercial products. All product names and trademarks cited are the property of their respective owners. The findings of this report are not to be construed as an official Department of the Army position unless so designated by other authorized documents.

DESTROY THIS REPORT WHEN NO LONGER NEEDED. DO NOT RETURN IT TO THE ORIGINATOR.

Contents

Abstract	ii
Figures and Tables.....	iv
Preface.....	vii
1 Introduction.....	1
1.1 Background.....	1
1.2 Objective.....	3
1.3 Approach	4
2 Methodology	5
2.1 Design and Construction of the Sectional Model Flume Model.....	5
2.2 Bed Material Scaling	7
2.3 Boundary Conditions and Flume Model Operation.....	8
2.4 Permeable Dam Model Design and Construction.....	8
2.4.1 Model Alternative 1: Untethered Tetrapods	12
2.4.2 Model Alternative 2: Interlocked, Untethered Tetrapods	14
2.4.3 Model Alternative 3: Tetrapods Replaced with Stone Structure	18
2.4.4 Model Alternative 4: Structural Changes.....	20
2.4.5 Model Alternative 5: Changes to Stone Structure.....	25
2.4.6 Model Alternative 6: Additional Structural Changes	28
2.5 Experiments and Testing Procedure.....	30
2.6 Data Processing and Analysis.....	31
3 Model Testing Results.....	32
4 Discussion	59
4.1 Untethered Tetrapod Configuration.....	59
4.2 Model Alternative 1: Untethered Tetrapods.....	62
4.3 Model Alternative 2: Interlocked, Untethered Tetrapods	62
4.4 Model Alternative 3: Tetrapods Replaced with Stone Structure.....	63
4.5 Model Alternative 4: Structural Changes	63
4.6 Model Alternative 5: Changes to Stone Structure	64
4.7 Model Alternative 6: Additional Structural Changes.....	64
5 Conclusions and Recommendations	66
Appendix: Permeable Dam Design Drawings.....	67
Abbreviations.....	76
Report Documentation Page (SF 298).....	77

Figures and Tables

Figures

1.	Location map of the permeable dam structure.....	2
2.	Piping failure conditions at the San Rafael Waterfall location (provided by US Army Corps of Engineers [USACE], Mobile District).....	3
3.	Top (<i>top</i>) and cross-sectional (<i>bottom</i>) views of the proposed permeable dam structure design (Electric Corporation of Ecuador [CELEC], with permission).	3
4.	The 3D and orthographic projections of the section model-design configuration.....	6
5.	Percent passing curve for model materials.	7
6.	Cross-sectional view of the permeable dam design (CELEC, with permission).	10
7.	Plan view of the permeable dam with the arrangement of tetrapods (CELEC, with permission).	10
8.	Permeable dam physical model.	11
9.	Representation of a tetrapod unit.	11
10.	Top view of model alternative 1.....	13
11.	Front view of model alternative 1.....	13
12.	Rear view of model alternative 1.....	14
13.	Geological profile of Coca River with the configuration proposed for model alternative 2 (CELEC, with permission).	15
14.	Side view of model alternative 2.	16
15.	Front view of model alternative 2.....	16
16.	Top view of model alternative 2.....	17
17.	Rear view of model alternative 2.....	17
18.	Geological profile of Coca River with the configuration proposed for model alternative 3 (CELEC, with permission).	18
19.	Side view of the model alternative 3.....	19
20.	Top view of model alternative 3.....	19
21.	Front (<i>top</i>) and rear (<i>bottom</i>) views of model alternative 3.....	20
22.	Geological profile of Coca River with the configuration proposed for model alternative 4 (CELEC, with permission).	21
23.	Gradation curves for prototype and model stone structure (prototype data provided by CELEC).	22
24.	Placement of third row of piles downstream of bridge: front (<i>left</i>) and side (<i>right</i>) views.....	22
25.	Side view of the model alternative 4.....	23
26.	Top view of model alternative 4.....	23
27.	Front view of model alternative 4.....	24
28.	Rear view of model alternative 4.....	24
29.	Geological profile of Coca River with the configuration proposed for model alternative 5 (CELEC, with permission).	25
30.	Side view of the model alternative 5.....	26

31. Top view of model alternative 5.....	26
32. Front view of model alternative 5.....	27
33. Rear view of model alternative 5.....	27
34. Side view of the model alternative 6.....	28
35. Top view of model alternative 6.....	29
36. Front view of model alternative 6.....	29
37. Rear view of model alternative 6.....	30
38. Side views of the initial (<i>top</i>) and final (<i>bottom</i>) conditions of model alternative 1.....	33
39. Side views of the initial (<i>top</i>) and final (<i>bottom</i>) conditions of model alternative 2.....	34
40. Side views of the initial (<i>top</i>) and final (<i>bottom</i>) conditions of model alternative 3.....	35
41. Side views of the initial (<i>top</i>) and final (<i>bottom</i>) conditions of model alternative 4.....	36
42. Side views of the initial (<i>top</i>) and final (<i>bottom</i>) conditions of model alternative 5.....	37
43. Side views of the initial (<i>top</i>) and final (<i>bottom</i>) conditions of model alternative 6.....	38
44. Scour profiles of model alternative 1.....	39
45. Scour profiles of model alternative 1 (continued).....	40
46. Scour profiles of model alternative 2.....	41
47. Scour profiles of model alternative 2 (continued).....	42
48. Scour profiles of model alternative 3.....	43
49. Scour profiles of model alternative 3 (continued).....	44
50. Scour profiles of model alternative 4.....	45
51. Scour profiles of model alternative 4 (continued).....	46
52. Scour profiles of model alternative 5.....	47
53. Scour profiles of model alternative 5 (continued).....	48
54. Scour profiles of model alternative 5 (continued).....	49
55. Scour profiles of model alternative 6.....	50
56. Scour profiles of model alternative 6 (continued).....	51
57. Comparison of scour depth and invert elevation for model alternative 1.....	53
58. Comparison of scour depth and invert elevation for model alternative 2.....	53
59. Comparison of scour depth and invert elevation for model alternative 3.....	54
60. Comparison of scour depth and invert elevation for model alternative 4.....	54
61. Comparison of scour depth and invert elevation for model alternative 5.....	55
62. Comparison of scour depth and invert elevation for model alternative 6.....	55
63. Comparison of modeled flow hydrograph and tailgate-lowering operation for test 1.....	56
64. Comparison of modelled flow hydrograph and tailgate lowering operation for test 2.....	57
65. Comparison of modelled flow hydrograph and tailgate lowering operation for test 3.....	57
66. Comparison of modelled flow hydrograph and tailgate lowering operation for tests 4 to 6.....	58
67. Posts scour images of a tethered grade control design (provided by the USACE team). The tethers tangled and kept the scour protection elements suspended above the scouring bed.....	61
68. Side view of the unsubmerged or free flow.....	65

A-1. Permeable dam plan and profile drawing (CELEC, with permission).	68
A-2. Initial permeable dam design—details of bridge and piers (CELEC, with permission).	69
A-3. Initial permeable dam design—details of tetrapods (CELEC, with permission).	70
A-4. Second permeable dam design change (CELEC, with permission).	71
A-5. Third permeable dam design change (CELEC, with permission).	72
A-6. Fourth permeable dam design change (CELEC, with permission).....	73
A-7. Fifth permeable dam design change (CELEC, with permission).	74
A-8. Sixth permeable dam design change (CELEC, with permission).	75

Tables

1. Physical model scale conversions.	5
2. Percent passing curve data for model bed material.	8
3. Comparison of the tetrapod unit model and prototype physical properties.	12
4. Physical model testing procedure.	31
5. Tailgate operation schedule.	31
6. Summary of experiments per model alternative.	32
7. Final slope values for the bed downstream of the bridge.....	56
8. Damage extension per model alternative.	59

Preface

The study was conducted for and funded by the US Army Corps of Engineers, Mobile District (USACE-SAM), under Funding Authorization/CO-8242-XX-8028-08, project identification Task 2.2—Permeable Dam Section Model, via a Labor Charge Code. The technical monitor for USACE-SAM was Mr. Adriel McConnell, project manager.

The work was performed by the River and Estuarine Engineering Branch of the Flood and Storm Protection Division, and the Harbors, Entrances, and Structures Branch of the Navigation Division, US Army Engineer Research and Development Center, Coastal and Hydraulics Laboratory (ERDC-CHL).

At the time of publication of this report, Mr. David P. May was chief, River and Estuarine Engineering Branch; Dr. Cary A. Talbot was chief, Flood and Storm Protection Division; Mr. Chad R. Bounds was chief, Harbors, Entrances, and Structures Branch; Ms. Ashley E. Frey was chief, Navigation Division; and Dr. Julie D. Rosati was the technical director for the Flood and Coastal Risk Management Research and Development. The deputy director of ERDC-CHL was Mr. Keith Flowers, and the director was Dr. Ty V. Wamsley.

COL Christian Patterson was commander of ERDC, and the director was Dr. David W. Pittman.

This page intentionally left blank.

1 Introduction

1.1 Background

The 140 m¹ tall San Rafael Waterfall was located 19 km downstream of the Coca Codo Sinclair (CCS) Hydroelectric Intake Structure (Figure 1). The CCS Intake Structure is located along the Coca River in Napo Province, Ecuador, 100 km east of Quito. It is the largest energy producer in Ecuador, with an installed capacity of 1,500 MW, providing up to 30% of the nation's energy. In February 2020, the Coca River undermined the basalt natural dam that formed the San Rafael waterfall, dropping the local hydraulic base elevation by approximately 150 m (Figure 2). This elevation drop activated the regressive erosion. In the subsequent 2 yr, the regressive erosion advanced 10 km upstream, eroding over 200 million tons of sediment and damaging pipelines, roads, bridges, and other infrastructure. Current projections predict the regressive erosion could threaten the CCS Intake Structure with as much as 45 m of erosion that could occur within the next decade.

The Electric Corporation of Ecuador (CELEC) and its Executive Commission for the Coca River (CERC) developed a strategy to deal with the effects of the regressive erosion in the Coca River. This strategy proposed implementing a set of grade-control structures along the river section between the CCS Intake Structure and the area of the former San Rafael waterfall. Among other goals, such structures aimed to maintain or increase the resistance to bed erosion in specific sections that will act as semihard areas along the river. CELEC CERC analyzed the development and morphological evolution of the river equilibrium profile and observed that creating local reinforcement reduces the degree of erosion upstream while the bed armor limits exposure of weak substrates. In this sense, the possible implementation of permeable dams along the segment between the CCS Intake Structure and the former waterfall would create sections that prevent the transport of coarse sediments and generate permanent equilibrium profiles in between sections.

¹ For a full list of the spelled-out forms of the units of measure and unit conversions used in this document, please refer to *US Government Publishing Office Style Manual*, 31st ed. (Washington, DC: US Government Publishing Office 2016), 248–52 and 345–7, respectively. <https://www.govinfo.gov/content/pkg/GPO-STYLEMANUAL-2016/pdf/GPO-STYLEMANUAL-2016.pdf>.

CELEC CERC proposed constructing a permeable dam structure in a location 8.4 km downstream of the CCS Intake Structure on the Coca River. The location was later revised to a location 7.7 km downstream due to site-condition challenges. The permeable dam design combines a bridge with an upstream set of piles and a tetrapod mat downstream (Figure 3). The 119 m long bridge, with piers spaced 7 m, would restore access to the river's right bank and allow routine maintenance work. For example, a crane could place bed protection during and between events. The original concept used concrete tetrapods attached to the bridge with cables. These mats of tetrapods would protect the downstream riverbed. Thus, as the regressive erosion passes through the reach, the tetrapods should form an armoring mat to maintain a steeper slope through the bridge that would effectively stop the head cut. The additional set of piles upstream of the bridge would provide other tethering anchors for the tetrapods.

Figure 1. Location map of the permeable dam structure.

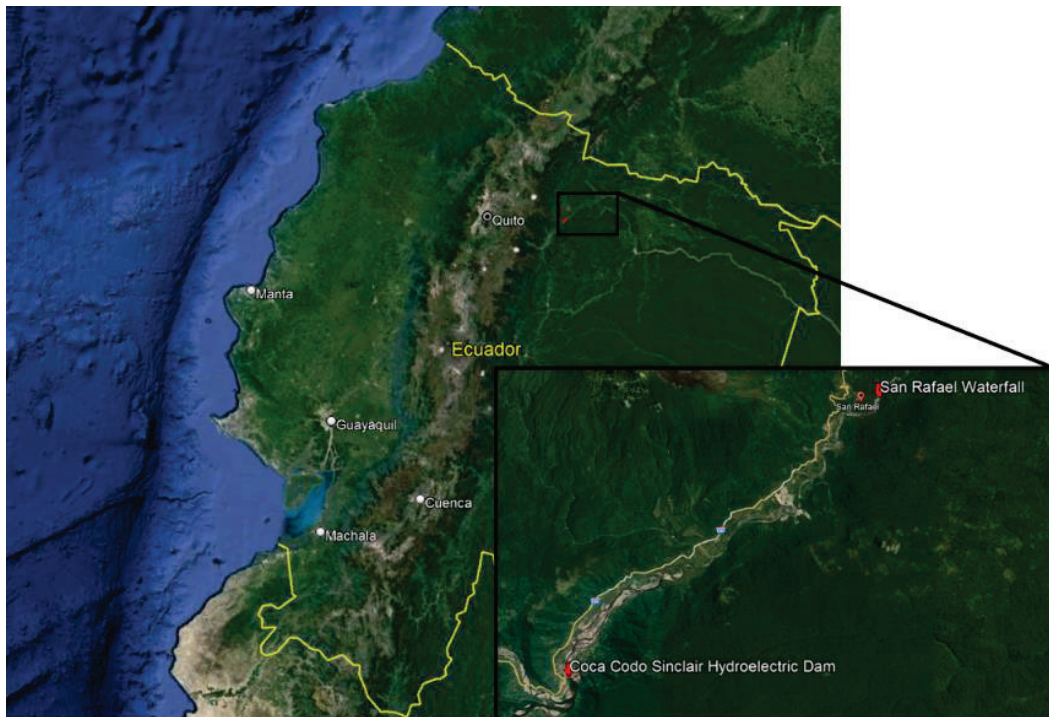
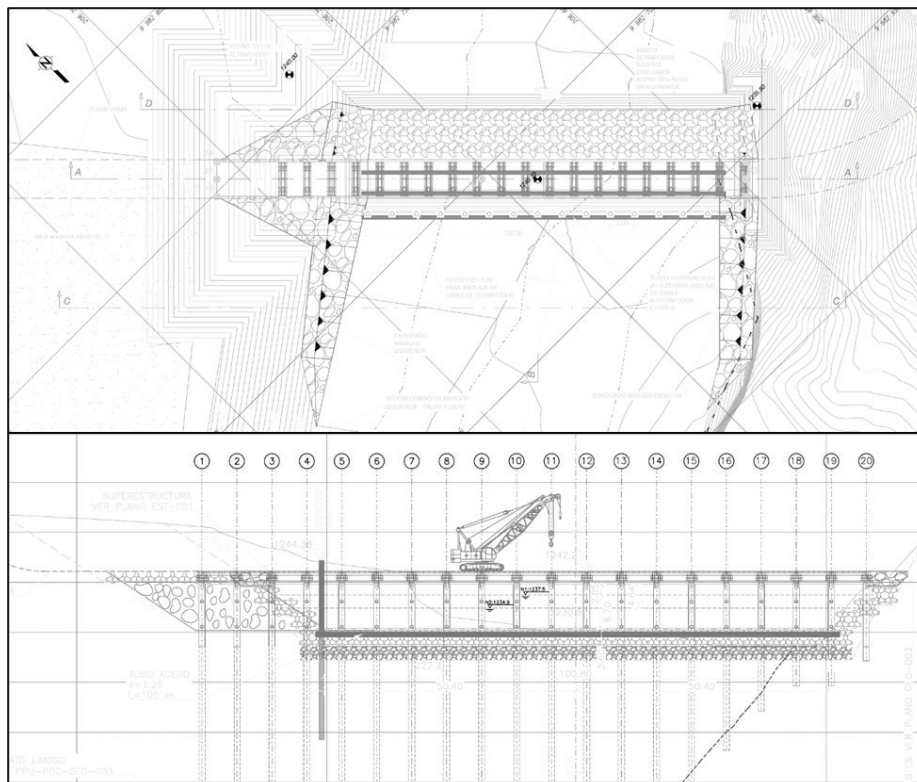


Figure 2. Piping failure conditions at the San Rafael Waterfall location (provided by US Army Corps of Engineers [USACE], Mobile District).



Figure 3. Top (*top*) and cross-sectional (*bottom*) views of the proposed permeable dam structure design (Electric Corporation of Ecuador [CELEC], with permission).



1.2 Objective

The US Army Engineer Research and Development Center, Coastal and Hydraulics Laboratory (ERDC-CHL), conducted a section physical model study to evaluate the hydraulic performance of the proposed permeable

dam. Specifically, this study sought to identify engineering modifications to improve the dam design and measure the local scour depth downstream of the proposed structure.

1.3 Approach

ERDC-CHL designed and built a movable bed section model at a 1:50 Froude scale. The model used the prototype's estimated critical shear stress (Shield's Scaling) to scale the model material for initiation of motion. Boundary conditions that allowed simulation of the regressive erosion in this model setup included a constant input hydrograph (i.e., constant peak flow) and a tailgate to regulate the invert elevation simulating the regressive erosion. An arrangement of three video recording cameras captured the model changes during tests. Finally, testing results combined with the expertise of the project delivery team (PDT) informed potential design changes to the permeable dam for each subsequent test.

2 Methodology

2.1 Design and Construction of the Sectional Model Flume Model

The permeable dam physical section model was a Froude-scaled 1:50 undistorted movable bed model (Figure 4). This model represented only 38.4% of the bridge prototype's total length (i.e., 45.7 m out of 119 m), reducing to a 2D analysis. The scale provides a fully turbulent flow with no surface tension influences for the selected flows. Table 1 includes the model scale conversions.

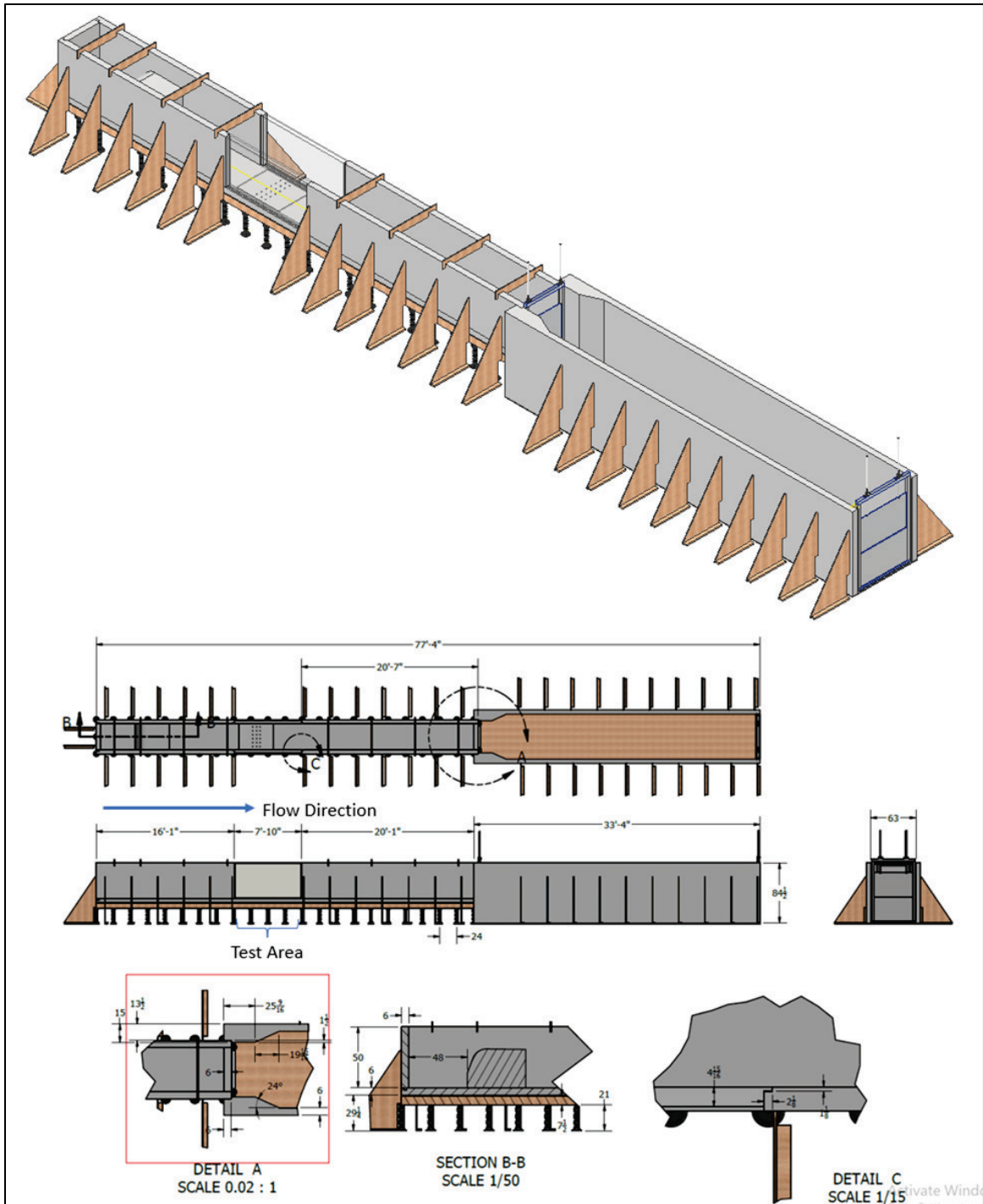
Table 1. Physical model scale conversions.

Variable	Froude Similitude Scale
Length	$L_r = 50$
Velocity	$L_r^{0.5} = 7.071$
Time	$L_r^{0.5} = 7.071$
Discharge	$L_r^{2.5} = 17,677$
Volume	$L_r^3 = 125,000$
Weight	$L_r^3 = 125,000$
Shear	$L_r = 50$

The construction method employed for the section model flume was the Waterways Lightweight Modeling System. The flume consists of a 2.3 m long head bay, 2.4 m test-section observation window (test section), 6.2 m of tailrace bathymetry, a sediment trap, and a catch basin. The flume was raised off the floor to house a bed invert gate. The bed invert gate controlled the rate of the regressive erosion and divided the tailrace bathymetry from the downstream sediment trap. At the end of the sediment trap, there is a tailwater control gate that facilitates the flooding of the model.

The initial permeable dam configuration for this model study is the original design. It consists of a bridge structure with an additional upstream set of piles and a tetrapod mat. The model bridge piers and upstream piles are acrylic, and the tetrapods are 3D printed.

Figure 4. The 3D and orthographic projections of the section model-design configuration.



2.2 Bed Material Scaling

The model intends to replicate the permeable dam design's local and regional scour potential and the impacts of the modifications. As scour is the primary driver, the initiation of motion is how the bed material is scaled (Shield's Scaling). The prototype material is a lacustrine deposit with an alluvial layer on top. Rocks with $D_{50} = 0.48$ m composed a superficial alluvial layer (approximately 5 m in thickness). For the model, the alluvial layer is geometrically scaled with 10 mm wash rock. The lacustrine layer underneath the alluvial layer is composed mainly of silt and clay, which are very susceptible to hydraulic erosion. The critical shear stress for this in situ material is 21 Pa (as validated in CELEC CERC's numerical modeling effort). Thus, applying the scaling relationship of L_r , the model's required critical shear stress is 0.42 Pa. At this shear stress, the size material needed is very coarse sand (less than 1 mm). The material used for the testing was US Silica NJ-1 (US Silica Company, Katy, Texas, USA) (Figure 5). The NJ-1 sand is a uniformly graded coarse sand with a D_{50} of 1.32 mm (Table 2) and a critical shear of 0.6 Pa. Particle settling was not scaled, and a time comparison between the model and prototype is impossible. In later tests, a top alluvial layer simulated with a washed pea-gravel material was added to the model, representing boulders up to 1 m in diameter on top of the lacustrine.

Figure 5. Percent passing curve for model materials.

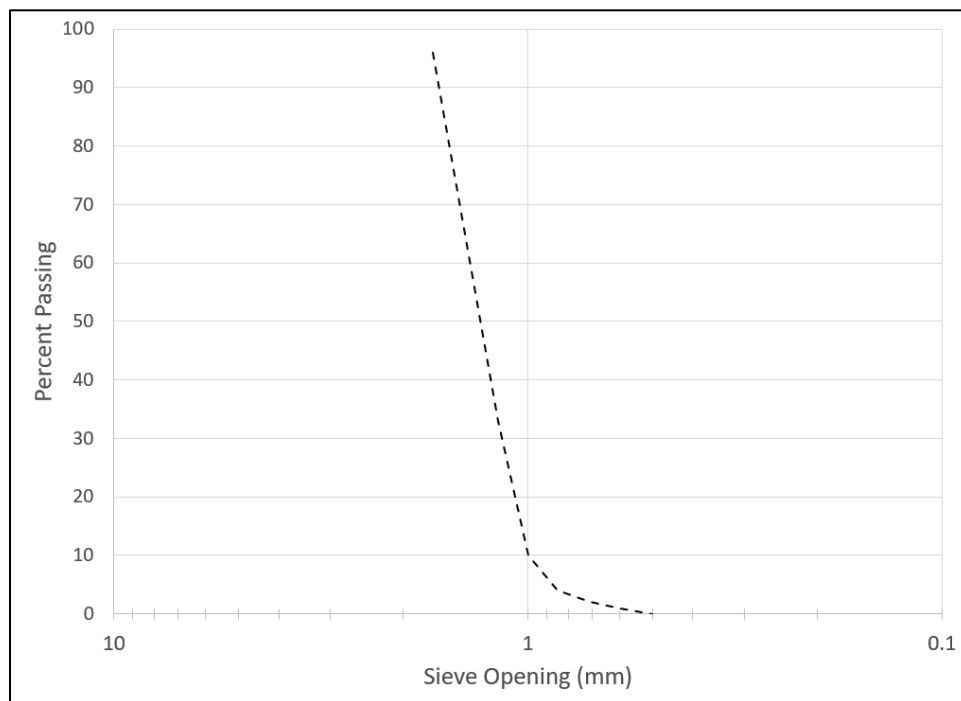


Table 2. Percent passing curve data for model bed material.

Percent Passing		
Opening (mm)	US Standard Sieve Size	NJ-1 (%)
1.70	12	96
1.18	16	33
1.00	18	10
0.85	20	4
0.71	25	2
0.60	30	1
0.50	35	0

2.3 Boundary Conditions and Flume Model Operation

The design event is the 20% annual exceedance probability (AEP, or 5 yr annual recurrence interval) event. In the model, the flow for the event is gradually increased from zero to full flow over 10 min to limit bed disturbance. Note that the model is a section model and represents only a portion of the total width of the prototype. Thus, the unit discharge is adjusted based on the model width. Here, the necessary adjustment is a flow reduction of 77.5% of the total flow for the section model.

Additionally, the entrance and exit slopes are 1.0% resulting in a Froude number near 1 or a critical flow condition. With a critical flow condition, there is no tailwater control for the downstream boundary, and the channel friction controls the water depth. During test initiation, the tailgate is raised to flood the model. Once the flow was near the peak, controlled via a 12 in. gate valve, the tailgate was lowered below the downstream channel invert, allowing for channel control through the bed invert gate and its progression (Figure 63 to Figure 66). The bed-invert tailgate was lowered continuously via a stepper motor for tests 1 to 4 and then manually for tests 5 and 6. For the manual lowering, the bed-invert gate was lowered in steps. Test times were 2 to 5.5 hr in length.

2.4 Permeable Dam Model Design and Construction

The permeable dam structure design proposed by CELEC CERC consisted of a bridge, an upstream set of piles, and a downstream dike formed by tetrapods with a riprap base (Figure 6). The tetrapod size is 2.4 m (7.9 ft). Two layers of concrete tetrapods resting over riprap provide the proposed

riverbed protection downstream of the bridge (Figure 7). Steel cables keep the tetrapods in place by tethering them to the bridge. More tetrapods placed in an interlocked pattern would protect the bridge footings. The 119 m long (390.4 ft) bridge had columns 1.25 m (4.1 ft) in diameter, spaced 7 m (22.9 ft) center-to-center, with a deck 10 m (32.8 ft) wide and 1.05 m (3.4 ft) deep. Three rows of transverse support members (0.6 m or 2.0 ft diameter) spaced at 4.5 m (17.1 ft) provided structural support to the columns. The bridge column's length was more than 30 m (98.4 ft). Piles upstream of the bridge were also 1.25 m (4.1 ft) in diameter but 20 m (65.6 ft) in length and located 5.75 m (18.9 ft) upstream of the bridge piers. Longitudinal support members (1.25 m diameter) were attached to each row of piers and upstream piles for tethering of tetrapods. The riprap subbase consisted of well-graded rock with sizes ranging from 0.3 to 1.0 m (1.0 to 3.2 ft). Appendix includes the design drawings for the complete structure, as provided by CELEC CERC.

ERDC-CHL designed and built a scaled model of the permeable dam design for this study based on prototype designs (Figure 8). The permeable dam components are the bridge deck, piles, riprap stones, and tetrapods. Structural aspects of the bridge deck and piles were simplified and fabricated from acrylic. The bridge components are attached to the flume walls and bottom with bolts and glue. The scope of this study did not consider the dam's structural stability.

The tetrapods were 3D printed with acrylonitrile butadiene styrene (ABS) plastic (Figure 9). Four brass rods were inserted into 3D printed holes for the tetrapods to meet weight requirements—the weight is 31,000 lb. (14,061 kg). The model's mass moment of inertia on the x -axis (I_{xx}), y -axis (I_{yy}), and z -axis (I_{zz}) were within sub-5% of the prototype (Table 3).

The model replicated the tetrapod arrangement as presented in the original design drawings (Figure 6 and Figure 7). Downstream of the bridge, two stacked layers of tetrapods were arranged in a noninterlocked pattern without tethering, resulting in 50% of voids. Two layers of interlocked tetrapods were placed underneath the bridge, resulting in 25% of voids. Another row of tetrapods was placed against the bridge between the upstream set of piles and the bridge. All voids were filled with edged, angular rock with sizes no larger than 1.98 cm (0.78 in. model; 1 m prototype).

Figure 6. Cross-sectional view of the permeable dam design (CELEC, with permission).

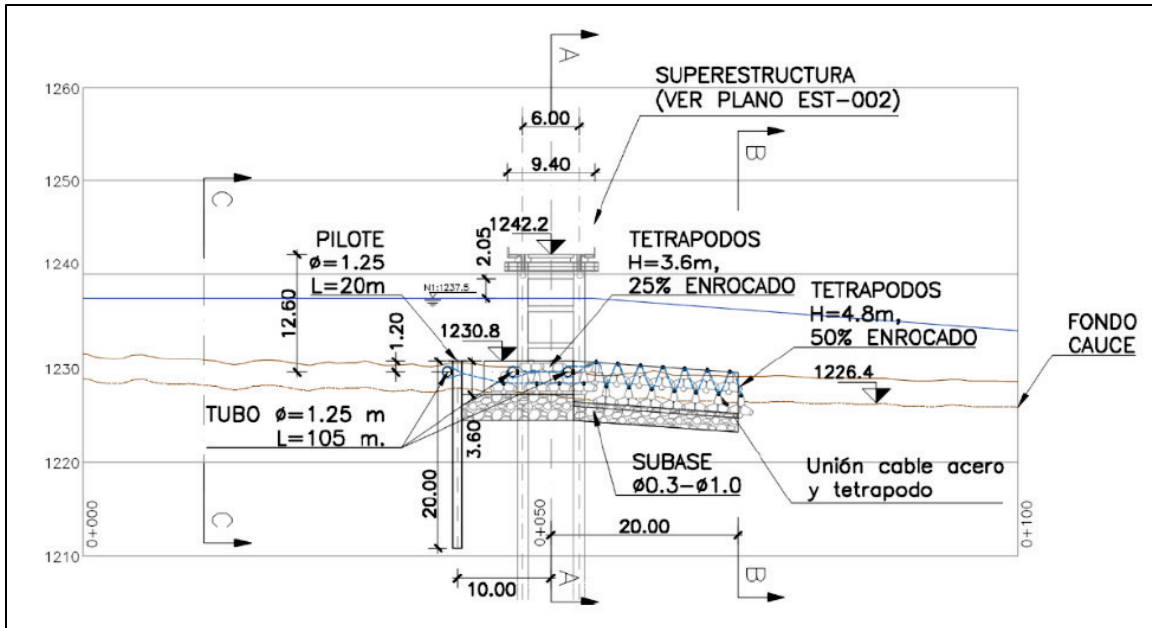


Figure 7. Plan view of the permeable dam with the arrangement of tetrapods (CELEC, with permission).

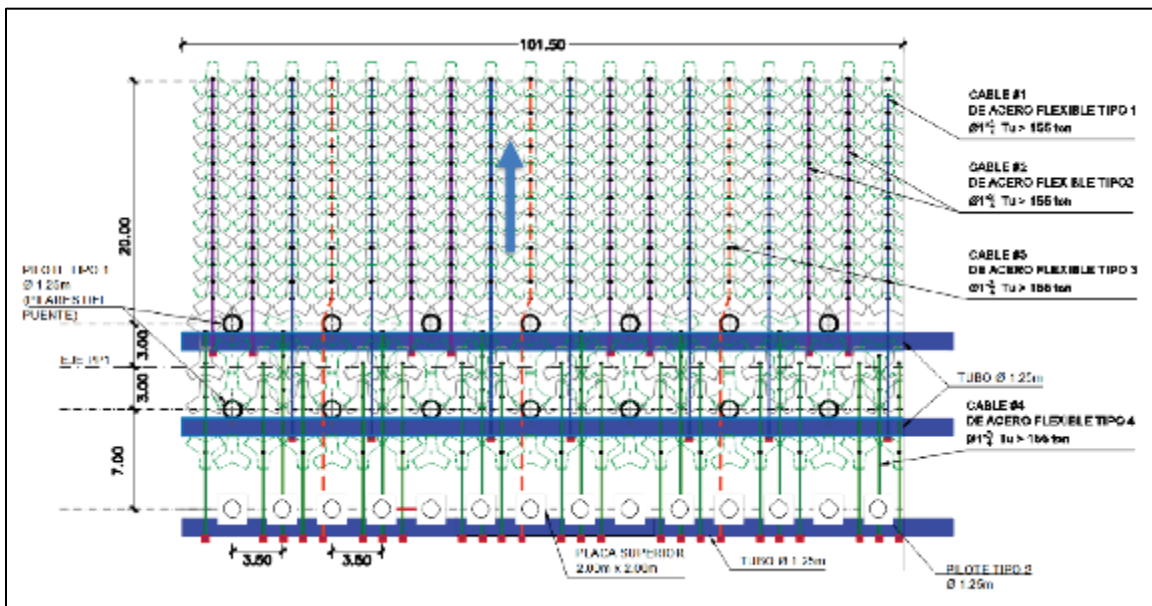


Figure 8. Permeable dam physical model.

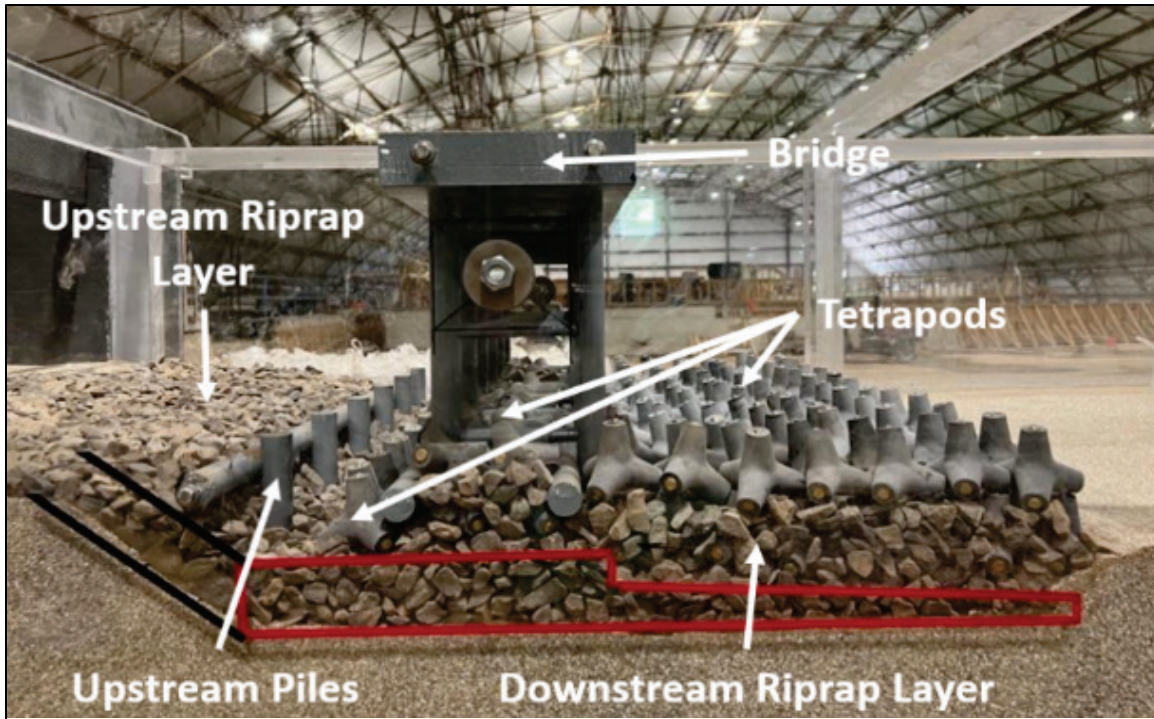
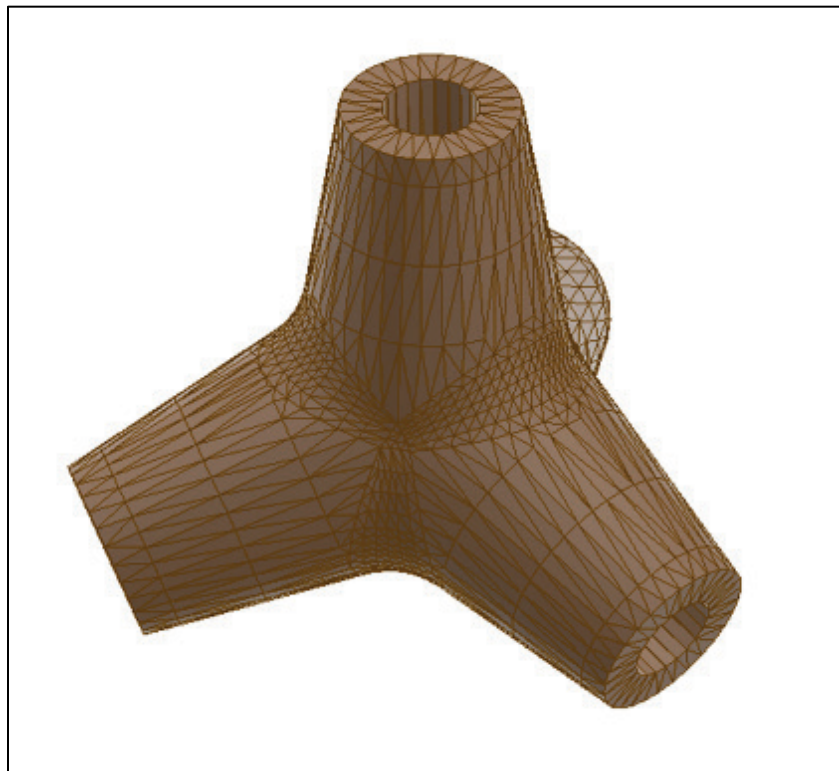


Figure 9. Representation of a tetrapod unit.



Multiple riprap layers were positioned in the model (Figure 8) as follows:

- a 2.54 cm thick (1 in. model) riprap layer downstream of the bridge
- a 5.08 cm thick (2 in. model) riprap layer running from under the bridge up to the upstream set of piles
- another 2.54 cm thick (1 in. model) riprap layer starting at the upstream set of piles and covering a portion of the upstream bed

As this physical model study progressed, six alternate versions of the proposed prototype design were tested. Results from each test informed the next design change to improve the permeable dam performance. The following subsections describe the resulting six model alternatives.

Table 3. Comparison of the tetrapod unit model and prototype physical properties.

Physical Properties	Prototype	Model	Model to Prototype	Model-Prototype	Error
lxx	36748089	0.123	38437500	1689411	4.6%
lyy	36750504	0.123	38437500	1686996	4.6%
lzz	36749127	0.123	38437500	1688373	4.6%
P-Mass	31,564	0.266	na	na	na
Density	2.407	Varies	na	na	na

2.4.1 Model Alternative 1: Untethered Tetrapods

The first model alternative represented the original permeable dam design described previously (Figure 10 to Figure 12). This alternative, however, excluded tethering the tetrapods for the following two reasons:

1. A hanging mesh-like structure does not protect or provide a stable invert elevation to hold channel grade. Hence, an unstable channel grade results in a lack of grade control, and the regressive erosion will migrate upstream through the structure.
2. Tetrapods are not designed to move or rotate. Movement can result in breaking of the arms of the tetrapod. The designed physical section model cannot simulate the tetrapods breaking. Because tetrapods break with movement, they will not have the same weight distribution across the mesh and channel. Thus, only the tethered section of the tetrapod would remain attached while the broken arms would wash downstream.

Figure 10. Top view of model alternative 1.



Figure 11. Front view of model alternative 1.



Figure 12. Rear view of model alternative 1.



2.4.2 Model Alternative 2: Interlocked, Untethered Tetrapods

The second version of the permeable dam design considered two significant changes: (1) untethered tetrapods with the interlocked arrangement and (2) the addition of geological layers on the prototype site. Model alternative 2 retained the tetrapods as the primary armoring units but experimented with an interlocking configuration that prevented the exposure of the tetrapod arms. This interlocking method would not follow any specific geometrical pattern but would fill all gaps between tetrapods.

Two significant geological layers are at the site (Figure 13). First, an alluvial material with a nominal diameter size (D_{50}) of 0.48 m (prototype) composed the top layer or the riverbed (*yellow layer*). The second layer rests underneath the alluvial material but is upstream of the piles (*brown layer*). This layer resulted from a debris flow of noncohesive material caused by the 1987 earthquake in that area. The particle D_{50} in the layer ranged from 0.870 m at the thinnest part to 5 m at the thickest part farther upstream in the river.

Alternative model 2 represented the additional prototype details and design changes in the following manner (Figure 14 to Figure 17). The downstream bed protection had a rectangular cross-sectional shape and consisted of three to four layers of interlocked tetrapods resting on a 2.54 cm thick (model) riprap bed. Riprap stone size ranged from 0.3 to 1 m (prototype),

with the exact placement as in alternative model 1. The debris flow layer consisted of angular material with diameters up to 5 m (prototype). Layer thickness went from 2 m (prototype) at the upstream piles, then tapered up to 7 m (prototype) going upstream. A 5 m (prototype) layer of rounded pea gravel with diameters close to 0.5 m (prototype) represented the alluvial layer. Upstream, this layer covered the debris flow layer until reaching the set of piles. On the downstream side, this layer covered the sand starting at the toe of the riprap and tetrapod mantle.

Figure 13. Geological profile of Coca River with the configuration proposed for model alternative 2 (CELEC, with permission).

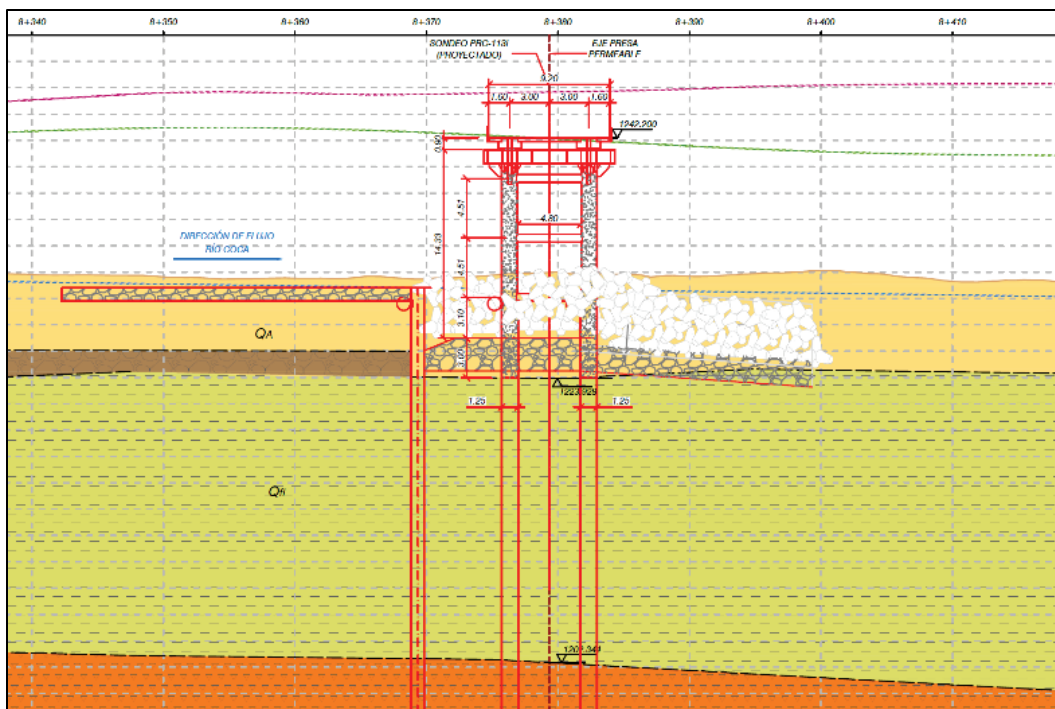


Figure 14. Side view of model alternative 2.

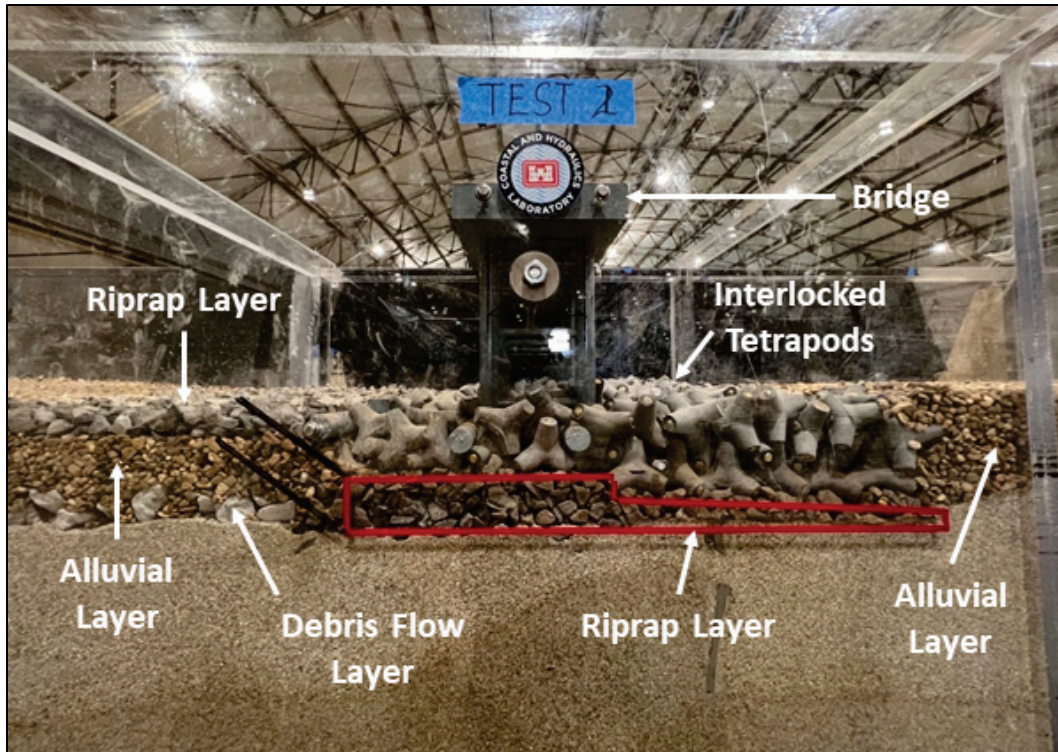


Figure 15. Front view of model alternative 2.



Figure 16. Top view of model alternative 2.

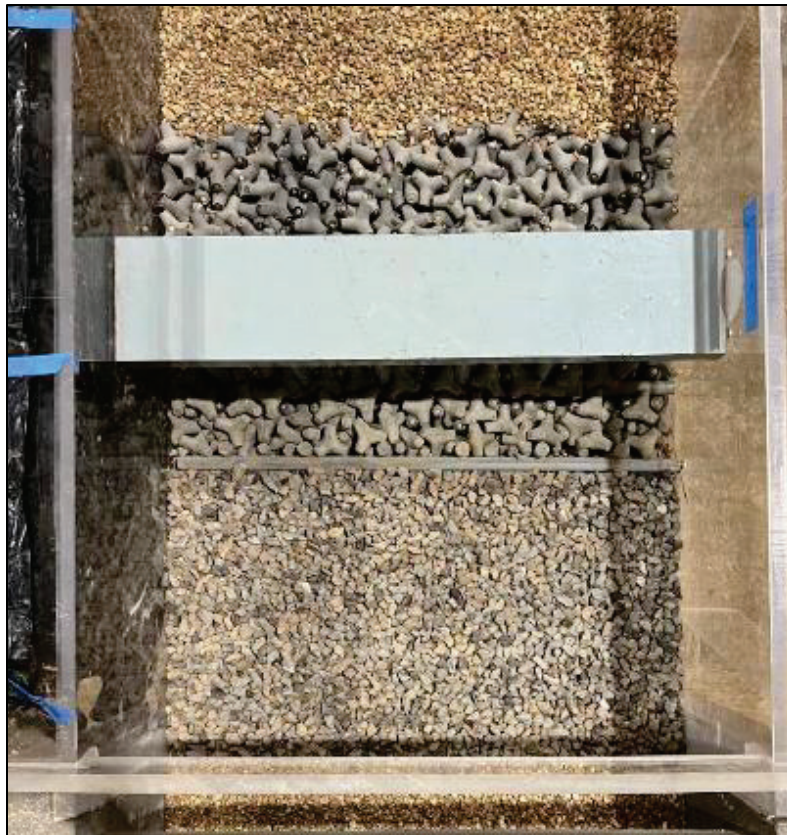


Figure 17. Rear view of model alternative 2.



2.4.3 Model Alternative 3: Tetrapods Replaced with Stone Structure

The third design change replaced the tetrapods and riprap with a stone structure (Figure 18). This structure had an irregular shape extending 20.31 m upstream and 23.31 m downstream of the bridge's center line. It had a solid core between bridge columns formed with stones of size 2.7 m (prototype) while having 2 m (prototype) size stones elsewhere. The upstream piles, the bridge, and the geological layers remained unchanged.

Alternative model 3 represented the prototype design changes by using 5.08 cm (2 in. model) edged gravel for the solid core and a mixture of 3.175 cm and 3.81 cm (1.25 in. and 1.5 in., respectively, model) round stone elsewhere (Figure 19 to Figure 21). The placement of the geological layers followed the setup of alternative model 2. From this point forward, the study did not consider the use of tetrapods but variations of the stone structure, for the reasons discussed in Section 4.1.

Figure 18. Geological profile of Coca River with the configuration proposed for model alternative 3 (CELEC, with permission).

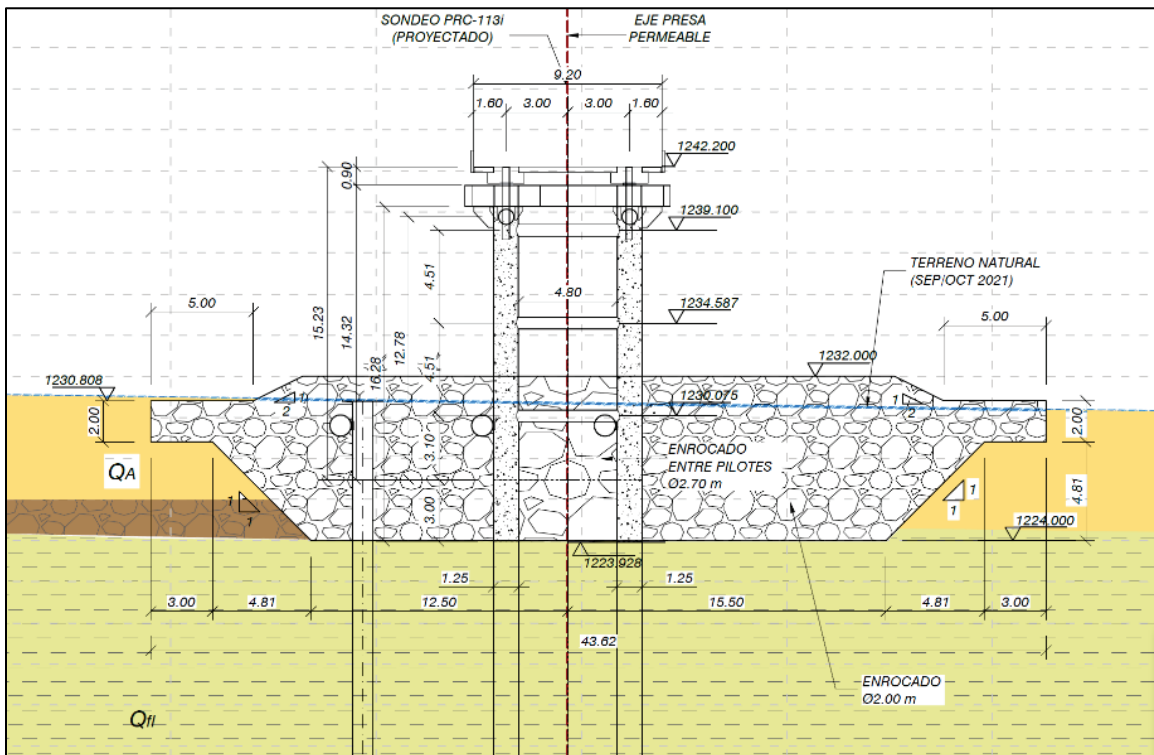


Figure 19. Side view of the model alternative 3.

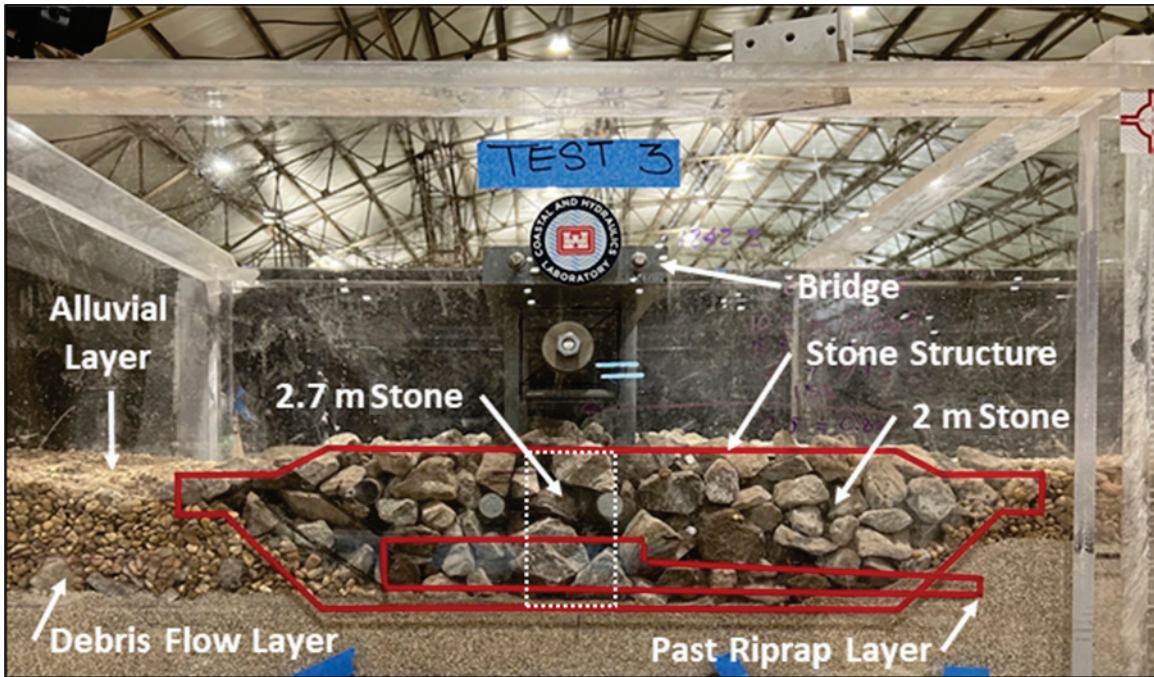
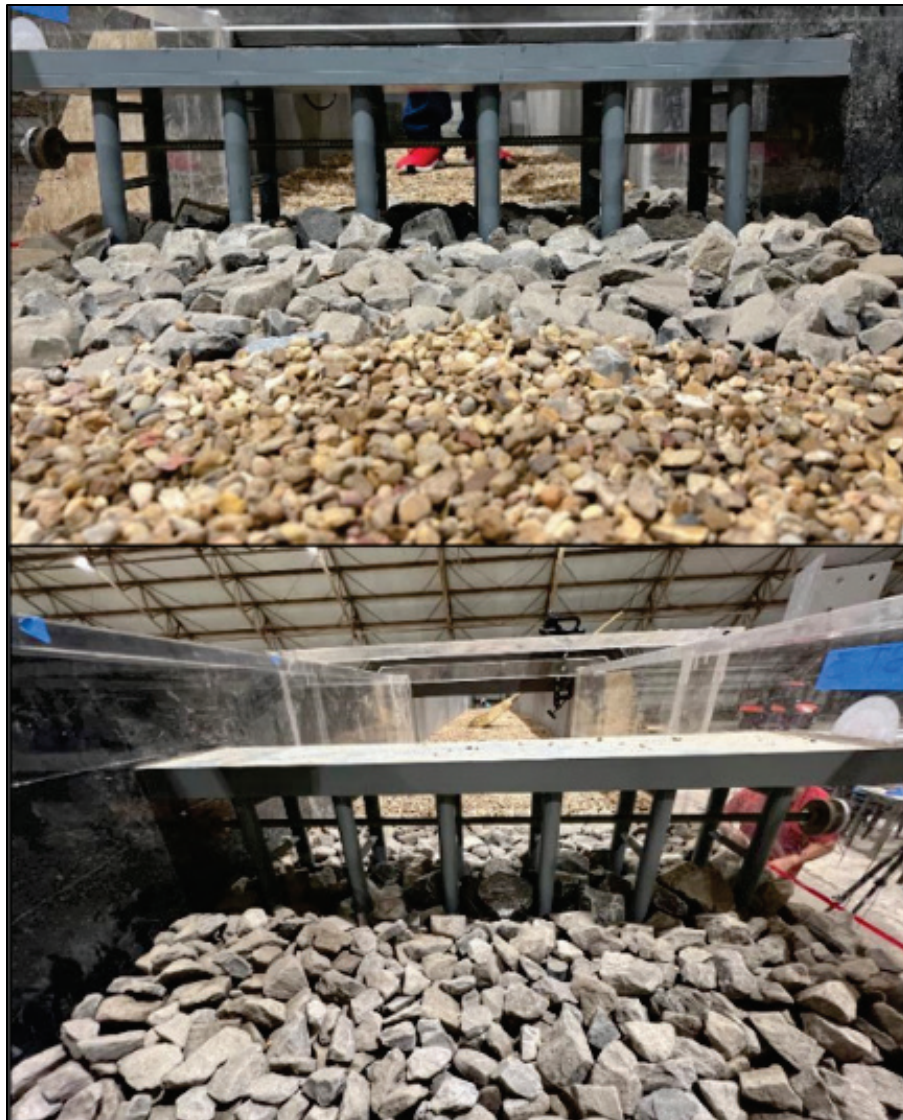


Figure 20. Top view of model alternative 3.



Figure 21. Front (*top*) and rear (*bottom*) views of model alternative 3.



2.4.4 Model Alternative 4: Structural Changes

The fourth design change retained the stone structure of alternative 3 with a few modifications (Figure 22). Changes included removing the three longitudinal piles, moving the set of piles downstream of the bridge's center line by 5.65 m (prototype), and using different granulometry for the stone structure. The structure's solid core stone size was reduced from 2.7 m to 2.5 m (prototype) while using a mixture of stone sizes with D100 of 2.09 m (prototype) elsewhere (Figure 23).

Alternative model 4 applied the structural changes to the permeable dam model as proposed (Figure 24) but kept the 5.08 cm (2 in. model) edged

gravel for the solid core (Figure 25 to Figure 28). This model, however, slightly changed the granulometry by replacing the D100 with 5.08 cm (2 in. model; 2.5 m prototype). Reasons to make this change included material availability and an expected performance reduction using 3.81 cm (1.5 in. model; approximately 2.09 m prototype) as the largest stone size. The placement of the geological layers followed the setup of alternative model 2.

Figure 22. Geological profile of Coca River with the configuration proposed for model alternative 4 (CELEC, with permission).

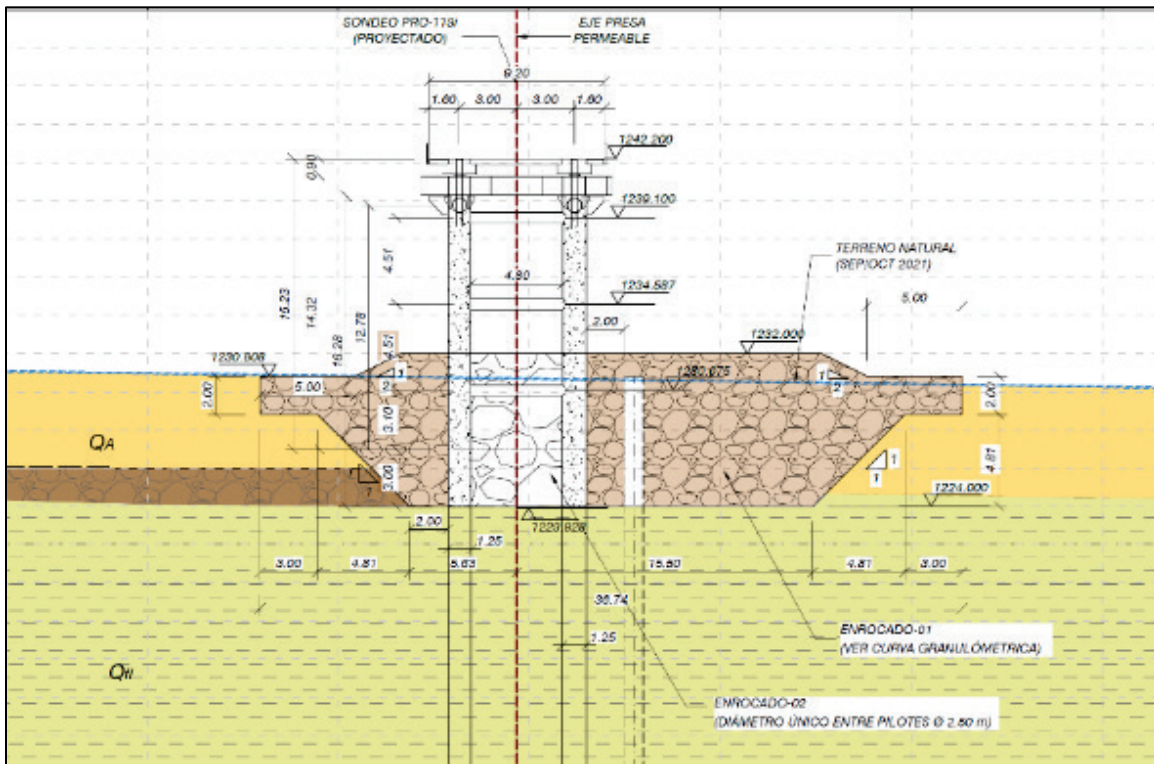


Figure 23. Gradation curves for prototype and model stone structure (prototype data provided by CELEC).

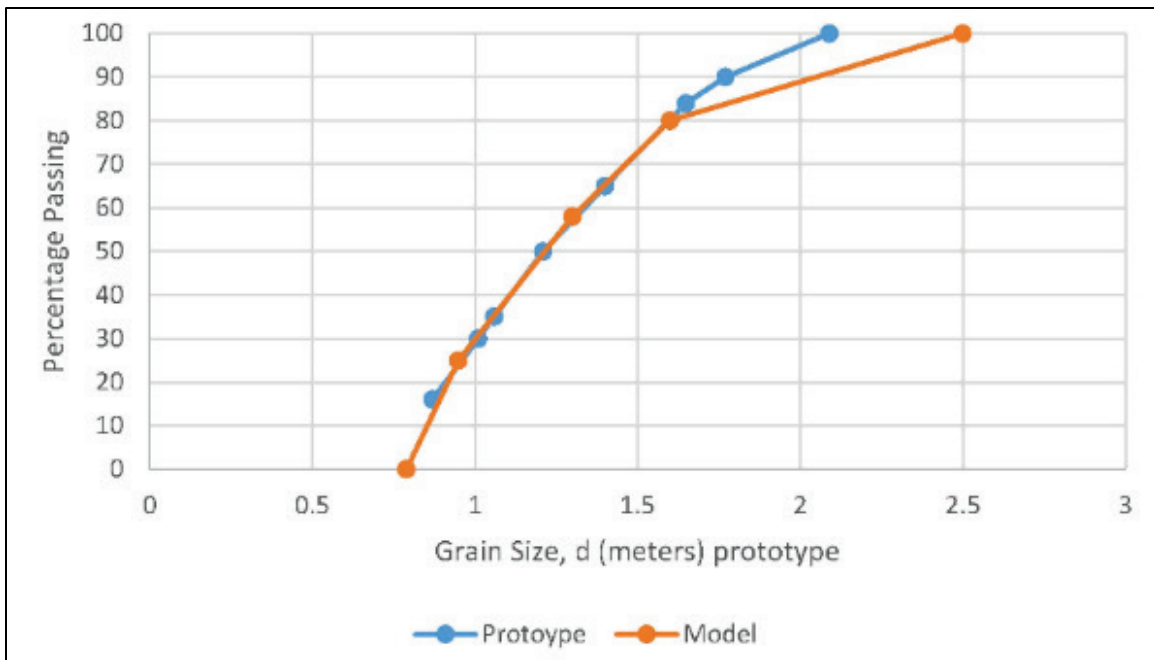


Figure 24. Placement of third row of piles downstream of bridge: front (*left*) and side (*right*) views.



Figure 25. Side view of the model alternative 4.

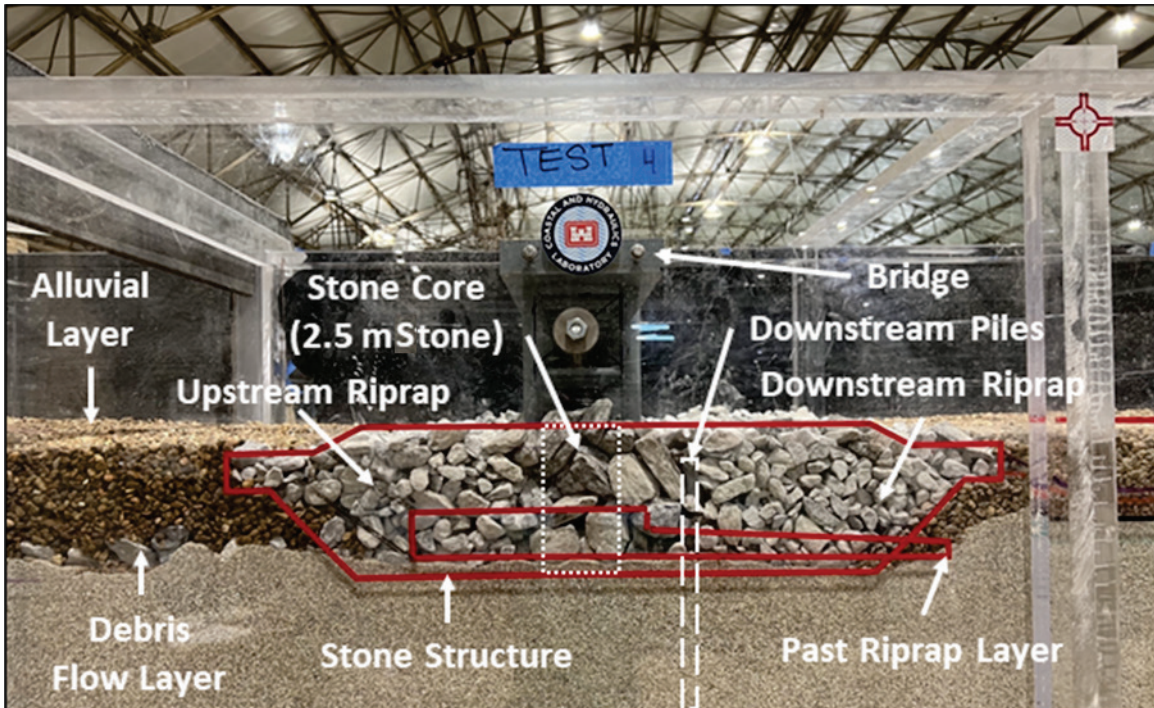


Figure 26. Top view of model alternative 4.



Figure 27. Front view of model alternative 4.



Figure 28. Rear view of model alternative 4.



2.4.5 Model Alternative 5: Changes to Stone Structure

The fifth version of the permeable dam combined the structural configuration of model alternative 4 with the stone structure of alternative 3 (Figure 29). The stone structure in model alternative 5 had a solid core of 5.08 cm (2 in. model; 2.5 m prototype) stones while 3.81 cm (1.5 in. model; 2 m prototype) size stones elsewhere (Figure 30 to Figure 33). The placement of the geological layers followed the setup of alternative model 2.

Figure 29. Geological profile of Coca River with the configuration proposed for model alternative 5 (CELEC, with permission).

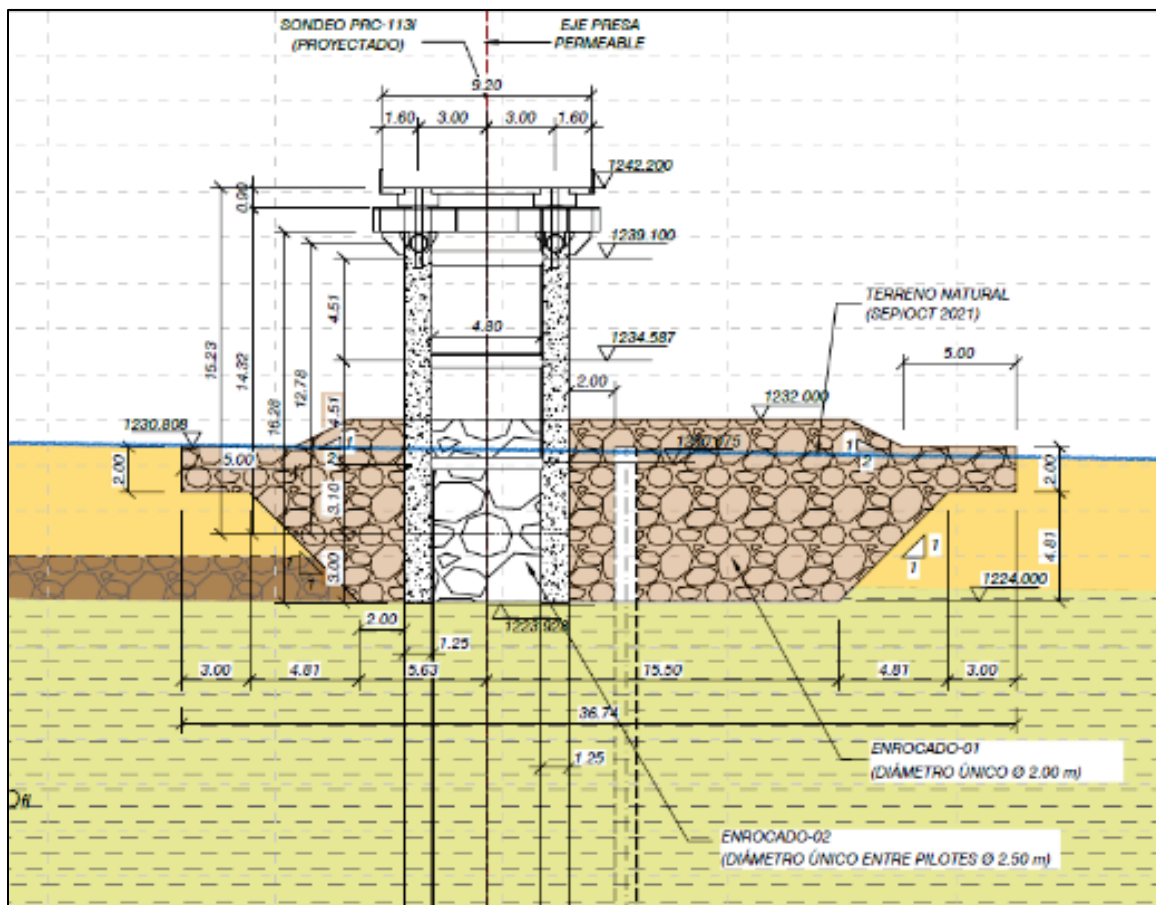


Figure 30. Side view of the model alternative 5.

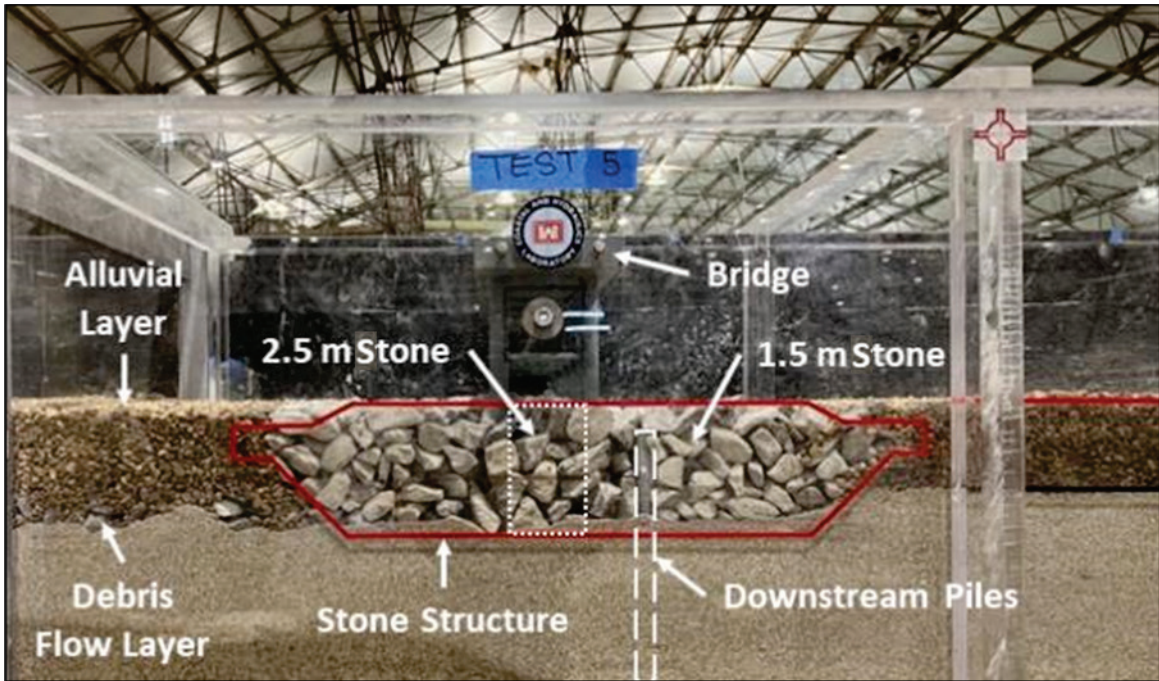


Figure 31. Top view of model alternative 5.



Figure 32. Front view of model alternative 5.



Figure 33. Rear view of model alternative 5.



2.4.6 Model Alternative 6: Additional Structural Changes

The sixth version of the permeable dam modified alternative 5 by (1) removing the downstream set of piles and (2) adding a sheet pile cut-off wall behind the downstream bridge columns. Model alternative 6 simulated the sheet piles with a piece of sheet metal that extended to the flume bottom (Figure 34 to Figure 37).

Figure 34. Side view of the model alternative 6.

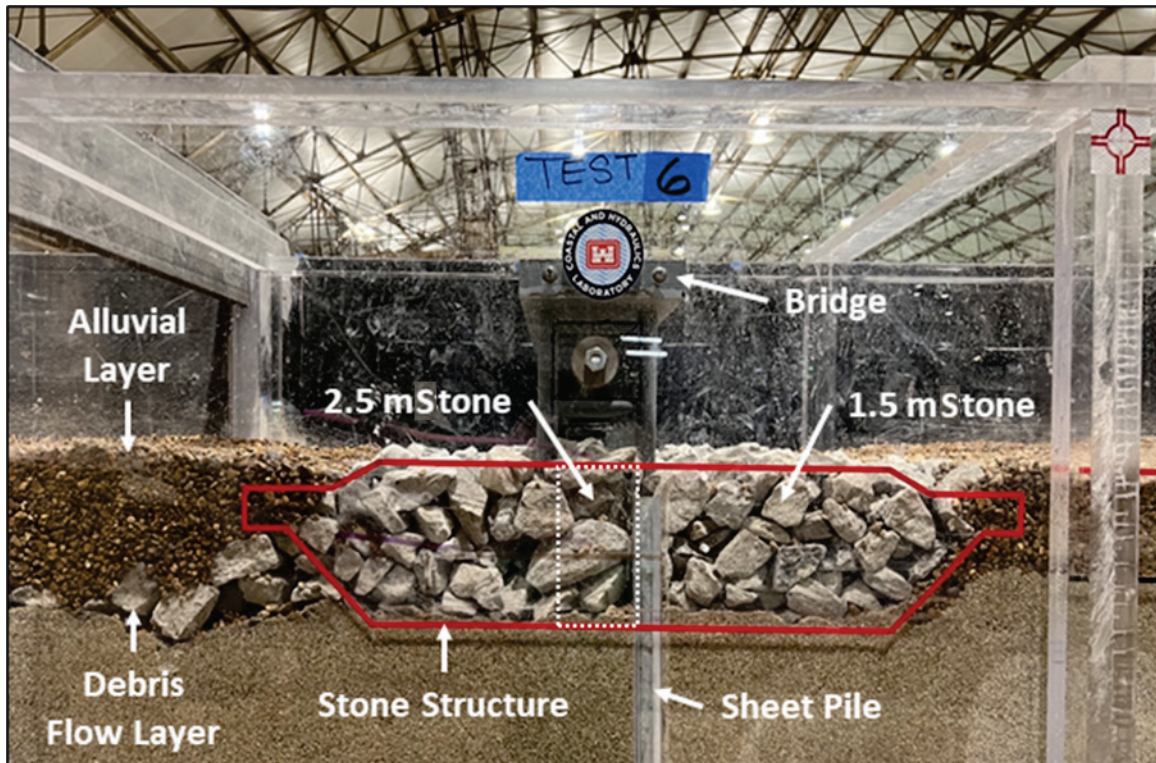


Figure 35. Top view of model alternative 6.



Figure 36. Front view of model alternative 6.



Figure 37. Rear view of model alternative 6.



2.5 Experiments and Testing Procedure

The testing process in this study consisted of seven steps for each model alternative (Table 4). First, the flume was cleaned from any mixed materials from the previous test run and debris using a loader and shovels. Gravels were sourced, then cleaned and sieved to get the required model stone sizes. The staff set up the permeable dam model alternative with the geological layers. Remolding the surface was necessary to establish the initial invert elevation and channel slope. Having all three cameras recording, a test started by slowly opening the water valve until achieving the target flow rate. An ultrasonic flowmeter from EESIFLO International (accuracy within $\pm 2\%$ of reading) measured the flow discharge. Testing duration varied from 3 to 5.5 hr depending on the proposed tailgate operation (Table 5) and observed scour or damage, or both. Photos of the model's final condition were collected for documentation, and results discussed with the PDT. Preparation for the next test started after gathering consensus on the permeable dam design changes and path forward.

Table 4. Physical model testing procedure.

Step	Description
1	Clean and fill the flume with sand, and source gravels.
2	Build the permeable dam model alternative.
3	Set the geological layers and remold surface to target elevation.
4	Set the video recording cameras and livestreaming.
5	Test the model alternative (3 to 5.5 hr) by changing the invert elevation with the tailgate.
6	Document the model's final condition.
7	PDT discuss results and potential improvements.

Table 5. Tailgate operation schedule.

Test	Total Invert Elevation Change (m)	Rate (m/hr)
1	25	12.5
2	25	10
3	25	10
4	15	3
5	15	3
6	15	3

2.6 Data Processing and Analysis

Data collected during all tests consisted of videos and photos from different angles of the permeable dam model. ERDC-CHL transferred all video files to Mobile District via DoD SAFE and RDE Drive Pub. Side-view photos were taken multiple times during testing with a 12 MP 2× optical zoom camera. Bed profiles were digitized from these photos using Autodesk AutoCAD. Additional information computed from such profiles included scour depth, the rate of change of scour depth to invert elevation, and downstream bed slope.

3 Model Testing Results

The ERDC-CHL team successfully applied the testing procedure to the six model alternatives. Each model alternative was evaluated qualitatively to determine the performance against the regressive erosion. Both the tailgate operation schedule (Table 5) and the damage progression influenced the maximum flow run time. Table 6 summarizes the experiments.

Table 6. Summary of experiments per model alternative.

Model Alternative	Structural Components	Downstream Protection	Geological Layers	Hydrograph Raise Time (min)	Max Flow Run Time (hr)
1	bridge, upstream piles	tetrapods, riprap	sand	12	1.80
2	bridge, upstream piles	interlocked tetrapods, riprap	sand, alluvial, debris flow	12	3.20
3	bridge, upstream piles	stone structure core: 2.7 m elsewhere: 2 m	sand, alluvial, debris flow	5	3.20
4	bridge, downstream piles	stone structure core: 2.5 m elsewhere: mixed	sand, alluvial, debris flow	5	5.33
5	bridge, downstream piles	stone structure core: 2.5 m elsewhere: 2 m	sand, alluvial, debris flow	5	5.45
6	bridge, sheet piles	stone structure core: 2.5 m elsewhere: 2 m	sand, alluvial, debris flow	5	5.33

Figure 38 to Figure 43 present side views of each model alternative's initial and final conditions. In addition, the digitized bed profiles for several time-steps per model alternative are Figure 44 to Figure 56. Estimated scour depths and rates per alternative are in Figure 57 to Figure 62. The scour depths were computed with respect to an initial bed elevation of 1,232 m (prototype). Scour rates represent the ratio of scour depth to invert elevation. Slopes were computed for the bed-profile portion downstream of the bridge piers (Table 7). The comparison of flow hydrographs with tailgate lowering operation are in Figure 63 to Figure 66.

Figure 38. Side views of the initial (*top*) and final (*bottom*) conditions of model alternative 1.

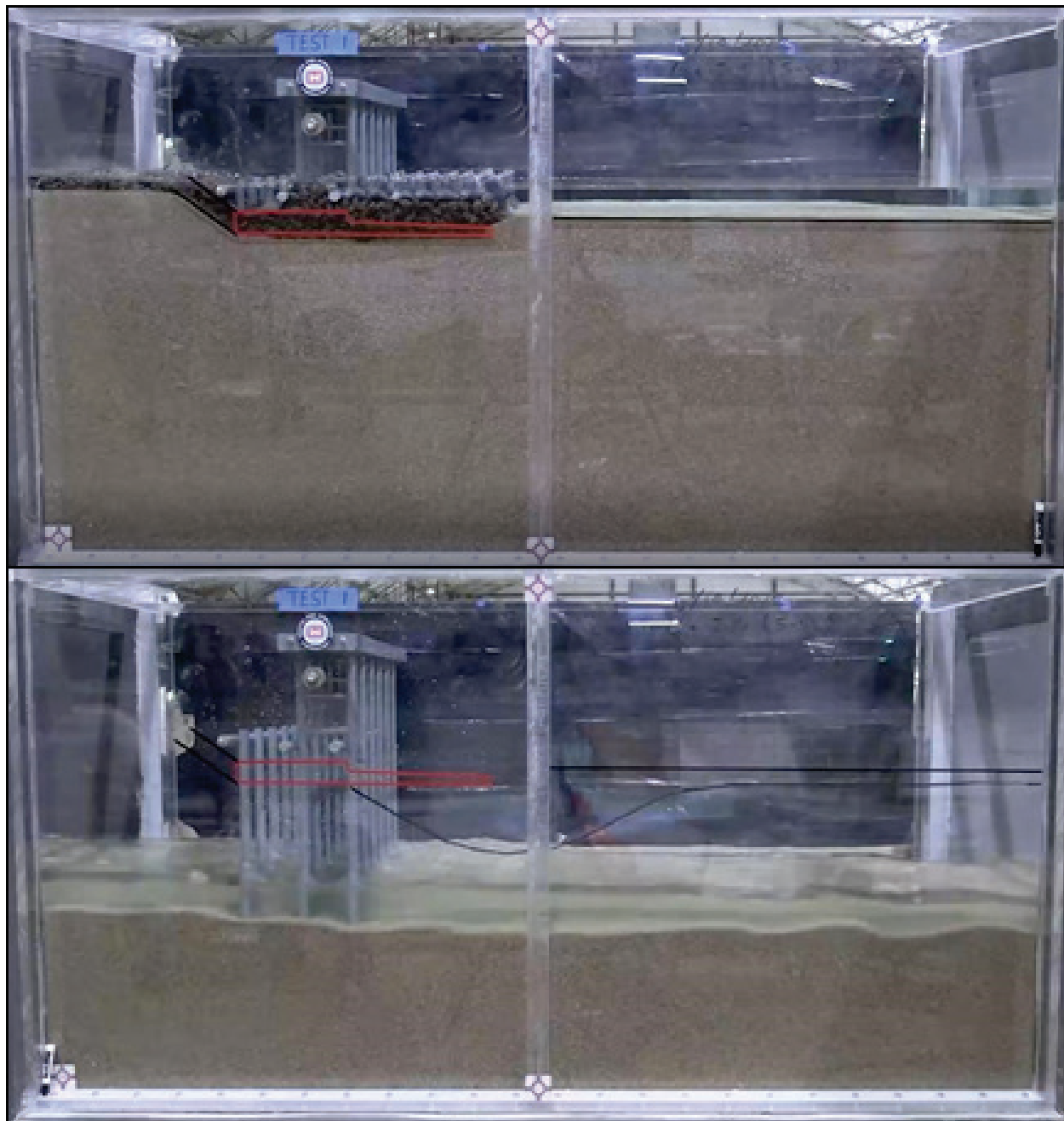


Figure 39. Side views of the initial (*top*) and final (*bottom*) conditions of model alternative 2.

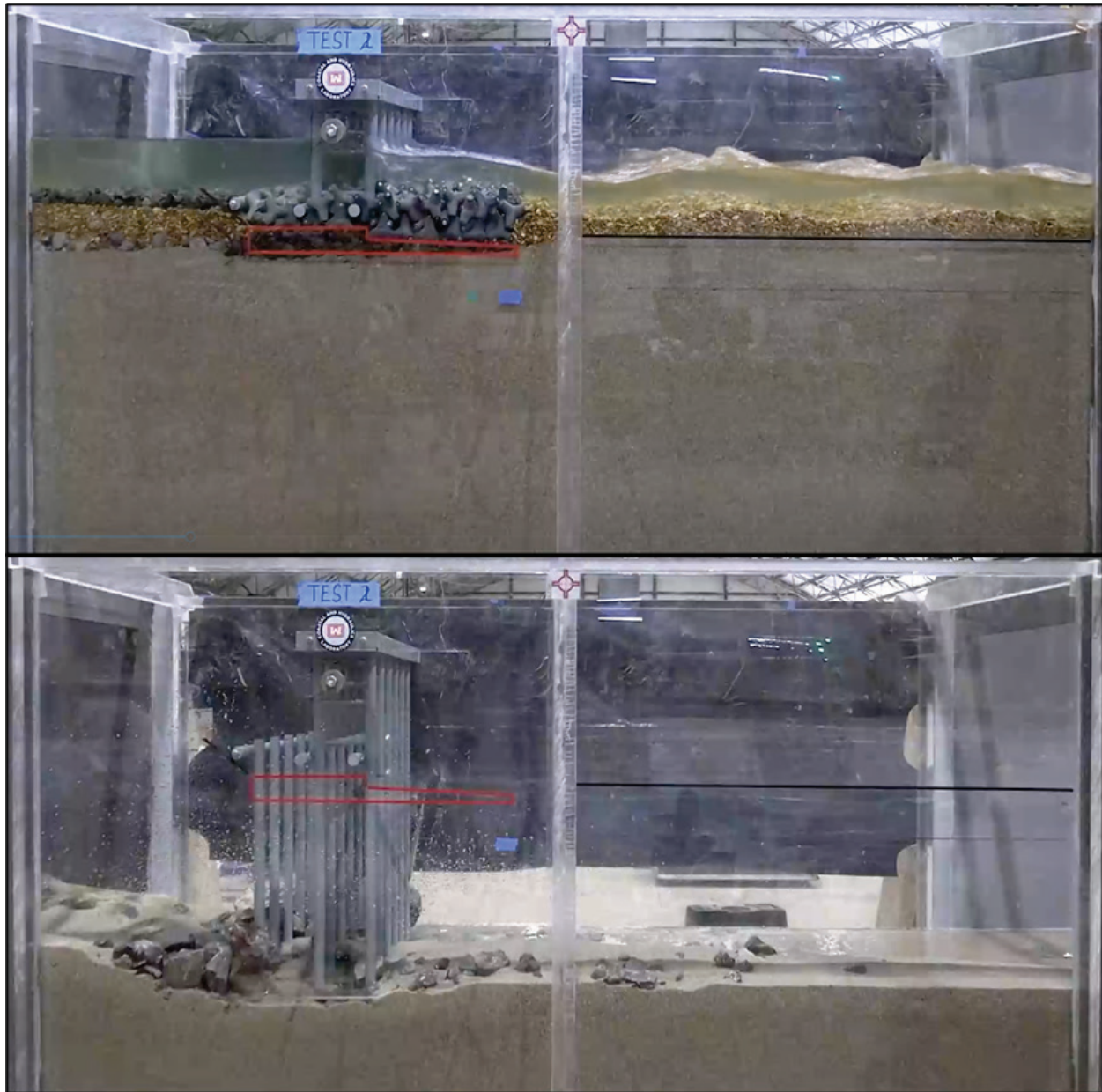


Figure 40. Side views of the initial (*top*) and final (*bottom*) conditions of model alternative 3.

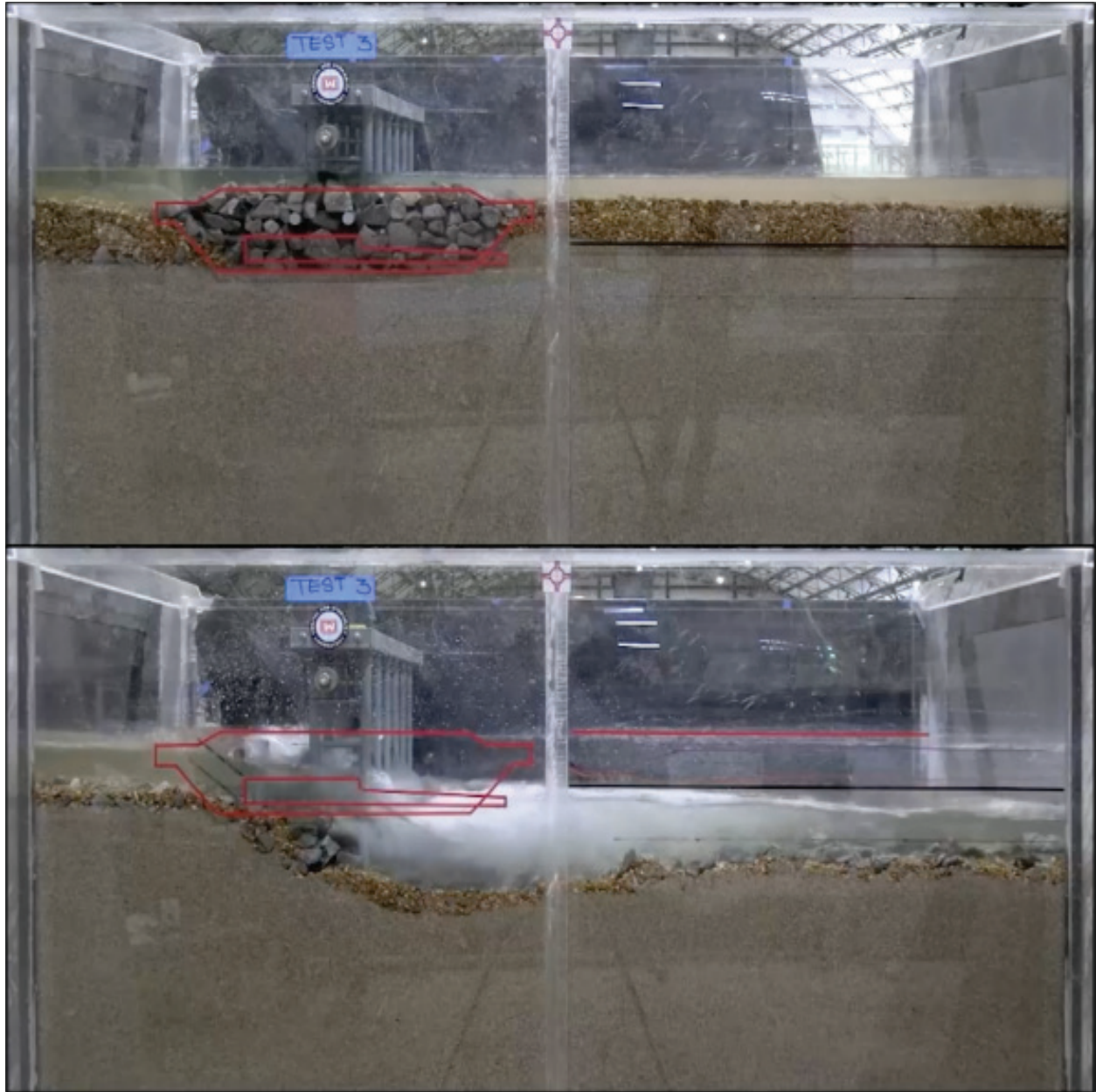


Figure 41. Side views of the initial (*top*) and final (*bottom*) conditions of model alternative 4.

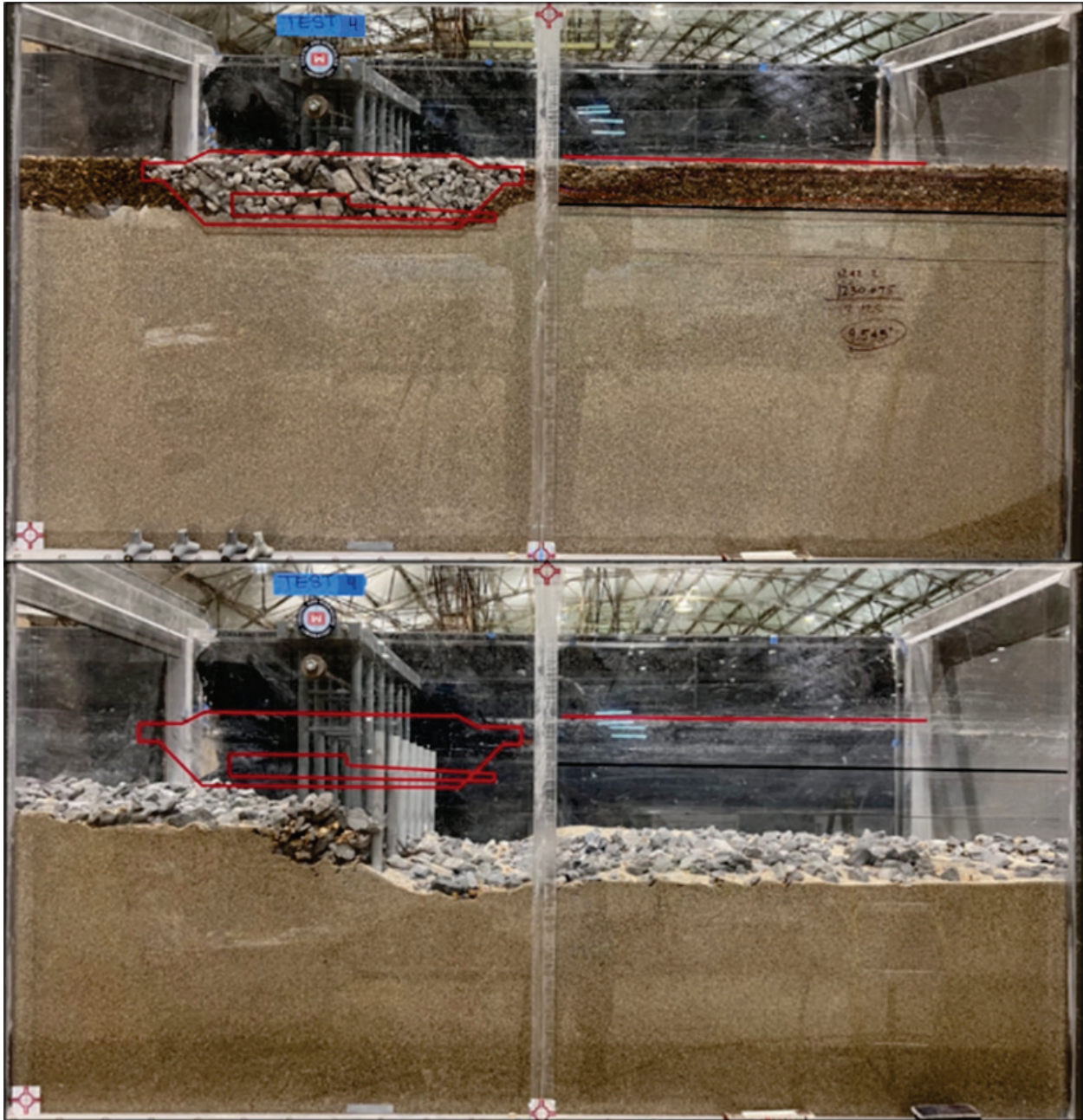


Figure 42. Side views of the initial (*top*) and final (*bottom*) conditions of model alternative 5.

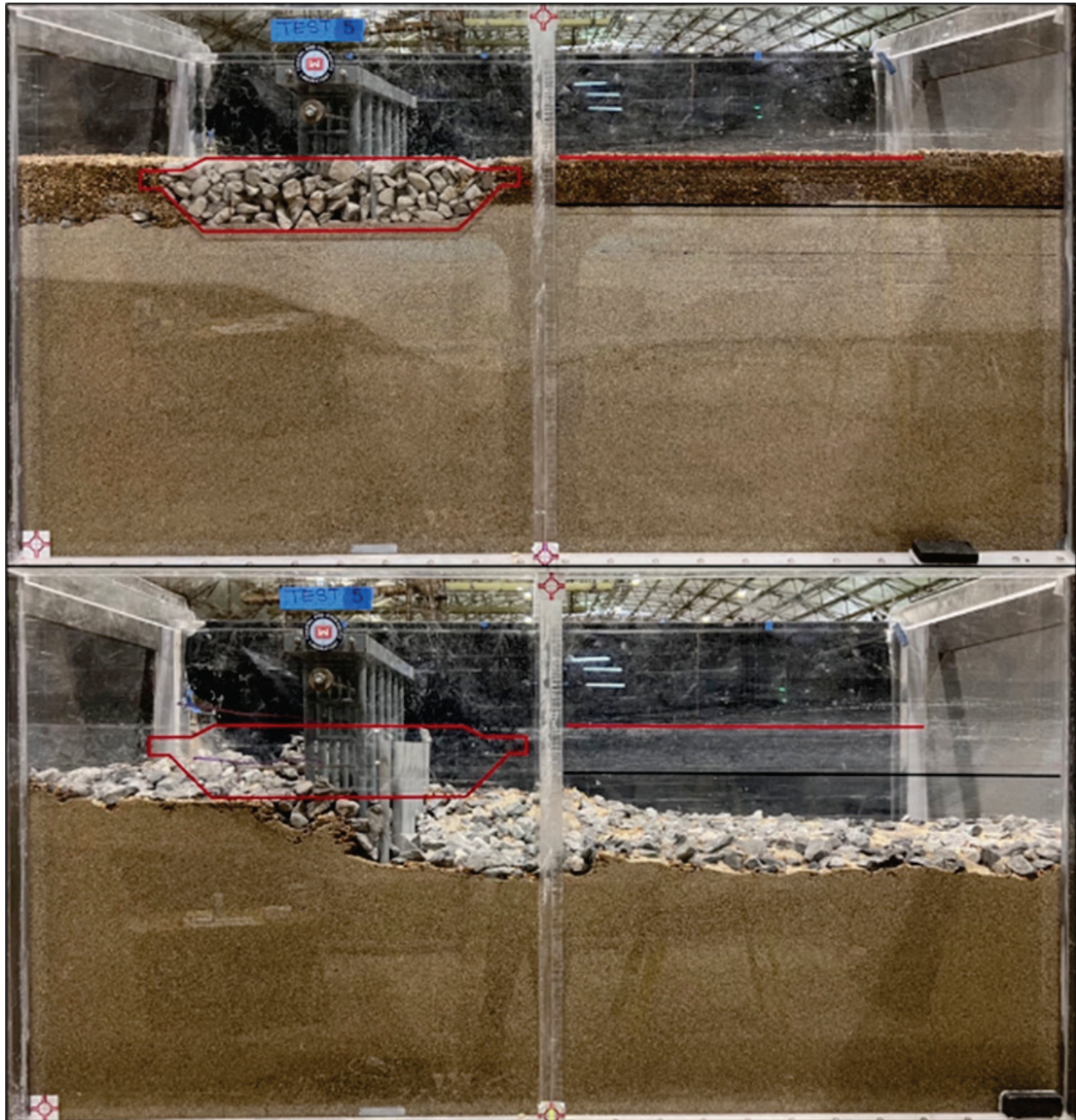


Figure 43. Side views of the initial (*top*) and final (*bottom*) conditions of model alternative 6.

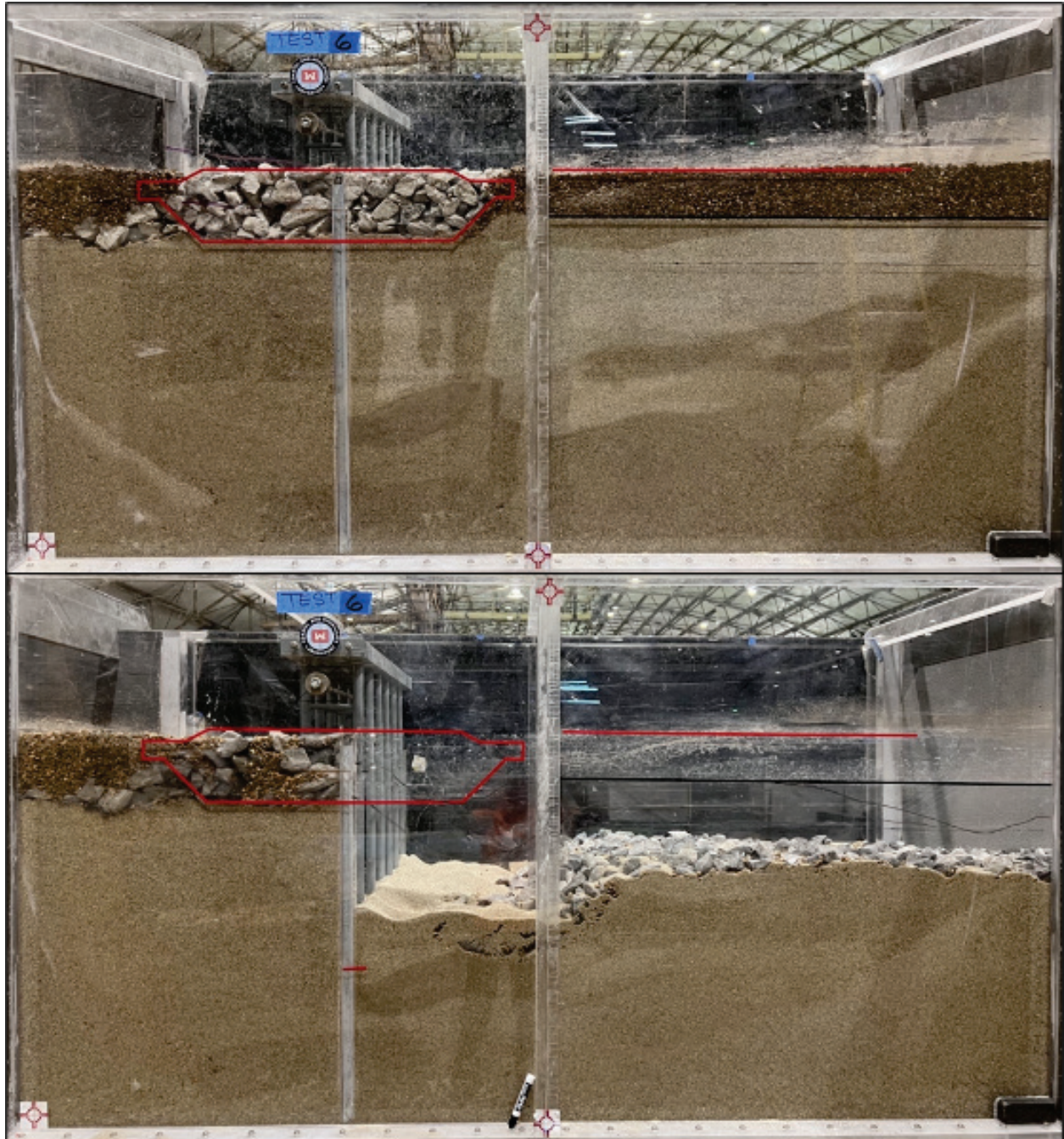


Figure 44. Scour profiles of model alternative 1.

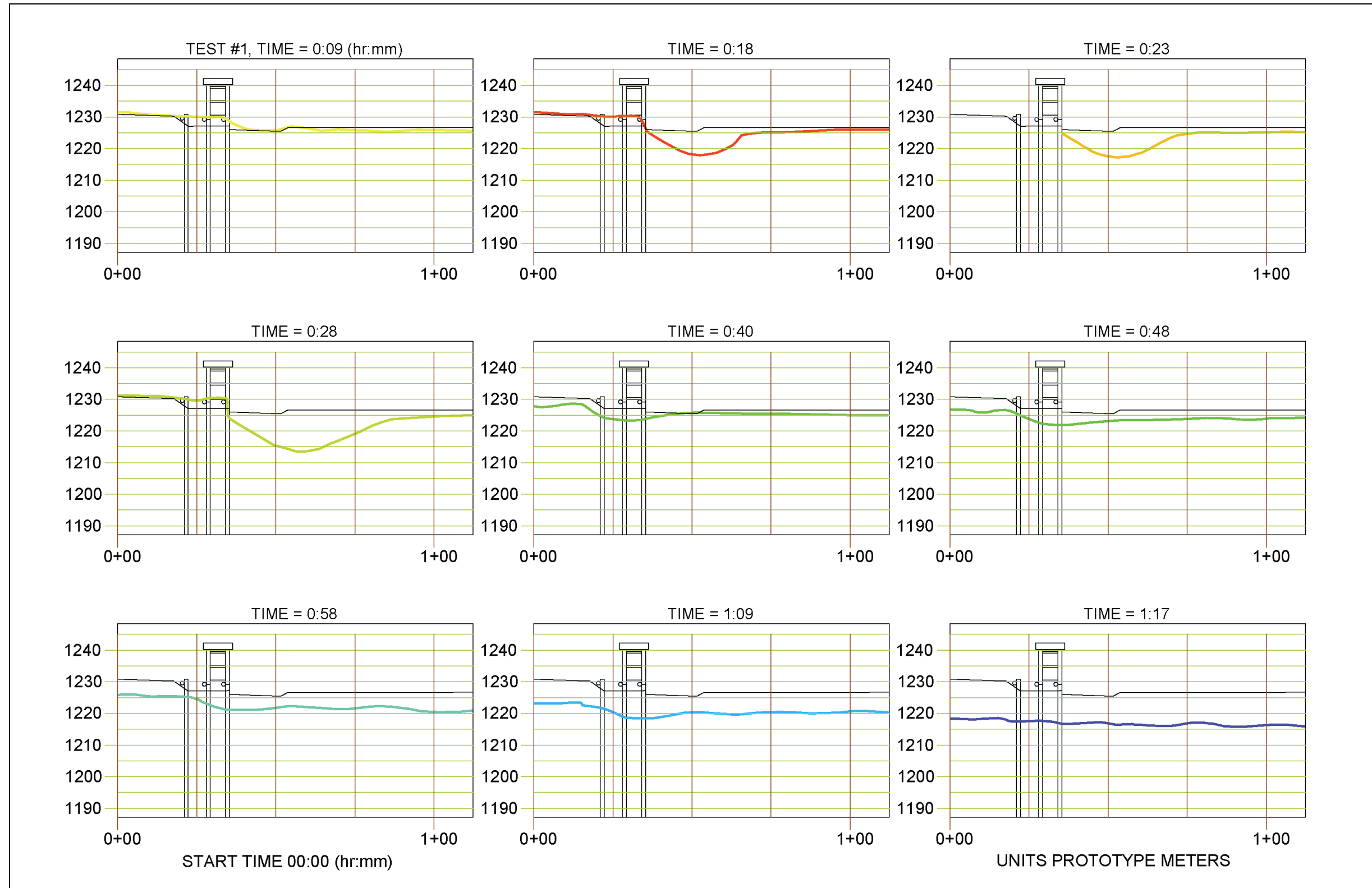


Figure 45. Scour profiles of model alternative 1 (continued).

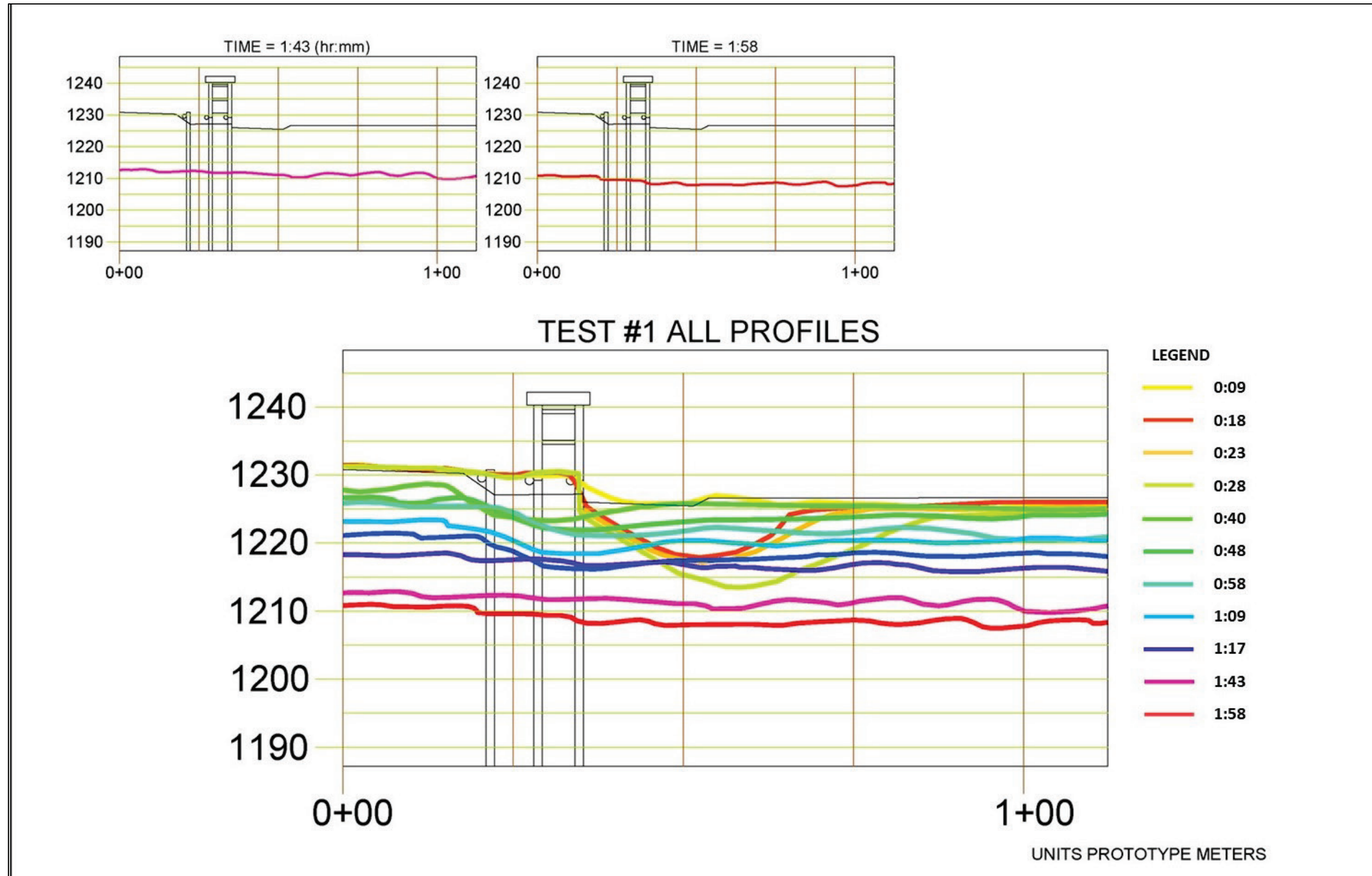


Figure 46. Scour profiles of model alternative 2.

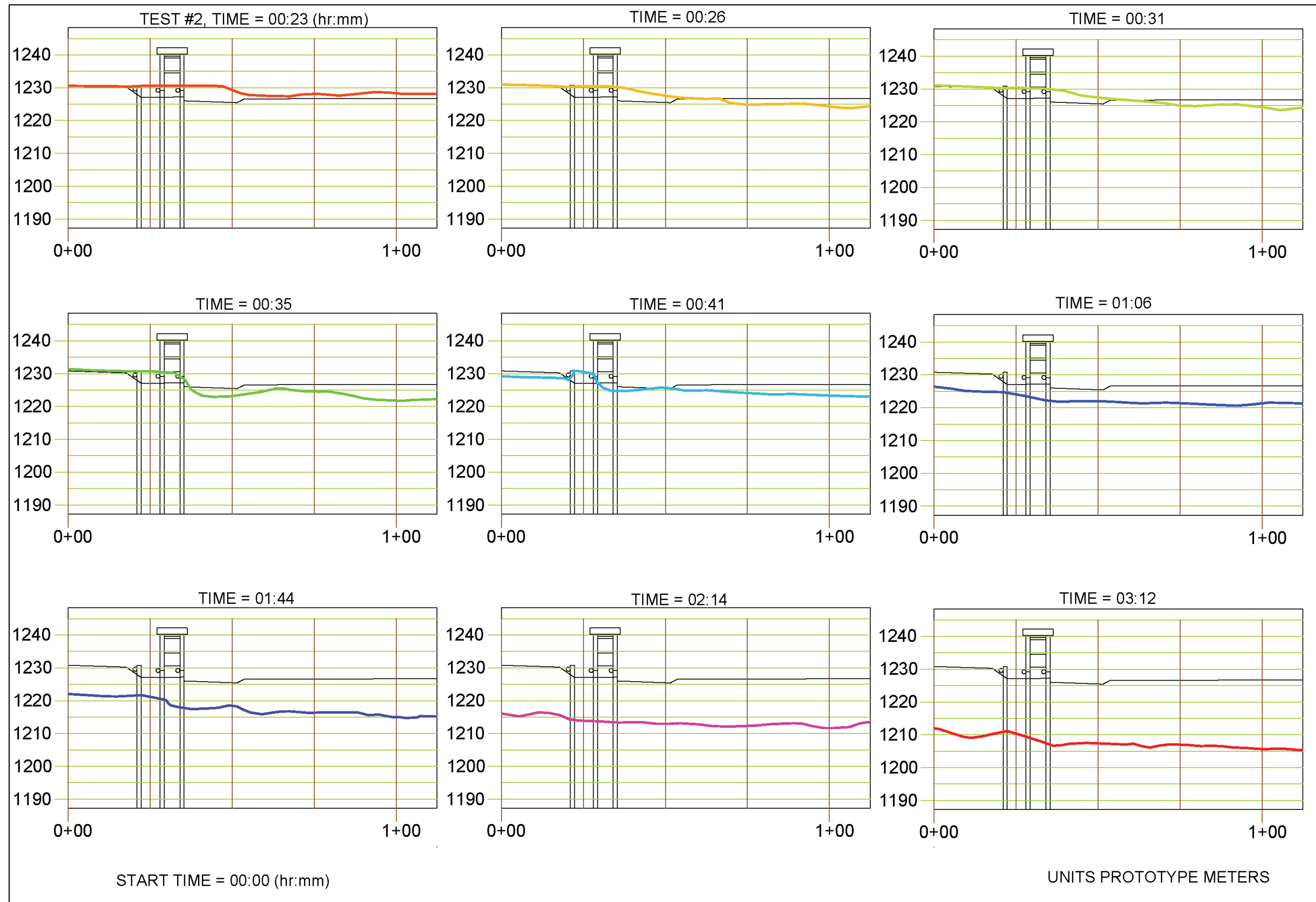


Figure 47. Scour profiles of model alternative 2 (continued).

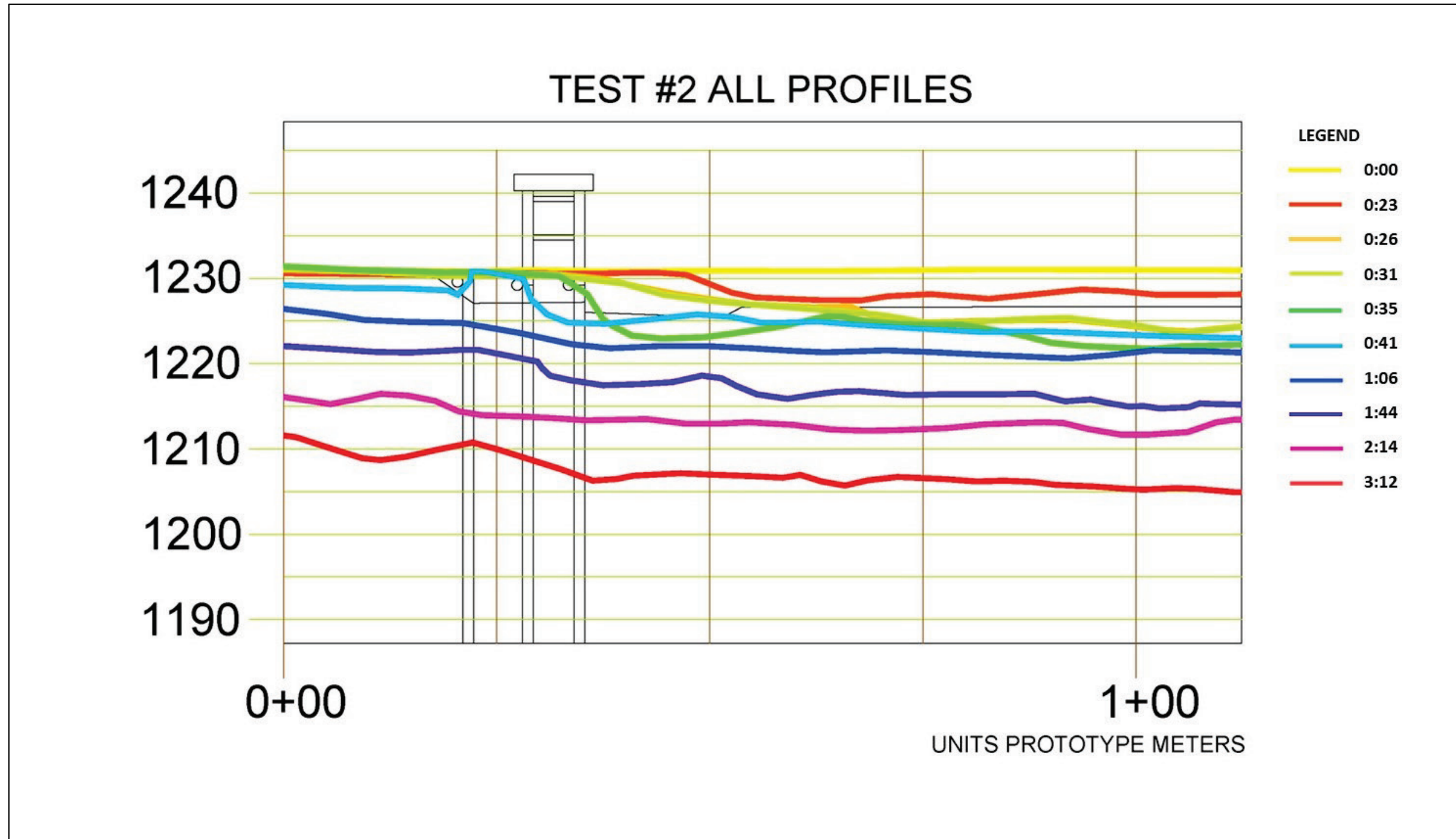


Figure 48. Scour profiles of model alternative 3.



Figure 49. Scour profiles of model alternative 3 (continued).

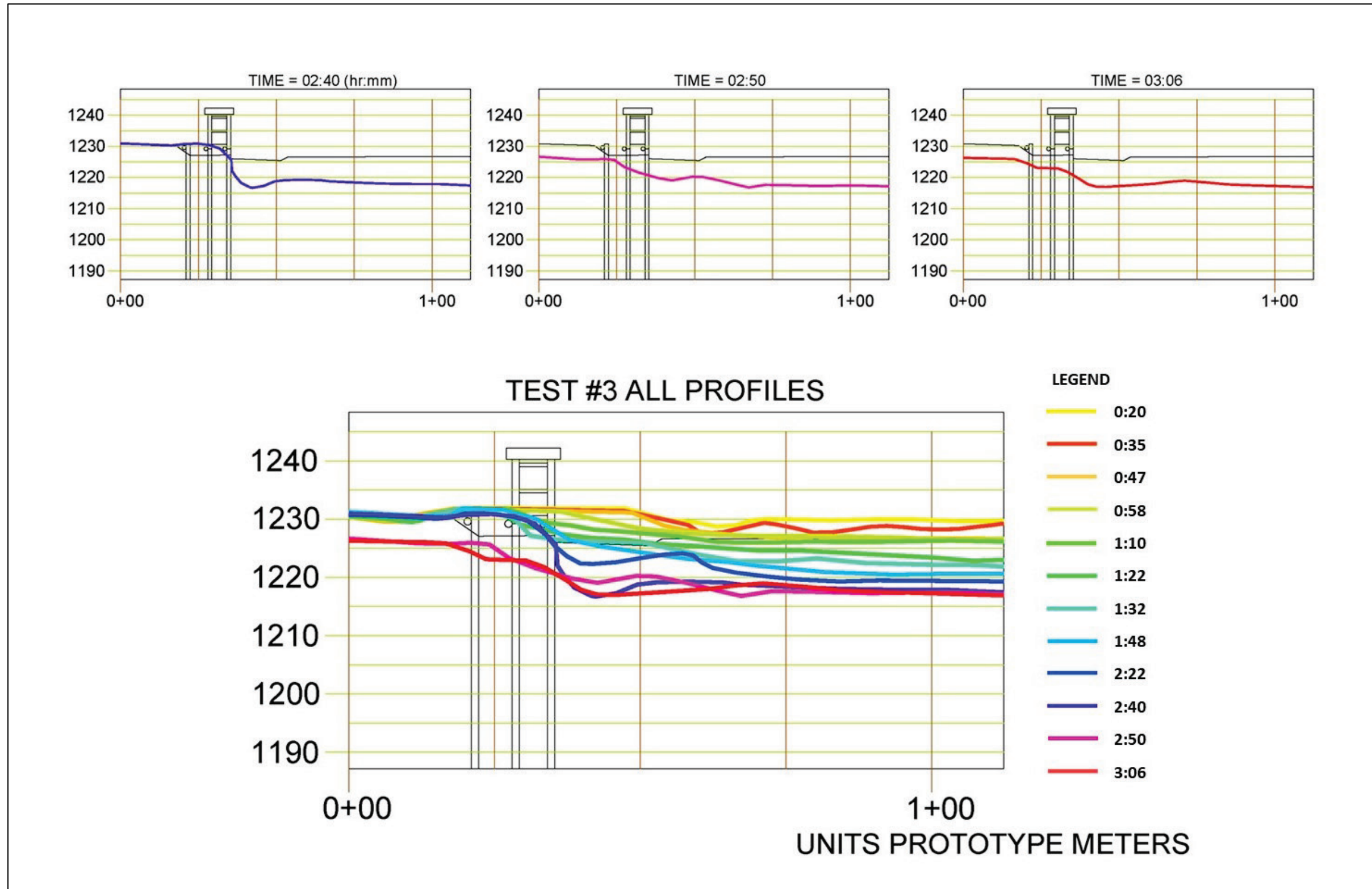


Figure 50. Scour profiles of model alternative 4.

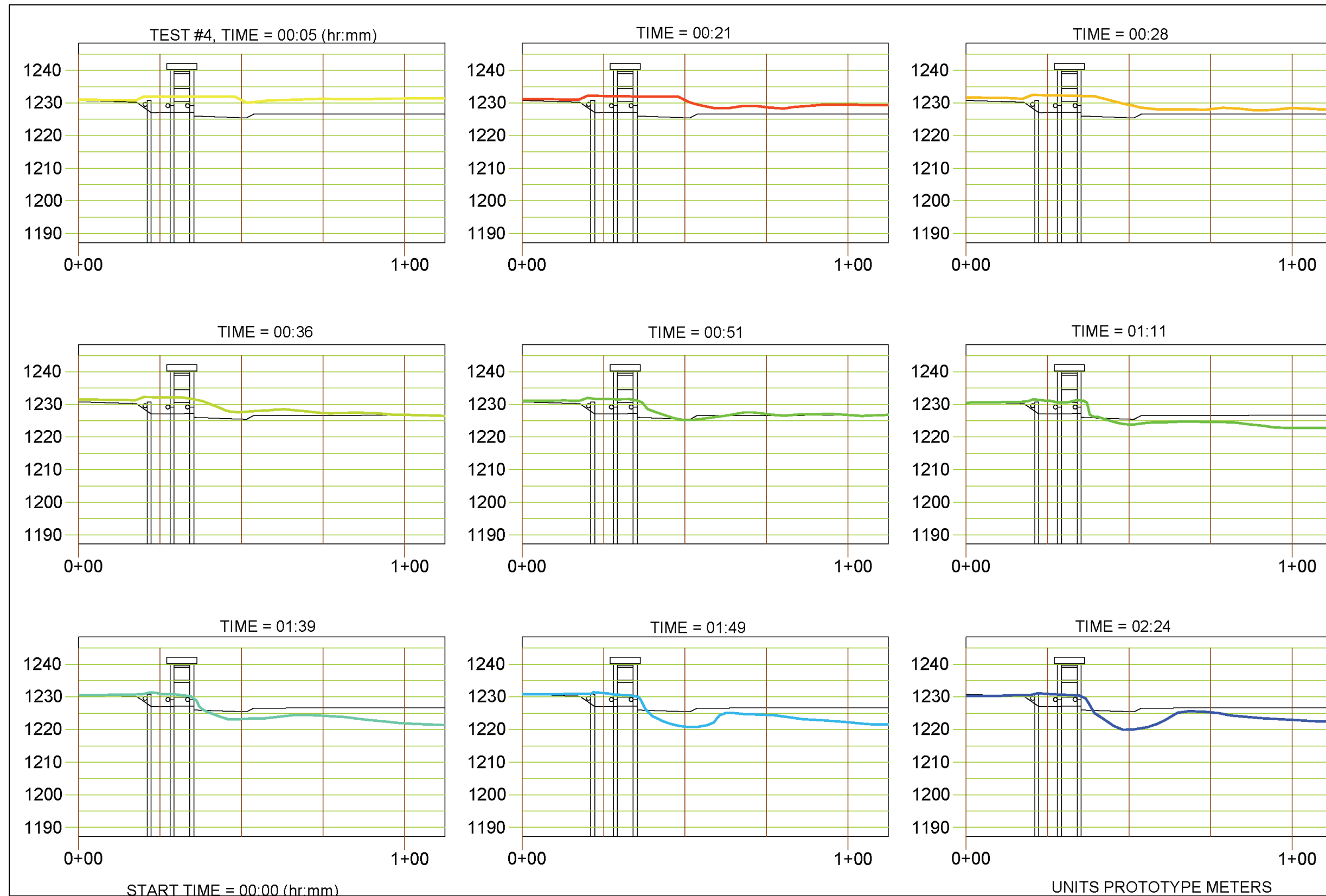


Figure 51. Scour profiles of model alternative 4 (continued).

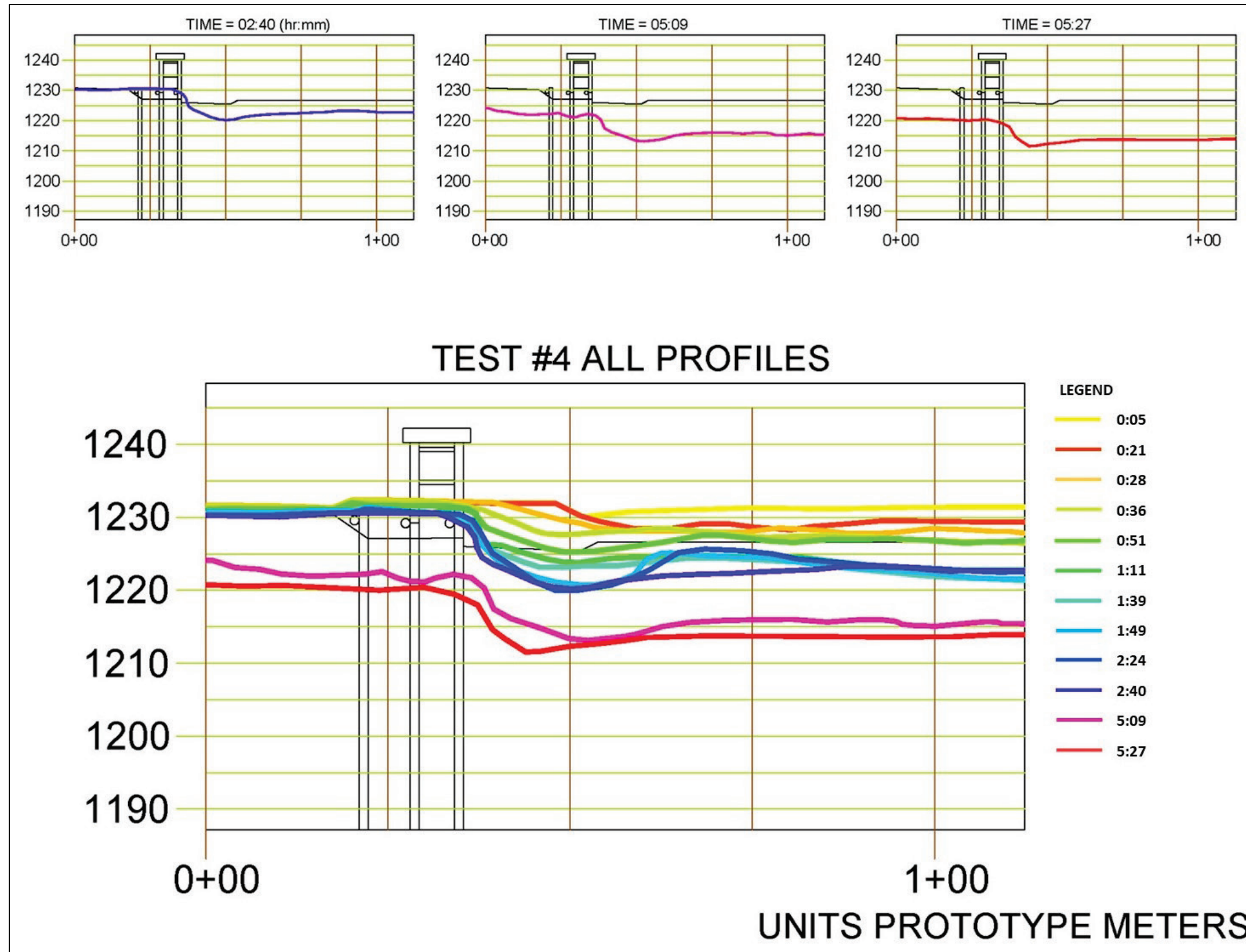


Figure 52. Scour profiles of model alternative 5.

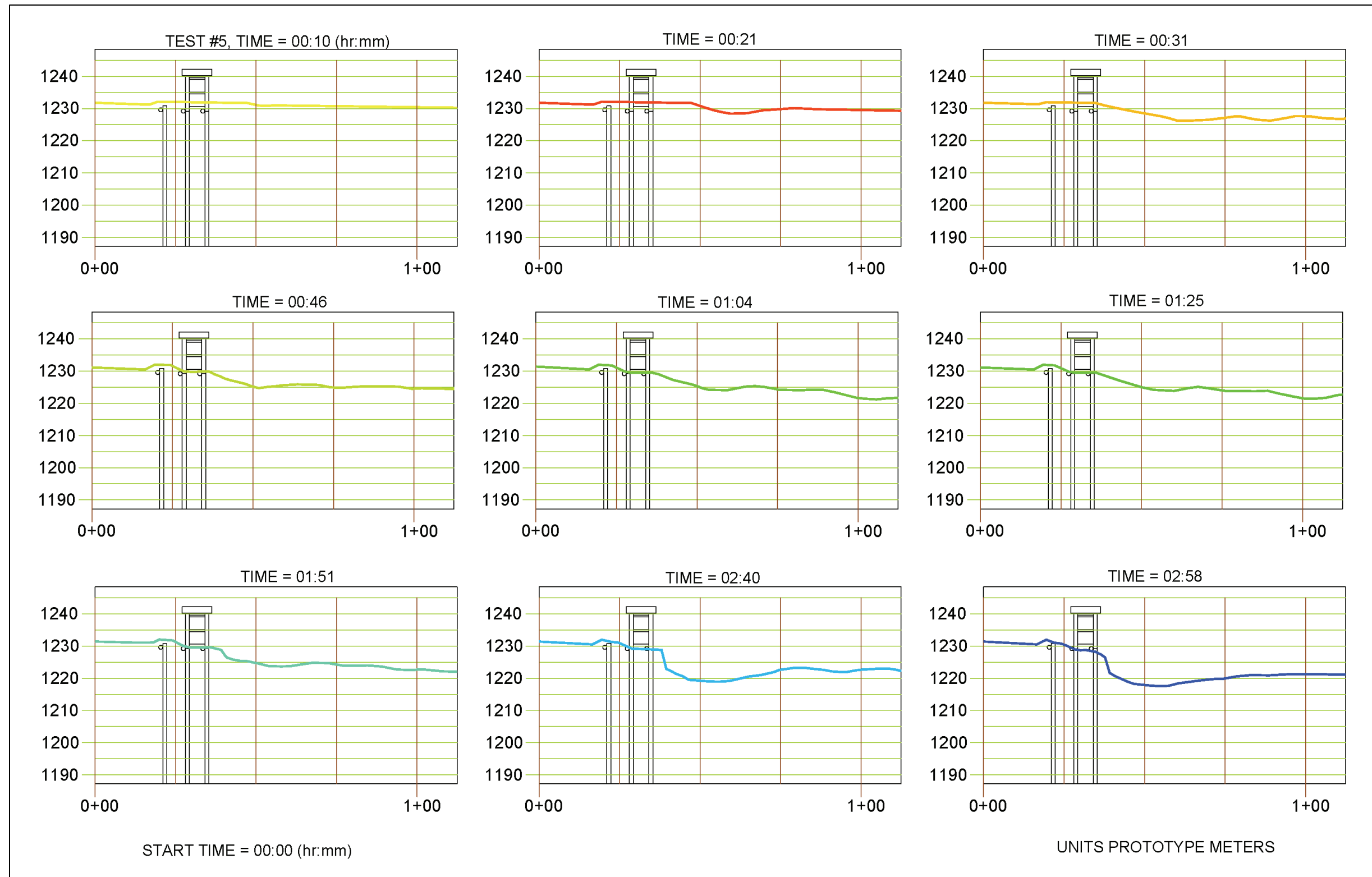


Figure 53. Scour profiles of model alternative 5 (continued).

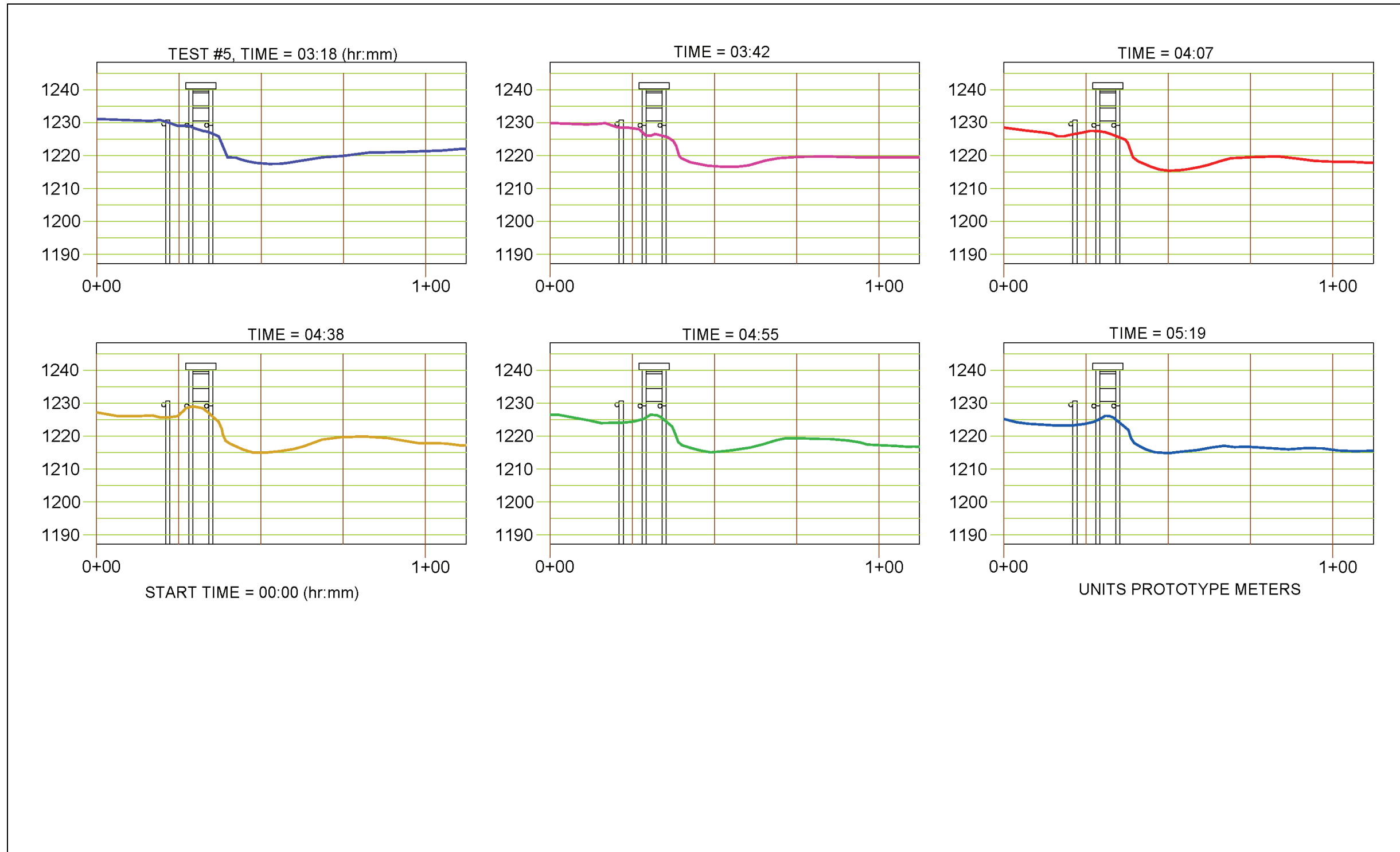


Figure 54. Scour profiles of model alternative 5 (continued).

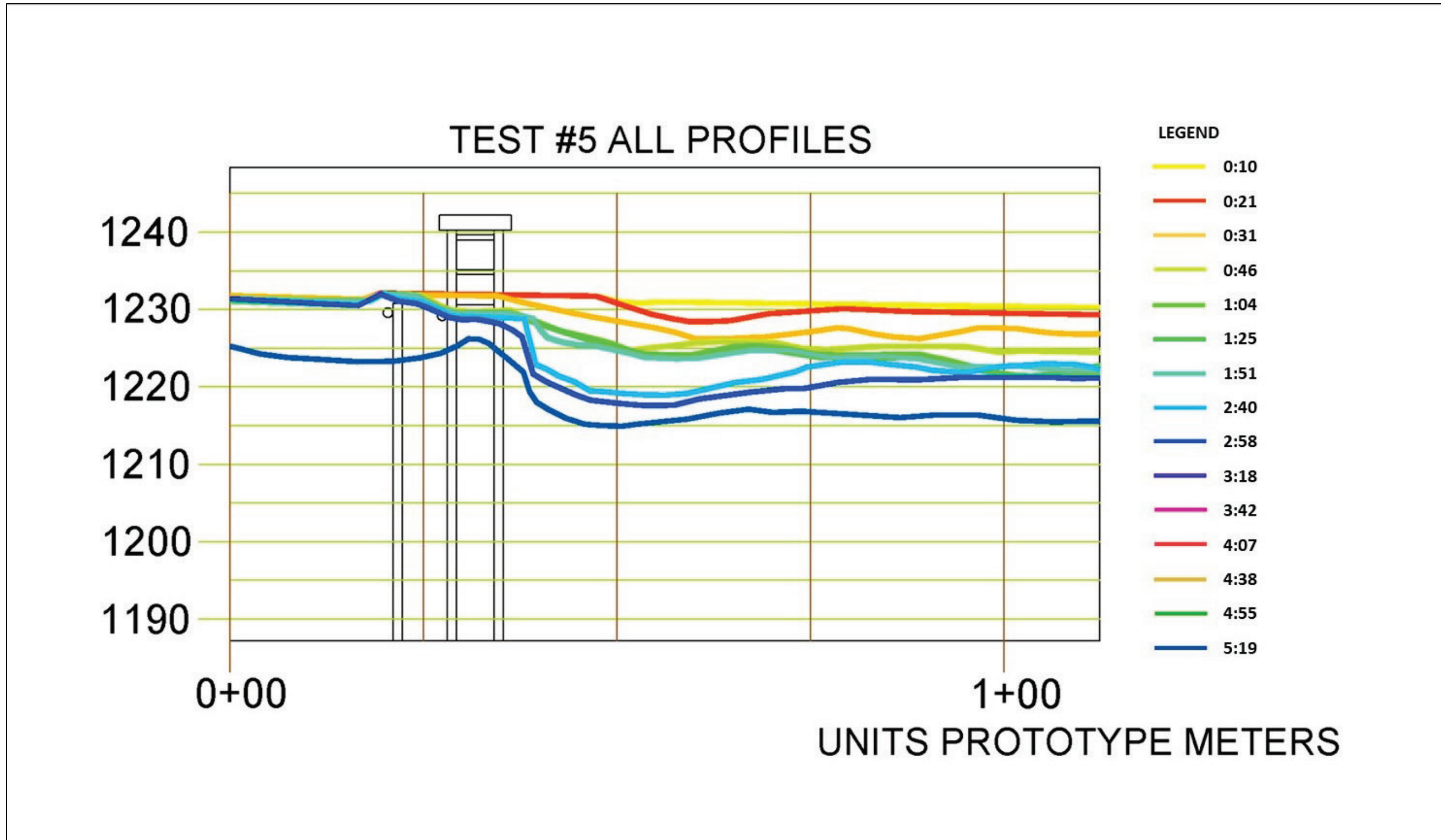


Figure 55. Scour profiles of model alternative 6.

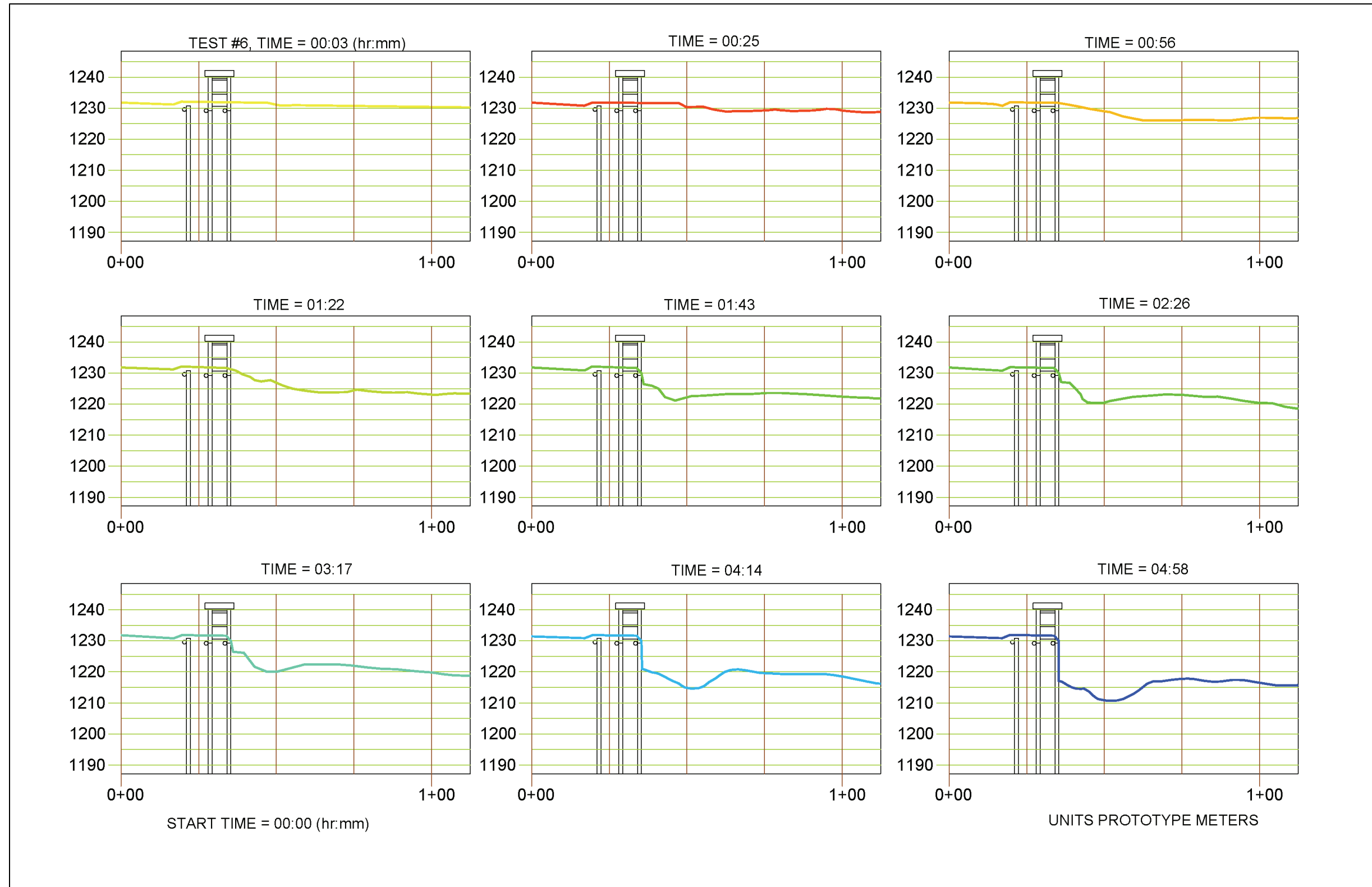
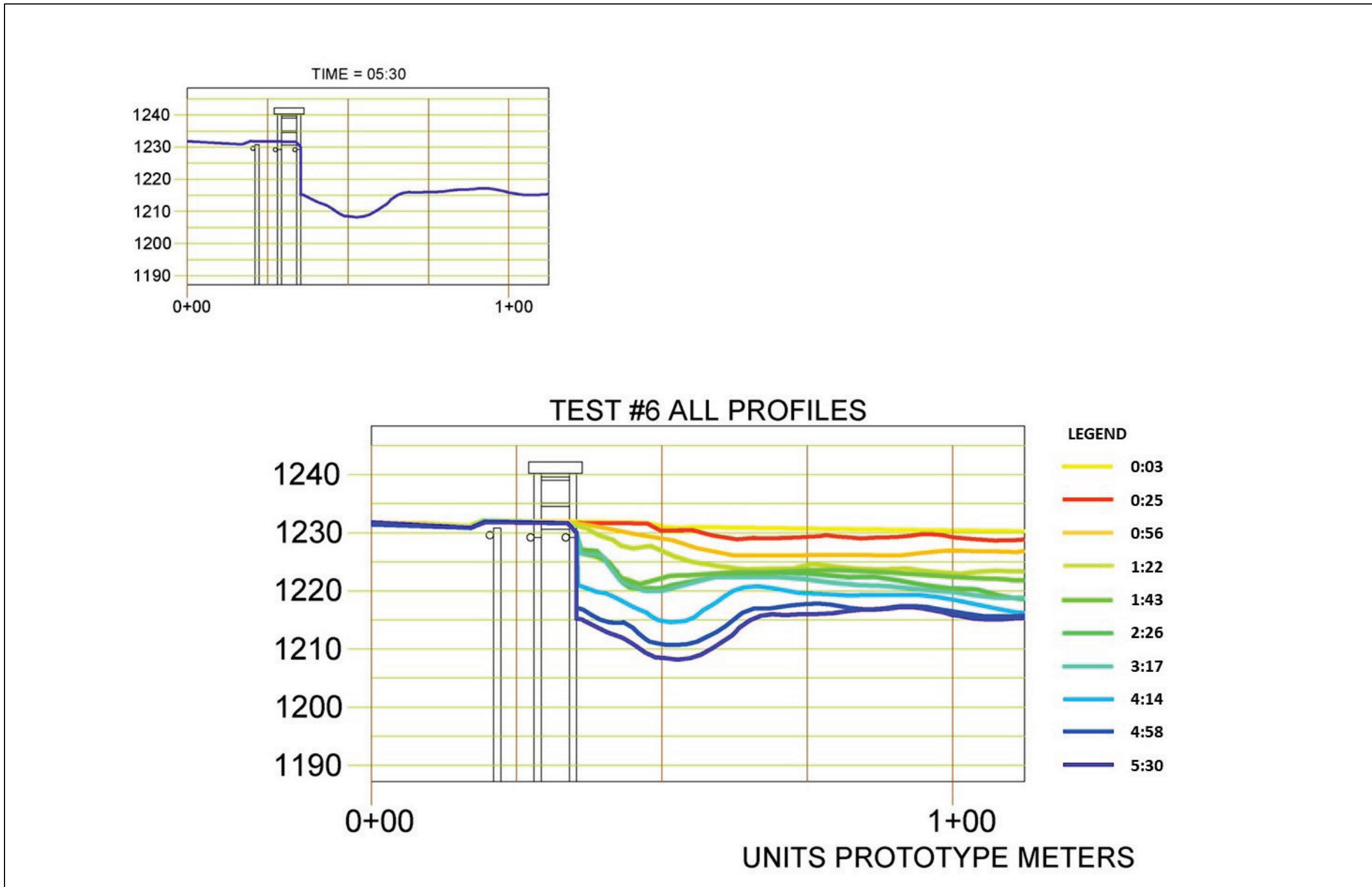


Figure 56. Scour profiles of model alternative 6 (continued).



This page intentionally left blank.

Figure 57. Comparison of scour depth and invert elevation for model alternative 1.

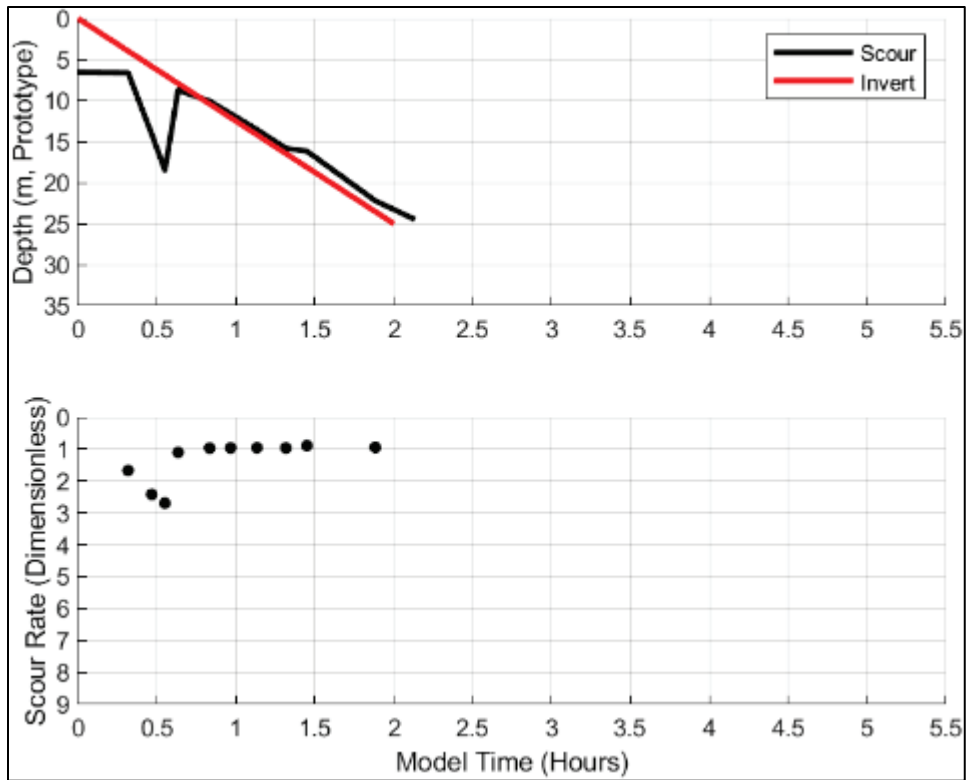


Figure 58. Comparison of scour depth and invert elevation for model alternative 2.

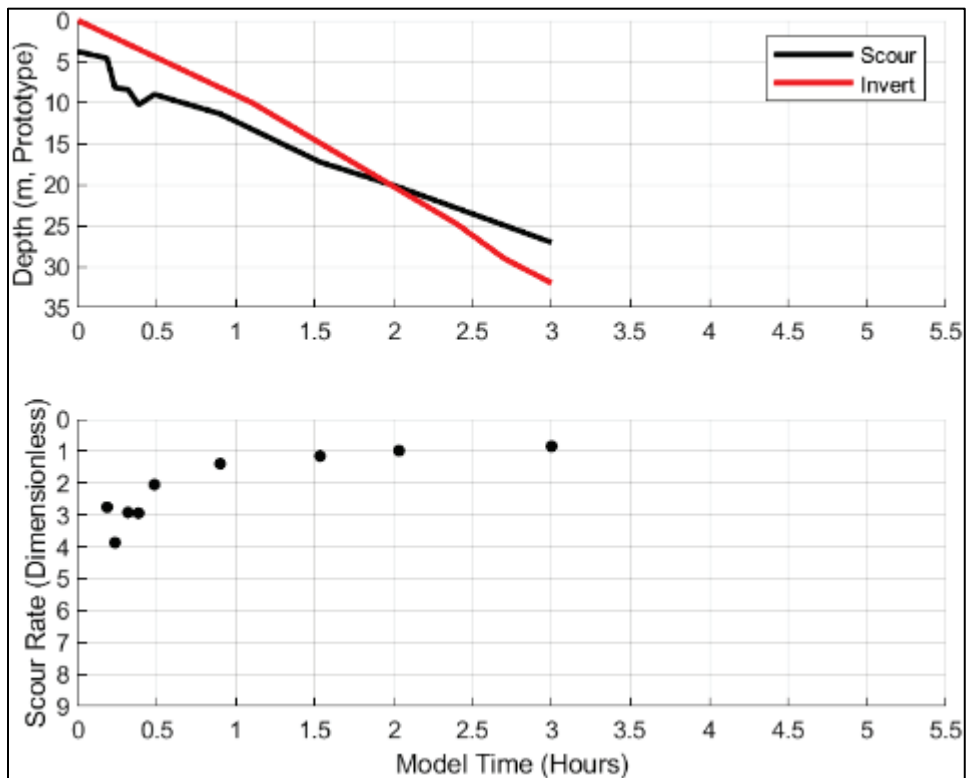


Figure 59. Comparison of scour depth and invert elevation for model alternative 3.

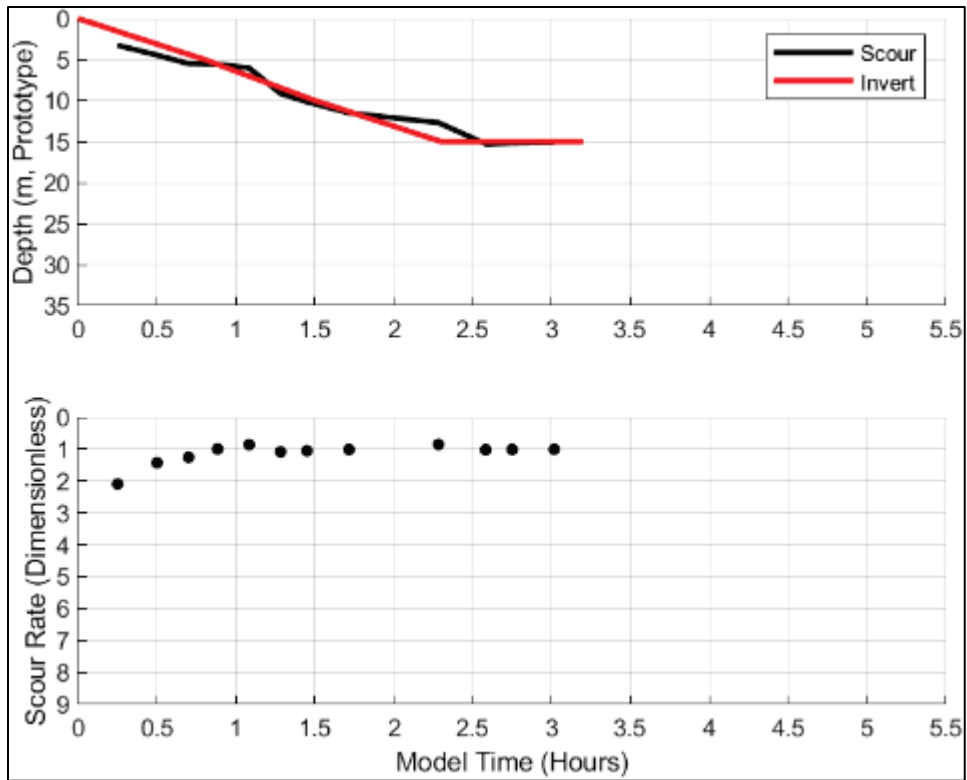


Figure 60. Comparison of scour depth and invert elevation for model alternative 4.

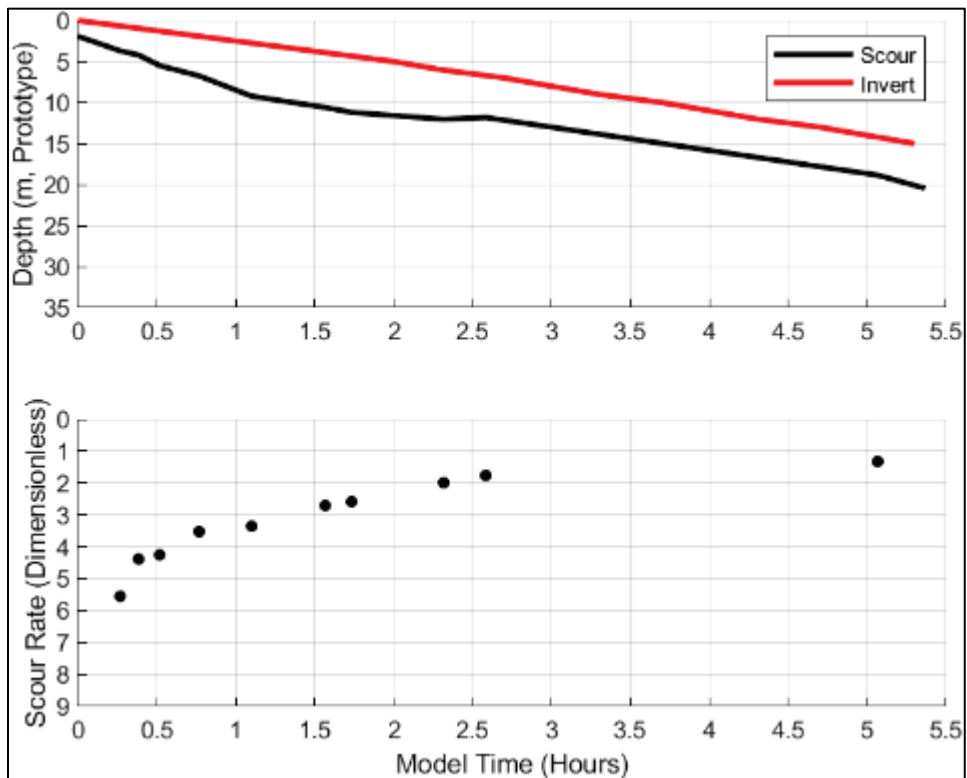


Figure 61. Comparison of scour depth and invert elevation for model alternative 5.

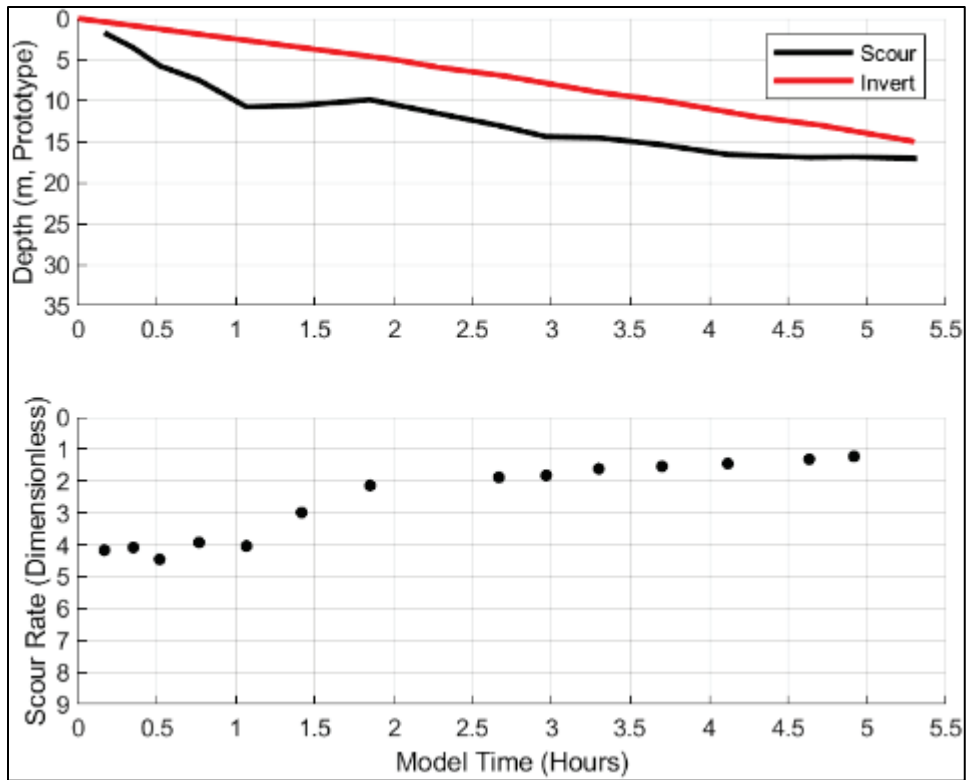


Figure 62. Comparison of scour depth and invert elevation for model alternative 6.

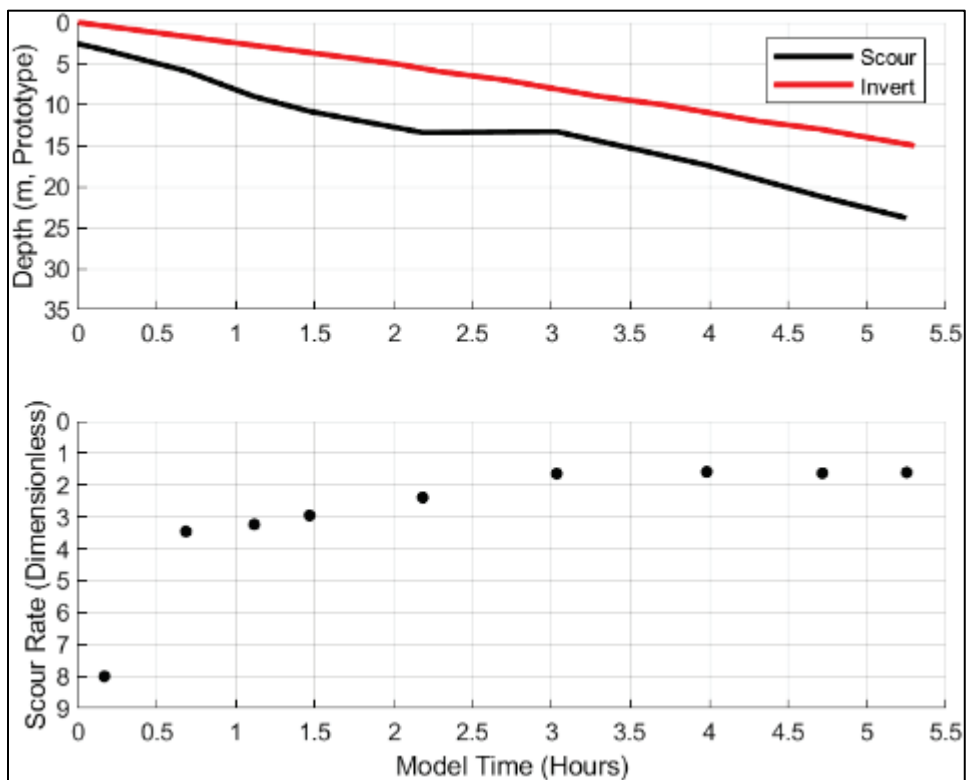


Table 7. Final slope values for the bed downstream of the bridge.

Model Alternative	Slope
1	0.005
2	0.027
3	0.057
4	0.070
5	0.121
6	0.163

Figure 63. Comparison of modeled flow hydrograph and tailgate-lowering operation for test 1.

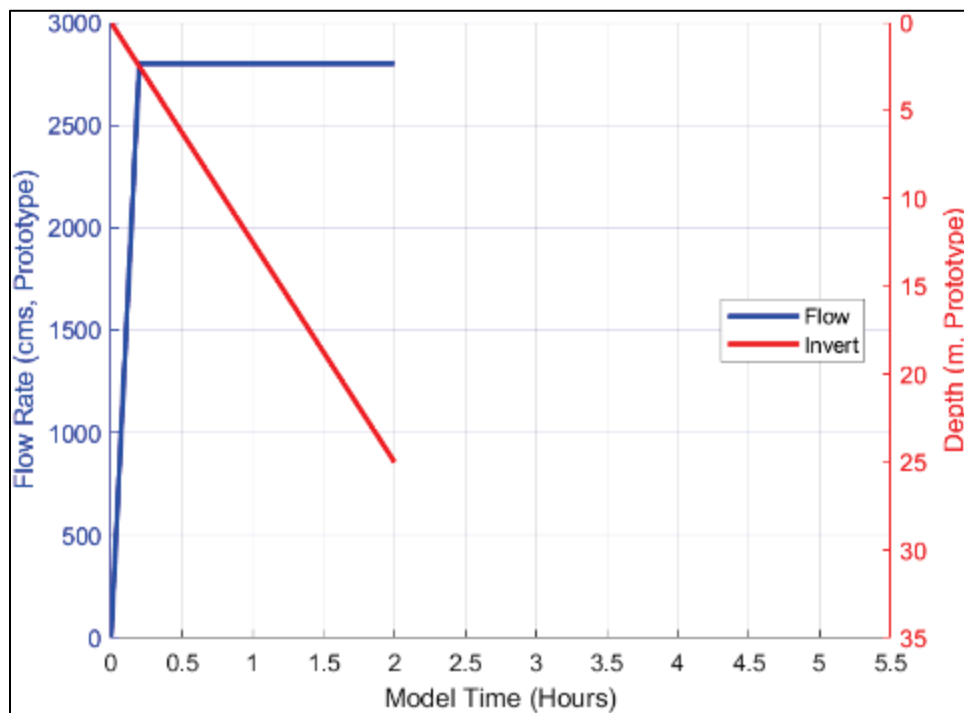


Figure 64. Comparison of modelled flow hydrograph and tailgate lowering operation for test 2.

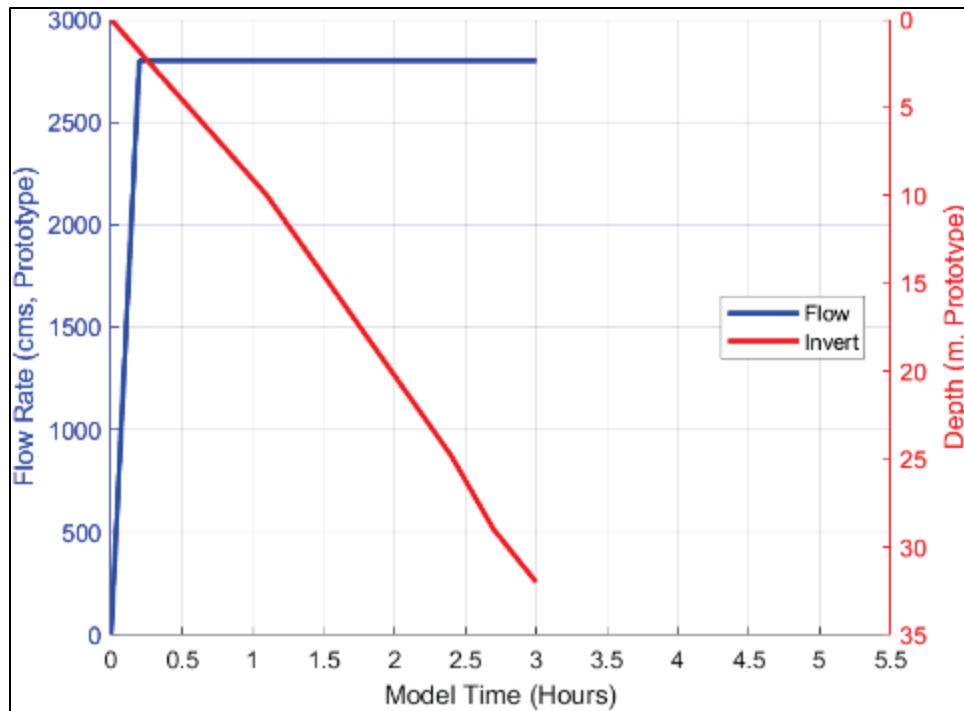


Figure 65. Comparison of modelled flow hydrograph and tailgate lowering operation for test 3.

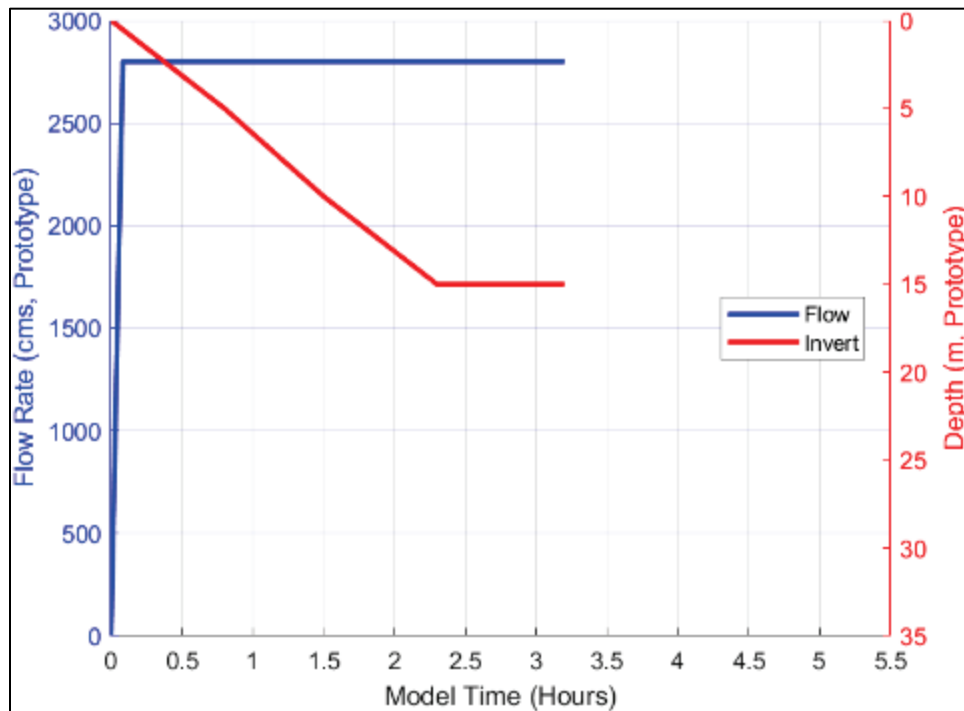
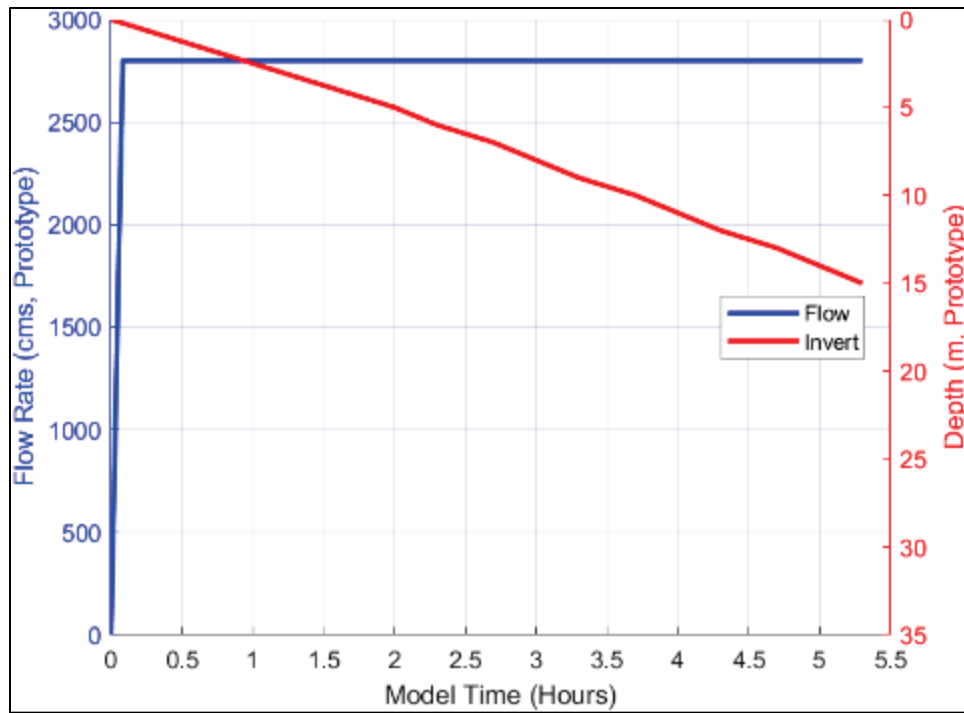


Figure 66. Comparison of modelled flow hydrograph and tailgate lowering operation for tests 4 to 6.



4 Discussion

The study qualified the level of damage on each permeable dam model alternative as a function of damage extension (Table 8). Using the bridge as the reference point, *total damage* implied that the model alternative did not survive the regressive erosion, where the regressive erosion went through the bridge section. *Moderate damage* meant that the regressive erosion could not travel beyond the bridge. *Low damage* indicated the regressive erosion scoured the downstream bed protection but could not get through the bridge. Based on these criteria, model alternatives 1 to 5 suffered total damage while model alternative 6 sustained low damage. The configuration of model alternative 6 successfully contained the regressive erosion downstream of the sheet-pile cut-off wall. As the bed invert elevation decreased, the cut-off wall acted as a weir with an invert control that promoted the formation and armoring of a scour hole. The following subsections discuss specific details of the findings obtained at each test and the reasoning for not tethering the tetrapods.

Table 8. Damage extension per model alternative.

Model Alternative	Damage Extension			Level of Damage
	Downstream of Bridge	Under Bridge	Upstream of Bridge	
1	Yes	Yes	Yes	Total
2	Yes	Yes	Yes	Total
3	Yes	Yes	Yes	Total
4	Yes	Yes	Yes	Total
5	Yes	Yes	Yes	Total
6	Yes	No	No	Low

4.1 Untethered Tetrapod Configuration

ERDC-CHL chose each model configuration in coordination with CELEC representatives and input from the larger team of US Army Corps of Engineers (USACE) subject matter experts. The original permeable dam design (Section 2.4) included cast concrete tetrapods tethered together in pairs to the bridge piers and upstream piles with steel cables. However, the USACE team had several concerns with this design and recommended first testing untethered configurations. First, the team thought the tethers could fray and fail. Second, even if the tethers did not fail, they would

introduce additional failure modes as the regressive erosion arrived and the tetrapod field settled. Concerns associated with tether persistence include the following:

- Since the Coca River has large bedload material, the tethers will be exposed to bedload abrasion, which will weaken them, possibly creating knickpoints in the steel cables. This can create a dynamic and unpredictable loading condition where the cables will be exposed to potential damage, leading to failure of the tethers.
- As the tetrapods shift and settle in response to hydraulic forces, local erosion and, eventually, undercutting, the tethers will be exposed to uneven loading. As the tethers become tangled and settle, additional loading may be placed on individual tethers instead of evenly distributed as designed. This will overload individual cables leading to failure and progressive overload of other cables.
- As failure of the tetrapods begins, or due to the debris or large bedload, additional load will be placed on the remaining tetrapods due to the failed tetrapods becoming tangled and wedged in place or due to the dynamic force of the tetrapods colliding during the event. This will lead to higher loads on the remaining tethers leading to overstressing and failure of the steel cables.

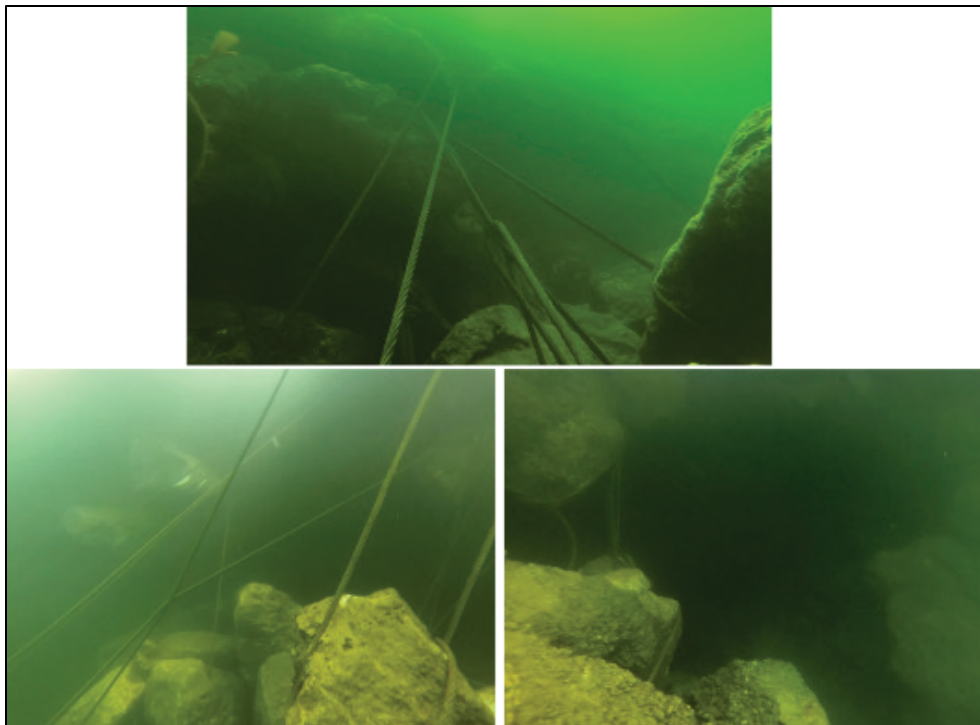
Concerns associated with intact tethers include the following:

- As the regressive erosion moves upstream and undercuts the tetrapod mat, it is possible that tethered tetrapods may not provide the expected protection. If the tetrapods act independently and not become tangled, they may become suspended in the flow and allow for continued erosion at that location.
- It is more likely that as the tetrapods act as a mat, they become interlocked and settle as the riverbed degrades and the regressive erosion reaches the structure. It is possible that as the regressive erosion reaches the tetrapod mat, the mat may still become suspended in the large flow event and allow the scour below the protection rather than settling into the scour hole as the event occurs. This bridging of the tetrapods will put more pressure on the tetrapods and the tethers and can lead to failure as expressed above or can lead to continued erosion and undercutting towards the bridge structure and eventual failure due to undercutting and seepage under the individual piles. Members of the USACE team have been involved with a project that

- used tethered scour protection like that proposed in the design. It performed poorly. As the bed scoured, the tethered elements bridged and the tethers tangled, leaving a web of suspended boulders well above the scouring bed (Figure 67).
- If the tethers survive abrasion, settling, and, eventually, bearing the entire submerged weight of the tetrapod mat, the design did not demonstrate that the piers could resist the additional load applied to the structure especially as the river scours and exposes the piers, decreasing the resisting forces and increasing the applied moments.

Based on the information provided above, the general uncertainty in the loading conditions of the tetrapod mats and the ability to introduce additional failure modes to the system, the USACE team recommends using stone protection at the site instead of the tetrapods. While it is difficult to size rock that will hold a grade under the expected conditions, the team believes rock will provide a more dynamic and responsive design to the changing conditions at the site, where the individual protection elements can adjust to morphological change. Therefore, the ERDC-CHL team proceeded to model the first two alternatives without tethering the tetrapods.

Figure 67. Postscour images of a tethered grade control design (provided by the USACE team). The tethers tangled and kept the scour protection elements suspended above the scouring bed.



4.2 Model Alternative 1: Untethered Tetrapods

Model alternative 1 (Section 2.4.1) did not perform satisfactorily. The flow carried away all tetrapods in the downstream mantle for 8 min (model) after achieving the peak flow. As the downstream grade protection weakened, a scour hole formed. This scour hole deepened in front of the bridge until 30 min into the test (Figure 44). In this time frame, the scour hole achieved a maximum depth of 18.5 m (prototype; 14.5 in. model; Figure 57). Two min afterward, the flow eroded the bed under the bridge, and the regressive erosion made its way upstream. The riverbed lowered 24.5 m (prototype; 19.3 in. model) to an elevation of 1207.5 m (prototype). Testing concluded at the 2 hr (model) mark since the model had already suffered total damage (Figure 38).

4.3 Model Alternative 2: Interlocked, Untethered Tetrapods

Like the first model, model alternative 2 (Section 2.4.2) could not arrest the regressive erosion (Figure 39). In this case, the downstream alluvial layer started eroding before achieving peak flow (Figure 46). It took 12 min (model) to establish the peak flow. The flow carried away the downstream tetrapods and riprap layer in 24 min (model). A few seconds later, while the bed invert elevation was 10 m (prototype), a scour hole formed downstream of the bridge. It deepened approximately 8 m (prototype; Figure 58) and moved quickly upstream, eroding the bed under the bridge.

In summary, the alluvial layer and the bed protection (tetrapods and riprap) became eroded within 30 min (model). Most of the stones from the debris flow layer piled up against the upstream piles. These stones armored the bridge structure, but some managed to move across and farther downstream.

The riverbed lowered 27 m (prototype; 21.2 in. model) to an elevation of 1205 m (prototype). Visual inspection after testing confirmed that most of the cast tetrapods had fractured during transport. Testing concluded at the 3 hr (model) mark since the model had already suffered total damage (Figure 39).

4.4 Model Alternative 3: Tetrapods Replaced with Stone Structure

Model alternative 3 allowed the formation of a shallow scour hole at the toe of the stone structure 13 min (model) after achieving peak flow (Figure 48). The tailgate reached the 5 m (prototype) mark 26 min (model) later, although initial rock movement was not observed until 12 min later. Visual inspection at 1.5 hr (model) into the test found most of the downstream alluvial layer eroded while stones of the permeable dam settled. About two-thirds of the stone structure collapsed after 2 hr of testing. Most debris rocks were carried downstream in the flume while some got stuck between the bridge piers. In addition, the upstream alluvial material armored the downstream bed.

The riverbed lowered 15 m (prototype) to an elevation of 1217 m (prototype). In this test, changes in bed elevation were consistent with invert elevation drops (Figure 60). Testing concluded after 3 hr and 20 min (model) since the model had already suffered total damage (Figure 40). Model alternative 3 resisted damage for longer than the first two alternatives.

4.5 Model Alternative 4: Structural Changes

Model alternative 4 performed similarly to the third alternative (Figure 41). However, before operating the tailgate, there was a 2 hr (model) waiting period to allow the erosion of the alluvial layer at the end of the tailrace (5 m prototype). The stone structure toe started eroding 10 min (model) after achieving peak flow, collapsing 40 min (model) later and exposing the downstream piles. At this point, the rocks under the bridge had carved down about 3.81 cm (1.5 in. model), and a shallow scour hole formed (Figure 50). The flow entirely eroded the downstream alluvial layer after an hour of achieving peak flow, armoring it with upstream material. After 3 hr into the test and with an invert elevation at 10 m (prototype), the physical model conditions transitioned from 2D to 3D. The downstream piles closer to the flume walls retained the material of the stone structure and the upstream alluvial layer. This stone combination forced the flow through the dam's center, introducing 3D effects. Testing, however, continued for the collection of qualitative data. The flow pattern kept changing and forcing 3D effects until the end of testing.

Testing lasted 5 hr, 20 min (model), and the model suffered total damage (Table 8). The riverbed lowered 20.5 m (prototype; approximately 16 in. model) to an elevation of 1,211.5 m (prototype; Figure 60).

4.6 Model Alternative 5: Changes to Stone Structure

Model alternative 5 performed like the fourth alternative (Figure 42). Again, the tailgate was not operated until the invert elevation had lowered to 5 m (prototype). Erosion on the stone structure toe started 20 min (model) after achieving peak flow (Figure 52). As in models 4 and 5, before lowering the tailgate, the flow entirely eroded the downstream alluvial layer and armored the downstream bed with stones and upstream material. The rocks under the bridge also settled down. A scour hole formed downstream of the piles after 2.66 hr (model) into the test while the invert elevation was 7 m (model). The solid core under the bridge started eroding 50 min (model) later. Similar to model alternative 4, the model conditions transitioned from 2D to 3D while the invert elevation was 10 m (model). Once again, the downstream piles closest to the flume walls retained the upstream stones, forcing the flow toward the right side of the flume. The dam's solid core was breached after lowering the tailgate to 12 m (model).

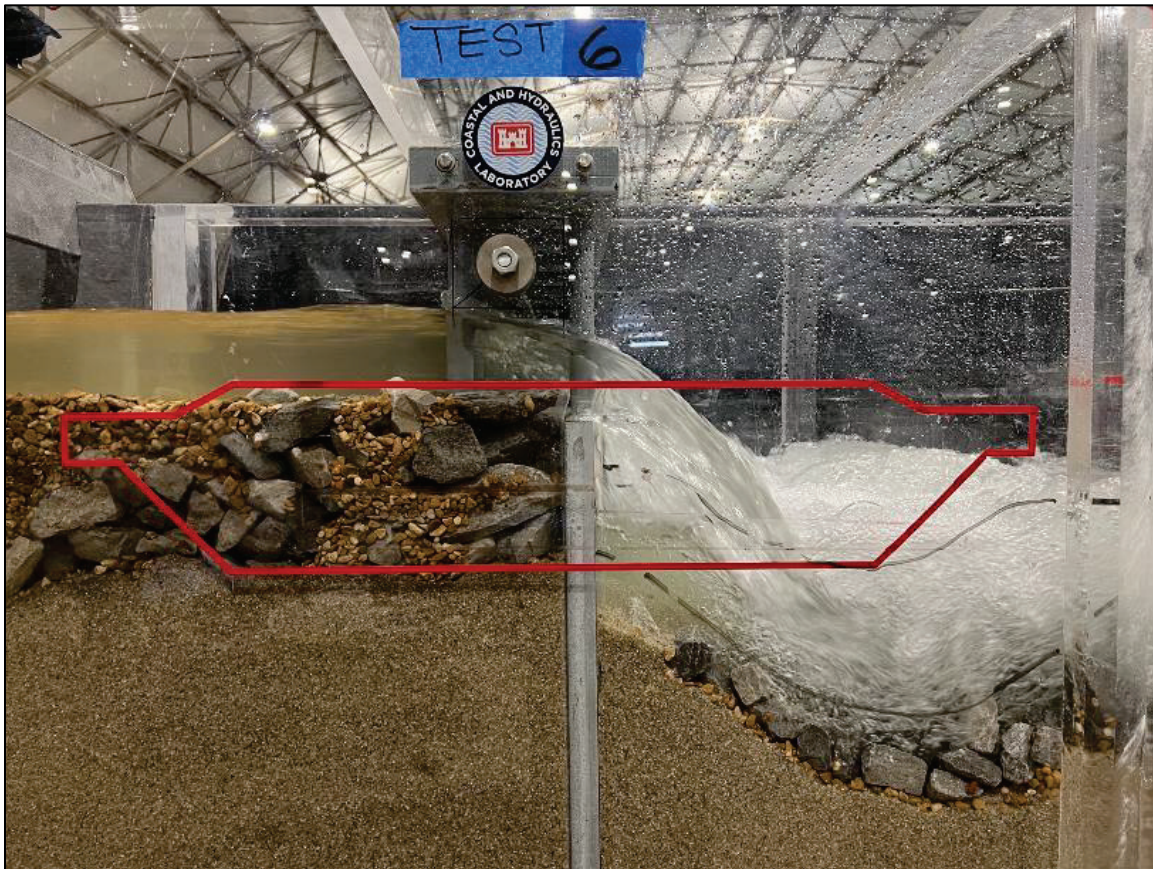
Testing lasted 5 hr 30 min (model), and the model suffered total damage (Table 8). The riverbed lowered 17 m (prototype; approximately 11 in. model) to an elevation of 1,214.9 m (prototype; Figure 61).

4.7 Model Alternative 6: Additional Structural Changes

Model alternative 6 outperformed the previous models (Figure 43). The tailgate was not operated until the invert elevation had lowered to 5 m. Erosion on the stone structure toe (downstream of sheet pile) started 14 min (model) after achieving peak flow. A scour hole formed about 17 min afterward. The downstream side of the stone structure became thoroughly scoured after 1.42 hr (model) into the test (Figure 55), but its material armored the downstream bed up to 2 ft past the flume's observation window. The scour hole was fully formed and armored with a thick layer on its right side (looking upstream). Unsubmerged flow (Figure 68) continued deepening and widening the scour hole as the invert elevation decreased. At approximately 4.5 hr into the test, the cut-off wall exposure above the scour hole (on top of 7 m scour depth) was 13 m, or at the same level as the invert.

Testing lasted 5 hr 20 min (model), and the model suffered low damage (Table 8). The downstream riverbed lowered 23.8 m (prototype; approximately 19 in. model) to an elevation of 1,208.2 m (prototype; Figure 62).

Figure 68. Side view of the unsubmerged or free flow.



5 Conclusions and Recommendations

This section model study of the permeable dam evaluated the performance of six different design alternatives against the regressive erosion currently affecting the prototype. The six alternatives included two variations of the tetrapod-based design (alternatives 1 and 2) and four runs that replaced tetrapods with rock (alternatives 3 to 6). Model alternatives 4, 5, and 6 evaluated the structural modifications with the large rock. For alternatives 4 and 5, the third row of piers was moved to just downstream of the structure. Then, in alternative 6, designers added a rigid pile wall between the bridge piers. All model alternatives included two rows of piers with 1.25 m diameter at 7 m (prototype) spacing on the center integrated with a bridge deck for access and maintenance. Each experiment ramped up to a maximum flow of 2,800 cms (20% AEP event) and lowered the downstream bed between 15 and 25 m to simulate the regressive erosion. The third row of piers, included in the original design for tethering of tetrapods, was included in the first five alternatives but moved downstream for alternatives 4 and 5 and removed in the sixth alternative. Top and side cameras recorded each alternative's effect against the regressive erosion in the physical model.

Photographs, digitized bed profiles, and estimates of scour depth supported the qualitative evaluation of each model alternative. Results confirmed that the first five alternatives could not stop the regressive erosion from moving upstream, sustaining total damage. Model alternative 6, however, outperformed the other models by successfully preventing the regressive erosion migration with the cut-off wall. This model alternative attained low damage, promoted the formation of an armored scour hole downstream, and provided a stable downstream bed slope. Fundamentally, the invert must be held to prevent the regressive erosion migration. An additional model study that focuses on the design may be beneficial to improving its efficiency.

Appendix: Permeable Dam Design Drawings

Figure A-1 through Figure A-8 present permeable dam design drawings.

Figure A-1. Permeable dam plan and profile drawing (CELEC, with permission).

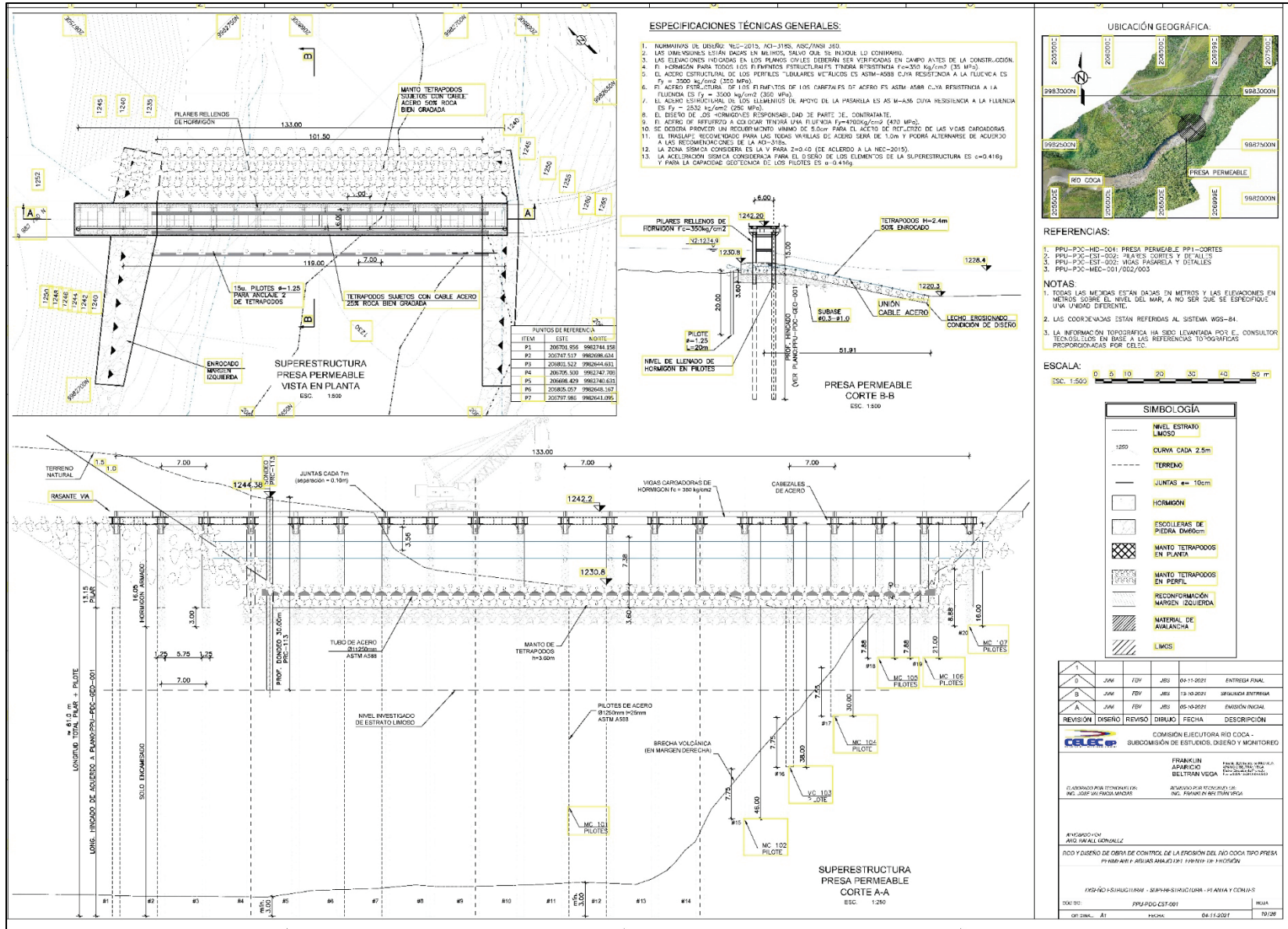


Figure A-2. Initial permeable dam design—details of bridge and piers (CELEC, with permission).

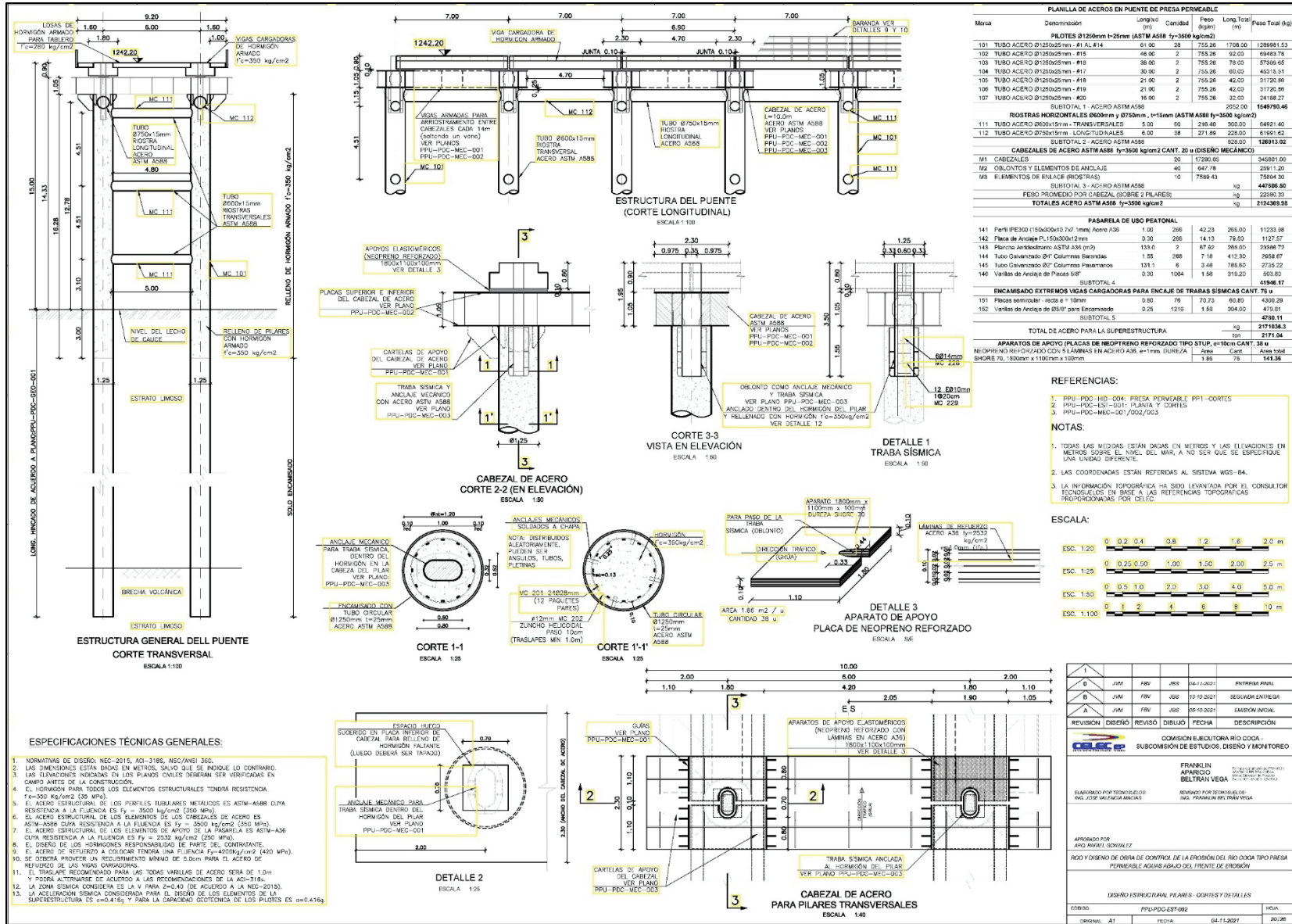


Figure A-3. Initial permeable dam design—details of tetrapods (CELEC, with permission).

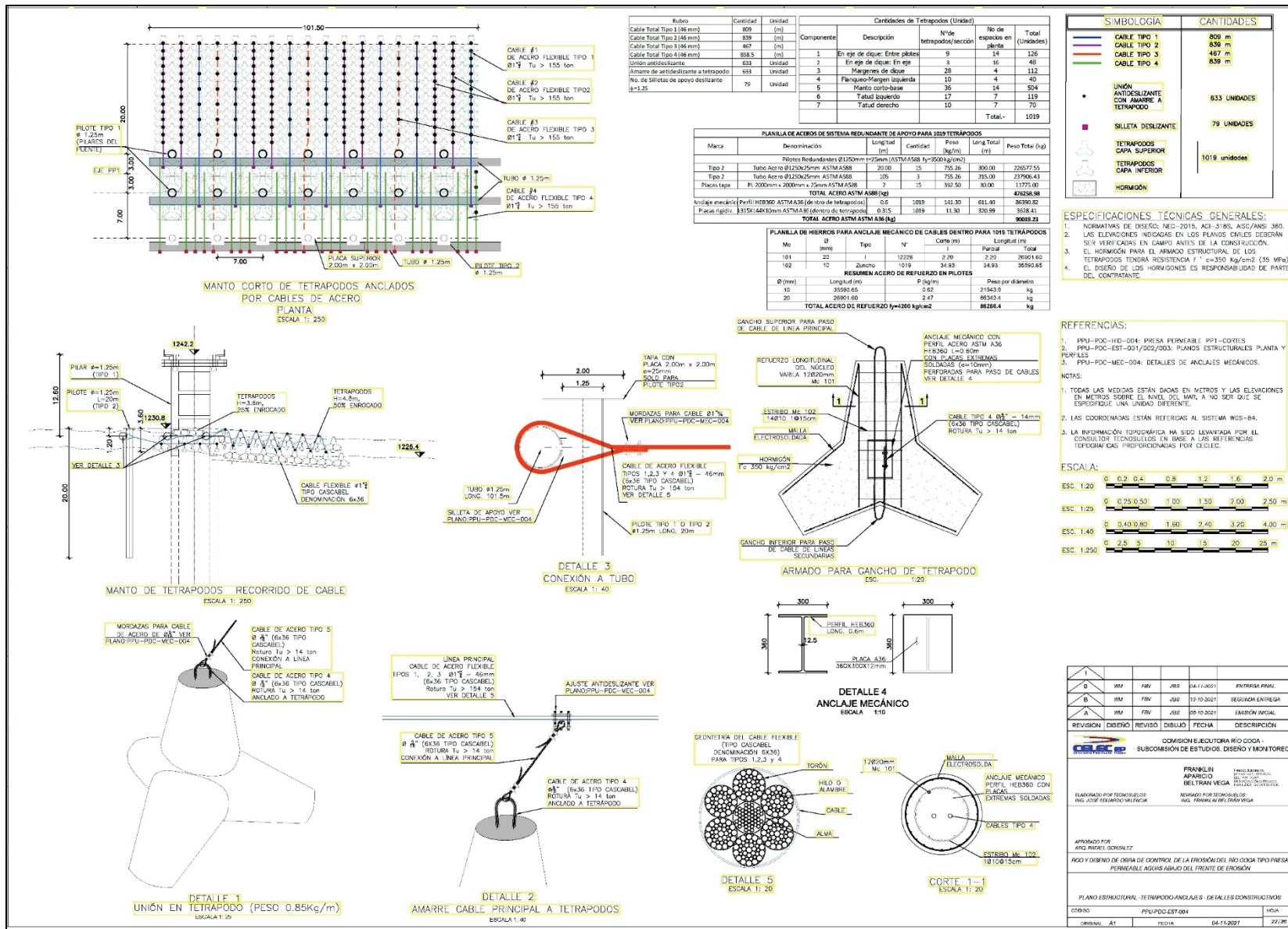


Figure A-4. Second permeable dam design change (CELEC, with permission).

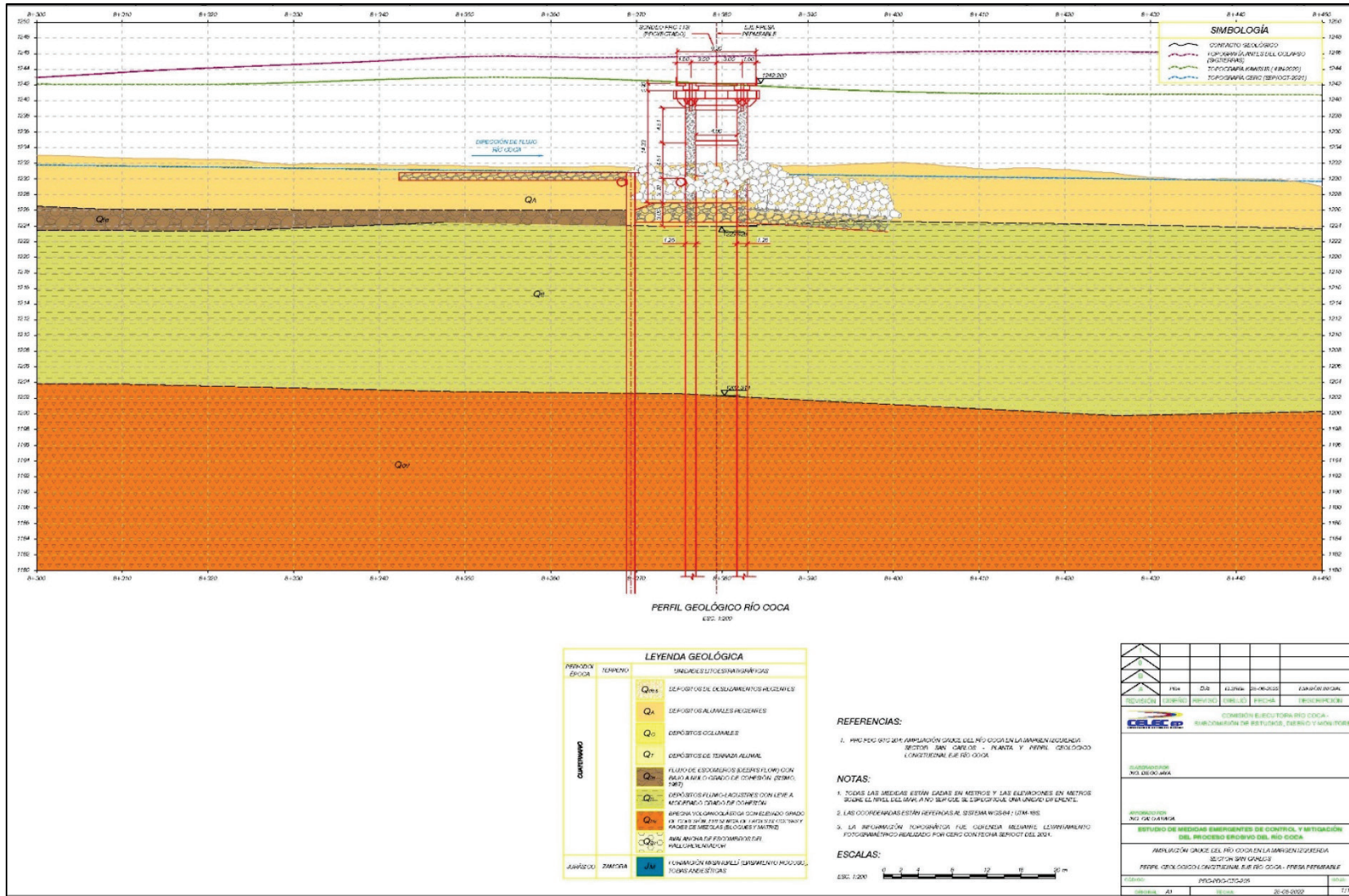


Figure A-5. Third permeable dam design change (CELEC, with permission).

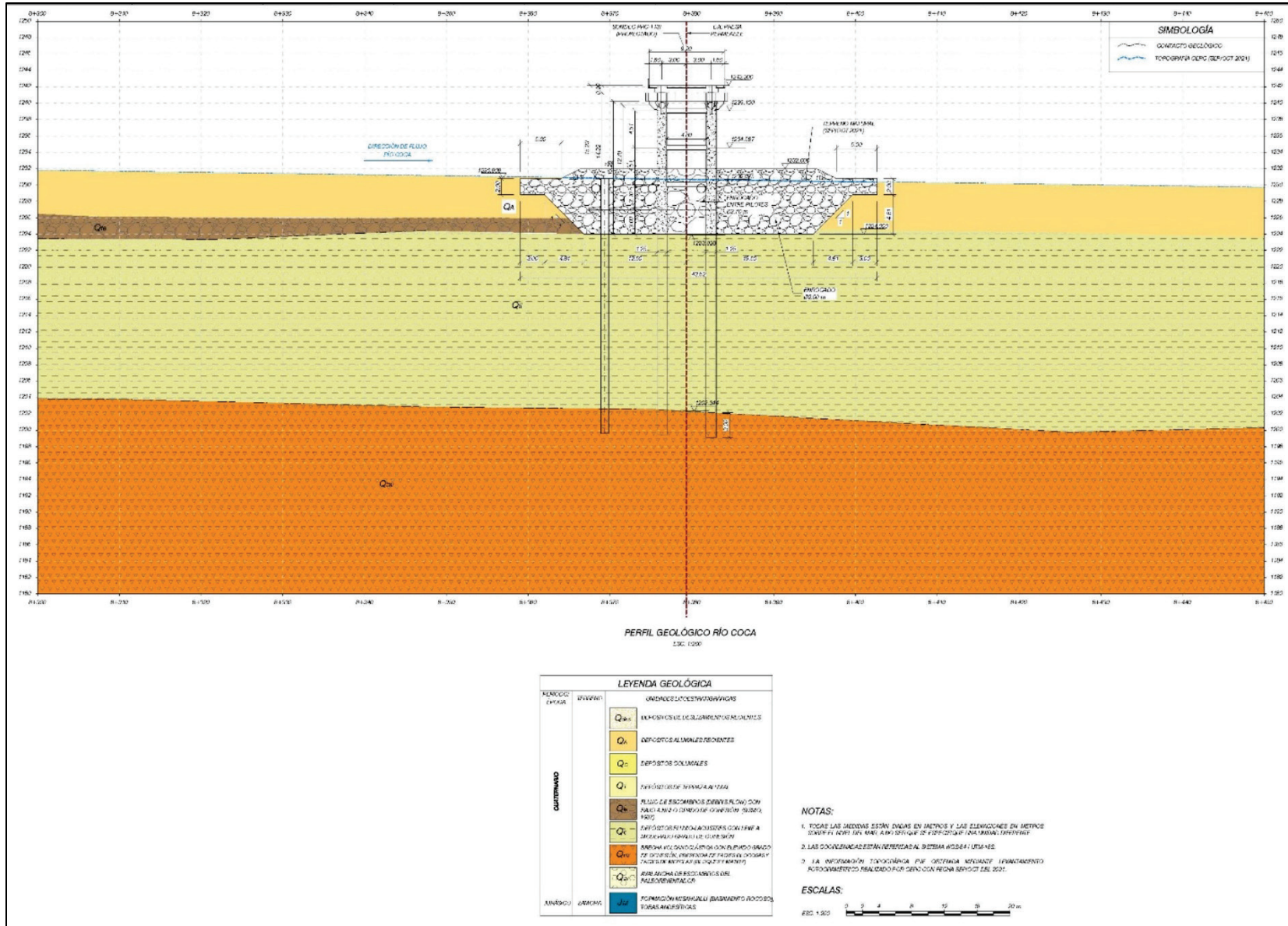


Figure A-6. Fourth permeable dam design change (CELEC, with permission).

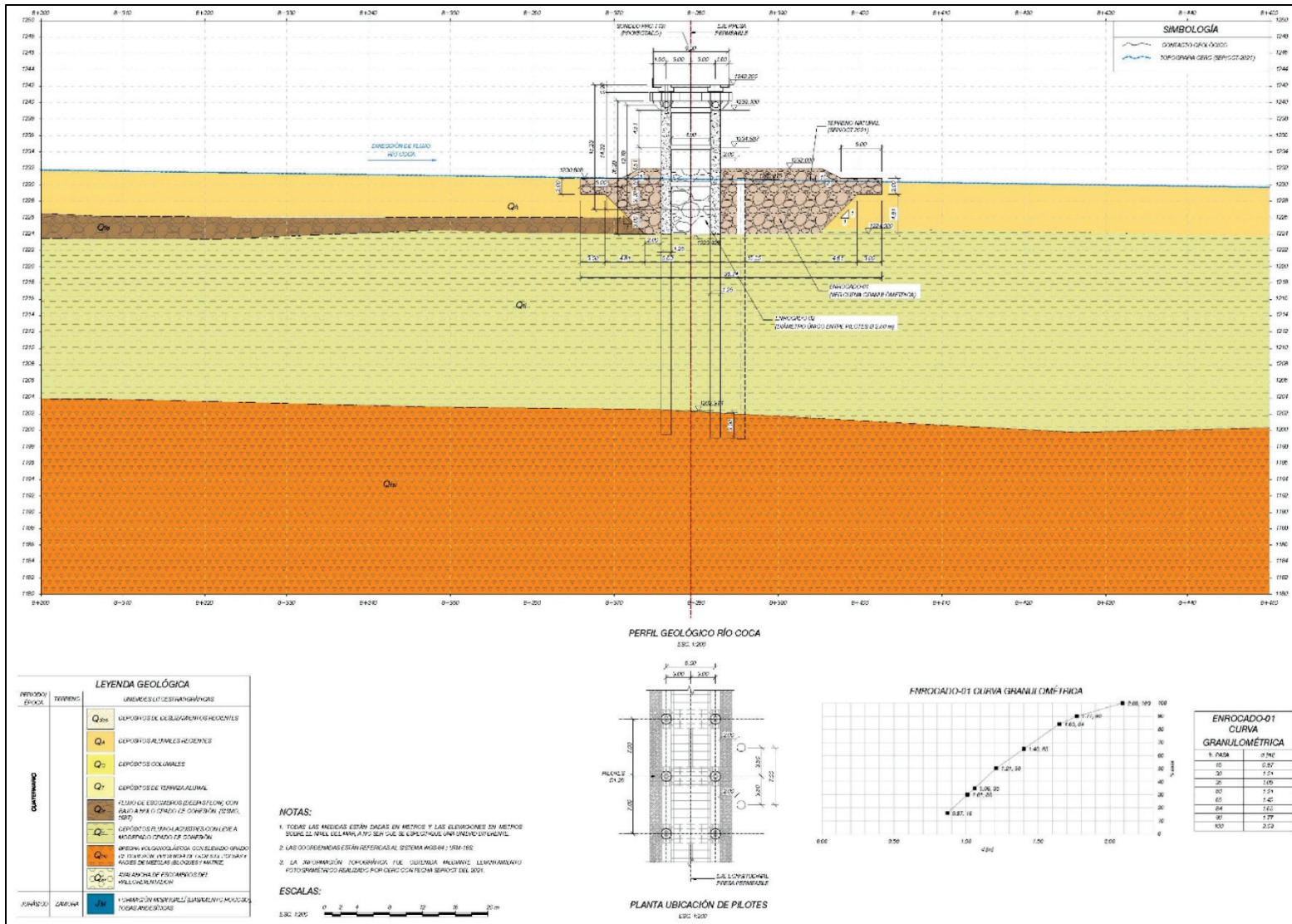


Figure A-7. Fifth permeable dam design change (CELEC, with permission).

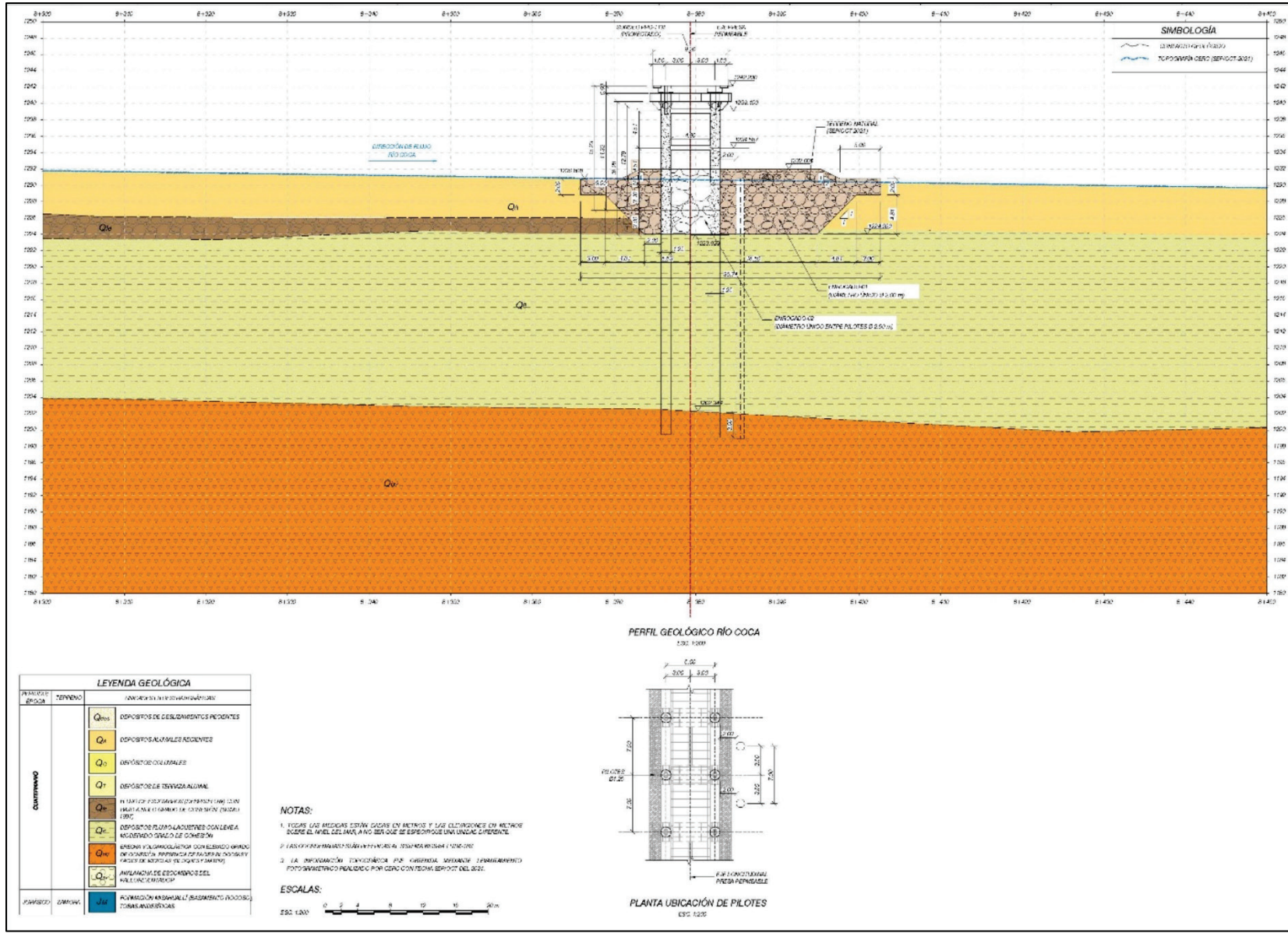
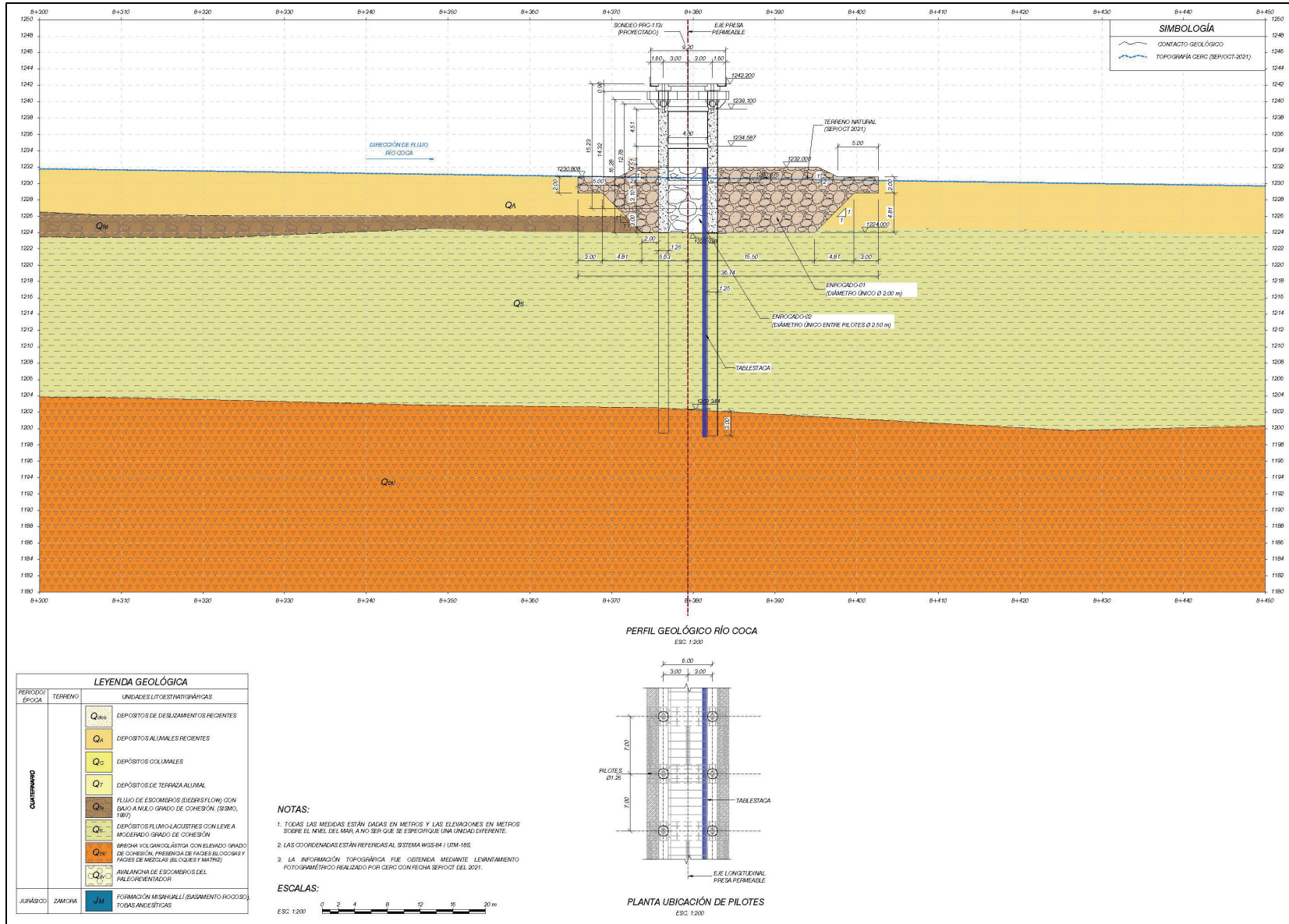


Figure A-8. Sixth permeable dam design change (CELEC, with permission).



Abbreviations

ABS	Acrylonitrile butadiene styrene
AEP	Annual exceedance probability
CCS	Coca Codo Sinclair
CELEC	Electric Corporation of Ecuador
CERC	Executive Commission for the Coca River
CHL	Coastal and Hydraulics Laboratory
ERDC	US Army Engineer Research and Development Center
PDT	Project development team
USACE	US Army Corps of Engineers

REPORT DOCUMENTATION PAGE

1. REPORT DATE June 2023		2. REPORT TYPE Final Report		3. DATES COVERED	
				START DATE FY22	END DATE FY23
4. TITLE AND SUBTITLE Evaluation of a Permeable Dam as an Erosion Control Structure on Coca River, Ecuador					
5a. CONTRACT NUMBER		5b. GRANT NUMBER		5c. PROGRAM ELEMENT	
5d. PROJECT NUMBER		5e. TASK NUMBER		5f. WORK UNIT NUMBER	
6. AUTHOR(S) Efraín Ramos-Santiago, Yamiretsy Pagán-Albelo, Jeremy A. Sharp, Curtis L. Blades, and Kevin L. Pigg					
7. PERFORMING ORGANIZATION NAME(S) AND ADDRESS(ES) US Army Engineer Research and Development Center (ERDC) Coastal and Hydraulics Laboratory (CHL) 3909 Halls Ferry Road Vicksburg, MS 39180-6199				8. PERFORMING ORGANIZATION REPORT NUMBER ERDC/CHL TR-23-6	
9. SPONSORING/MONITORING AGENCY NAME(S) AND ADDRESS(ES) Mobile District, US Army Corps of Engineers PO Box 2288, Mobile, AL 36628-0001			10. SPONSOR/MONITOR'S ACRONYM(S) USACE SAM		11. SPONSOR/MONITOR'S REPORT NUMBER(S)
12. DISTRIBUTION/AVAILABILITY STATEMENT Distribution Statement A: Approved for public release; distribution unlimited.					
13. SUPPLEMENTARY NOTES Funded via Labor Charge Code. Funding Authorization/CO-8242-XX-8028-08, "Task 2.2-Permeable Dam Section Model." Funded by US Army Corps of Engineers, Mobile District					
14. ABSTRACT The effort performed here describes the process to evaluate the scour-protection performance of the proposed permeable dam. The US Engineer Research and Development Center, Coastal and Hydraulics Laboratory, built a 1:50 Froude scaled movable bed section model of the permeable dam structure and tested in a specialized flume that simulates regressive erosion propagation. Profiles were collected at various times to track the progression of the scour. Tests evaluated variations of the proposed structure, which included tetrapods, riprap, bridge piers, and longitudinal piles. For the various proposed alternatives, a total of six tests were conducted. The collected profiles show the ability or inability of each alternative and its associated performance. From this analysis, untethered tetrapods could not effectively arrest the local scour around the structure. However, large rock along with invert control stopped the regressive erosion and held the upstream grade.					
15. SUBJECT TERMS Coco River (Ecuador); Dams; Erosion; Hydraulic structures; Scour (Hydraulic engineering)					
16. SECURITY CLASSIFICATION OF:			17. LIMITATION OF ABSTRACT		18. NUMBER OF PAGES
a. REPORT Unclassified	b. ABSTRACT Unclassified	c. THIS PAGE Unclassified	SAR		87
19a. NAME OF RESPONSIBLE PERSON Efraín Ramos-Santiago			19b. TELEPHONE NUMBER (include area code) 601-634-2775		